## Review Article

**Author for correspondence:**
Nicolas E. Beaudoin,
Email: nicolas.beaudoin@univ-pau.fr

**CAMBRIDGE**
UNIVERSITY PRESS

# How the geochemistry of syn-kinematic calcite cement depicts past fluid flow and assists structural interpretations: a review of concepts and applications in orogenic forelands

Nicolas E. Beaudoin[1] , Olivier Lacombe[2], Guilhem Hoareau[1] and Jean-Paul Callot[1]

[1]Universite de Pau et des Pays de l'Adour, E2S UPPA, LFCR, CNRS, Total Energies, Pau, France and [2]Sorbonne Université, CNRS-INSU, Institut des Sciences de la Terre de Paris – ISTeP, UMR7193, Paris, France

## Abstract

Orogenic forelands host interactions between deformation and static or migrating fluids. Given their accessibility and dimensions, these areas are not only historic landmarks for structural geology, but they are also areas of prime interest for georesource exploration and geological storage, and loci of potential geohazards. Geochemical techniques applied on cements filling tectonic structures and associated trapped fluids can constrain the temperature, pressure, origin and pathways of fluids during deformation and allow the characterization of the past fluid system. In this review focused on calcite cements, we first present and critically discuss the most used geochemical techniques to appraise specific parameters of the fluid system. Second, we summarize the outcomes of selected case studies where the past fluid system was reconstructed with consideration of tectonics, either at the scale of the individual fold/thrust or at the scale of the fold-and-thrust belt. At first order, the past fluid system evolves in a similar way with respect to the considered stage of deformation, being rather closed to external fluids when deformation is bounded to mesoscale structure development, and opening to vertical flow when thrust and folds develop. In a more detailed view, it seems that the past fluid system evolves and distributes under the influence of the structural style, of the geometry of the major faults and of the lithology of the sedimentary succession. Through this review, we illustrate the concept of geochemistry-assisted structural geology through case studies where the geochemistry of calcite veins constrained subsurface geometries and structural developments in orogenic forelands.

## 1. Introduction

Orogenic forelands are regions where fluid migration intimately entwined with the development of deformational structures. In both fold-and-thrust belt – foreland basin systems (FTB hereinafter) or broken forelands (BF hereinafter), fluid migrations occur at the large scale (in relation with e.g. major faults) and at the mesoscale (in relation with e.g. mesoscale faults, joints, bands and stylolites (Figs 1, 2; Roure *et al.* 2005; Groshong *et al.* 2014; Lacombe *et al.* 2014; Agosta *et al.* 2016; Lacombe & Rolland, 2016). The mesoscale structures directly affect the fluid transport by altering the porosity, either enhancing its connectivity with, for instance, fracturing, or reducing it with, for instance, cataclasis, consequently changing the permeability of a given rock volume. In turn, fluids interact with the rock to enhance the porosity locally by dissolution (e.g. Szymczak & Ladd, 2014) or to reduce it locally by either mineral precipitation (e.g. Bons *et al.* 2012) or mass transfer by pressure solution (e.g. Toussaint *et al.* 2018). Studies of the interplays between fluid flow and deformation processes are numerous (e.g. Mourgues & Cobbold, 2003; Laubach *et al.* 2010, 2019; Cobbold *et al.* 2013; Dielforder *et al.* 2015). Besides the reconstruction of the diagenetic evolution of rocks, a large literature has been dedicated to the reconstruction of past fluid flow associated to deformation by studying syn-kinematic mineralization associated to the development of large-scale fault zones (e.g. Lacroix *et al.* 2014; de Graaf *et al.* 2019; Smeraglia *et al.* 2019), deformation bands (Parry *et al.* 2004; Fossen *et al.* 2007; Zuluaga *et al.* 2016; del Sole *et al.* 2020), and vein networks at the scale of the fold and at the scale of the entire FTB/BF (e.g. Ferket *et al.* 2000; Roure *et al.* 2005; Sibson, 2005; Fischer *et al.* 2009; Beaudoin *et al.* 2011, 2014*a*, 2015; Fitz-Diaz *et al.* 2011*a*; Evans & Fischer, 2012; Crognier *et al.* 2018; de Graaf *et al.* 2019; Dielforder *et al.* 2022).

This approach implies the reconstruction of the past fluid system (Evans & Fischer, 2012) from studying the syn-kinematic cement properties. The fluid system is characterized by (1) the nature of the fluid (i.e. formational, meteoric, basement-derived) from which the cement precipitated, (2) the temperature of precipitation (hotter or cooler than, or at equilibrium with, the surrounding rock), (3) the pressure regime at which the cement precipitated (under hydrostatic to sub-lithostatic), (4) the amount of interaction the fluid phase had with the host rock, and (5)

### (a) Foreland fold-and-thrust belt
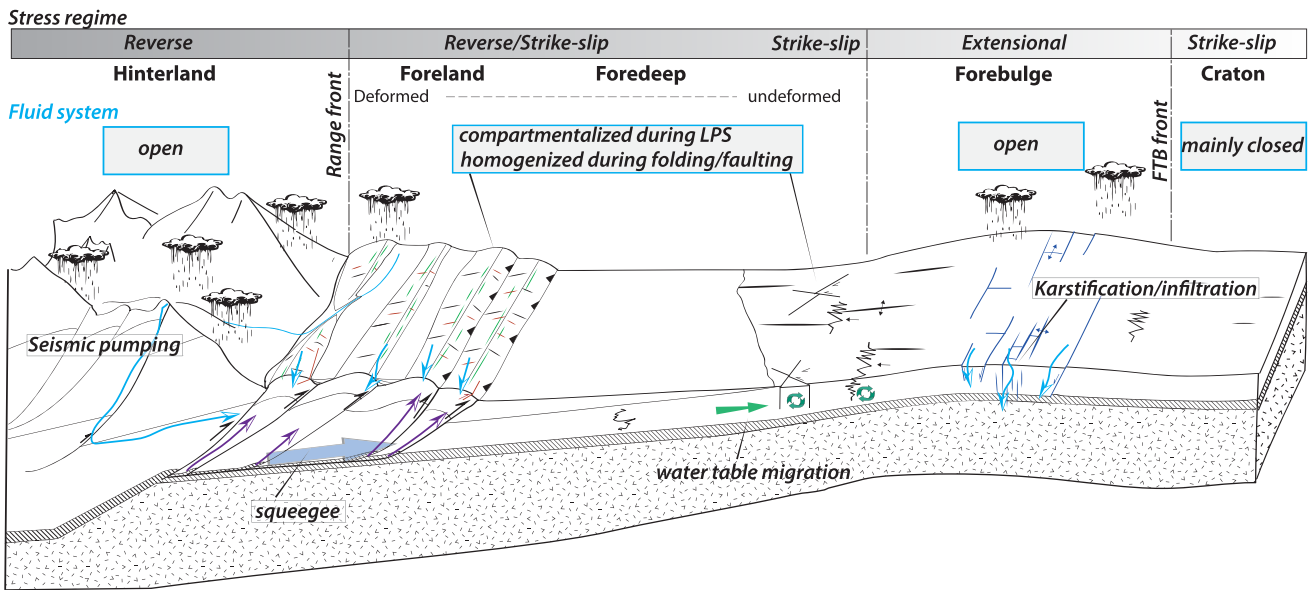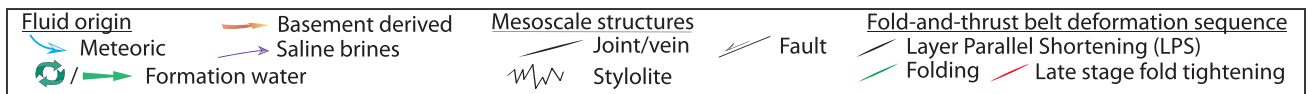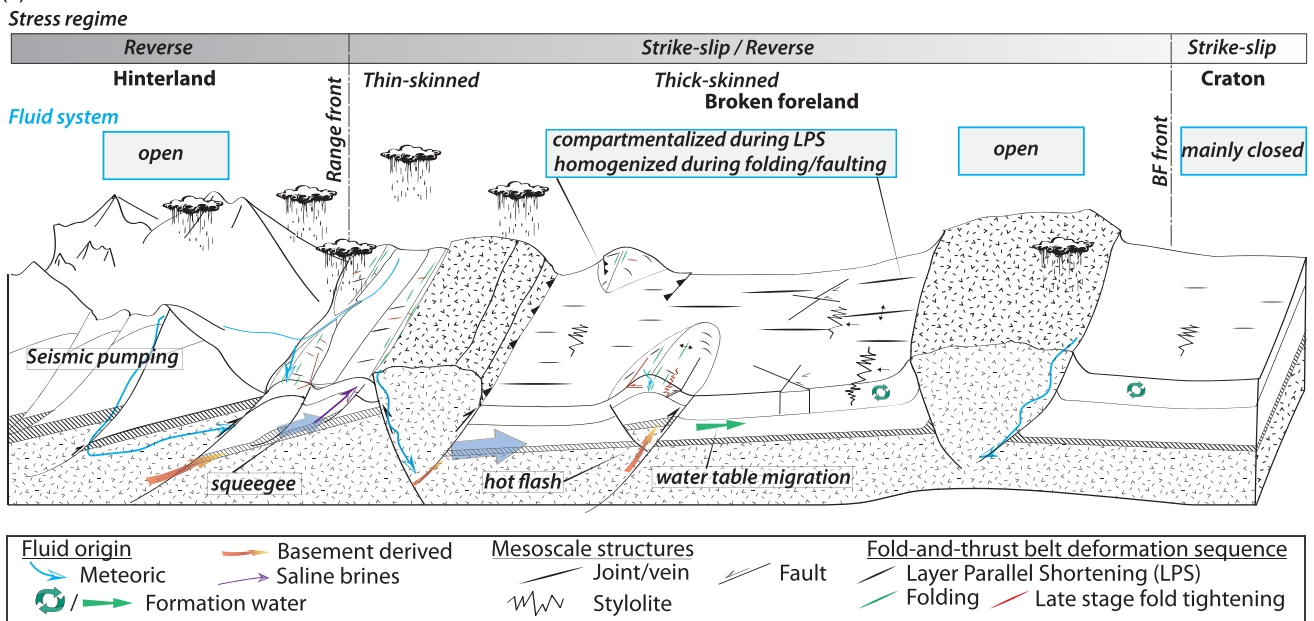


### (b) Broken foreland



**Fig. 1.** Sketches representing a fold-and-thrust belt – foreland basin system (a) and a broken foreland (b). Stress regime, fluid system, source of fluids and engine of migrations, and mesoscale structures related to the folding event, from layer-parallel shortening to late stage of fold tightening, are reported.

the timing of the cement precipitation with consideration as to whether this age may also be the age of deformation, and (6) the hydraulic structure of the reservoir rock. A reservoir can be closed, i.e. with no lateral or vertical migration of fluids; it can be open and compartmentalized with stratified lateral migrations (i.e. no fluid external to the reservoir is involved), or with vertical migration limited by tectonic barriers like faults; finally it can be open and homogenized (i.e. with drains connecting it to other reservoirs or to the surface). One of the prime means of access to the past fluid system lies in the study of cements associated to the sequence of deformation that affected a given rock. Mineral precipitation in major fault zones, along mesoscale fault planes, in veins, and to a lesser extent associated to stylolite development, is the main and most studied marker of past fluids (Fig. 2). In this

review, we focus on the mesoscale structures including fractures (faults, veins), bands and stylolite-related veins (e.g. tension gashes, reopened stylolites). For the sake of simplicity, we refer to all these mesoscale structures as the *fracture network*, as (1) all these develop following patterns (i.e. repetitive distribution) that arrange together as networks (Tavani *et al.* 2015) and (2) they all are host to past fluid-derived mineralization related to deformation. The fracture network comprises sets of structures that can develop either locally (e.g. curvature at the fold hinge) or regionally (e.g. far field contraction). The cement that can fill a mesoscale structure can thus provide a good picture of the past fluid system at the time the structure developed, providing the cement is indeed coeval with the structure development, and that its chemistry remained unaltered. In mesostructures developed in FTB and BF, quartz
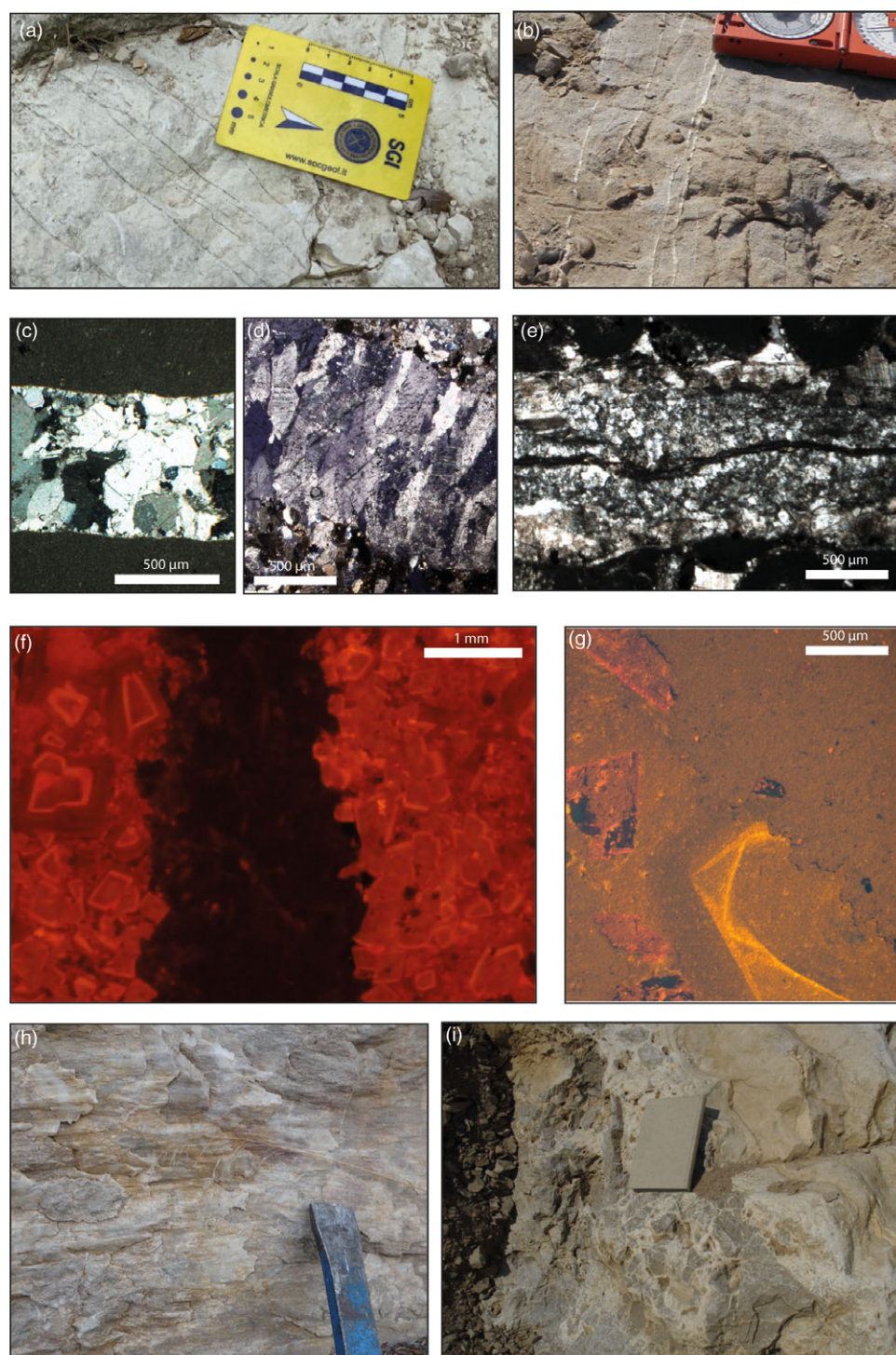
**Fig. 2.** Field and microscope photographs of mesoscale structures studied for past fluid system reconstruction. (a, b) Veins in a fracture network in the Apennines, Italy (a) and in the Laramide province, USA (b). (c, d) Examples of vein textures: blocky calcite from the Apennines, Italy (c); elongated blocky calcite from southern Pyrenees, Spain (d). (e) Multiple fluid flow events and related cement precipitation in a crack seal, Laramide province, USA. (f, g) Cathodoluminescence images of a single phase of cementation in a vein whose borders were affected by dolomitization, Laramide province, USA (f), and of multiple diagenetic phases affecting a vein, Southeast Basin, France (g). Note pressure-solution (stylolite) along the vein border in (g). (h, i) Striated calcite steps along a fault surface, Laramide province USA (h), and fault breccia, associated to local overpressure, Jaca Basin, Spain (i).

and calcite are the most common minerals encountered. In this review, we will focus on syn-kinematic calcite cement, because it is the most frequently encountered in orogenic forelands as a majority of deformed rocks are carbonates in type. Calcite also yields more information about the past fluid system, even when considering only carbonate host rock. Calcite veins, striated calcite steps or calcite slickenfibres on mesoscale fault surfaces, and calcite veins around stylolites are ubiquitous in deformed sedimentary rocks in FTB/BF. Understanding the evolution of the past fluid system from calcite cements is bound to both the evolution of concepts and the continuous development of geochemical tools

applied to calcite cements. Studying the syn-kinematic calcite cement geochemistry, some, if not all, of the parameters that constitute the fluid system can be understood for a given reservoir, providing a picture of the conduits used by the fluids during their migration, the so-called plumbing system. It also hints at the processes required to trigger and maintain the flow on a larger scale than the studied reservoir (Bjørlykke, 1994; Andresen, 2012). For instance, deciphering the past fluid system in FTB such as the Canadian Rocky Mountains has helped identify the main drains (faults/sedimentary interfaces) for hydrocarbon-rich fluids and the relative timing of the fluid migration along with the

topographic-driven migration engine (Roure *et al.* 2010). This kind of information provides boundary conditions to basin-scale fluid flow simulations that predict the migration pathways and rates, and ultimately the distribution of plays (Roure *et al.* 2005, 2010; Callot *et al.* 2017).

This review aims at defining the concept of geochemistry-assisted structural geology, by focusing on the various case studies that report syn-kinematic calcite cement geochemical analysis in carbonate host rocks. We wish to illustrate what geochemical analysis can be conducted on syn-kinematic calcite cements to reconstruct the fluid temperature and pressure at the time of precipitation, the fluid origin, the age of precipitation, or the migration pathways. In turn, we question how this information can be used to qualitatively infer the distribution and activation time of the conduits, leading to deciphering structural information such as extension of faults, the nature of decoupling level, and the timescale of deformation. Hereinafter, we provide an overview of the geochemical techniques that can be used to characterize the conditions of precipitation of calcite cements (and to a lesser extent, quartz), and the chemistry of the fluid it precipitated from. Among others, we present classical techniques such as $\delta^{18}O$, $\delta^{13}C$, $^{87}Sr/^{86}Sr$, elementary content, and fluid inclusion microthermometry, along with others under development such as $\Delta^{47}CO_2$ and U–Pb geochronology. The prerequisite to a proper geochemical investigation of past fluid systems, i.e. a petrologic and diagenetic characterization of samples, will be briefly introduced, including vein petrography and techniques such as cathodoluminescence. We then present detailed examples of how the past fluid system can be reconstructed from calcite cements precipitated in major faults and/or in fracture networks at the scale of individual folds and at the scale of FTB (Canadian Rockies, Central Apennines, southern Pyrenees) or at the scale of the BF (Laramide province). More cases are then summarized, based on the large-scale structural style, in order to draw a complete picture of the relationship between the past fluid system, its evolution during deformation, and the structural geology of the subsurface.

Beyond the study of syn-kinematic cements in fault rocks from major faults, this review reports numerous studies focusing on the mesoscale structures (comprising faults and veins, but extended to stylolites and bands). Studying the fracture network in strata potentially allows access to the past fluids during a deformation history, from the weak deformation related to foreland flexure to the involvement of the strata in folds and/or thrusts as the FTB/BF developed (Fig. 1). This review excludes past fluid systems reconstructed from (1) magmatic fluids (e.g. MacDonald *et al.* 2019) and related ore deposits (e.g. Jin *et al.* 2021), (2) hydrocarbon-dedicated geochemical techniques, and (3) geochemical techniques dedicated to non-carbonate veins, e.g. sulphur in gypsum cement (Machel, 1985*b*; Moragas *et al.* 2013). This review also does not examine how the understanding of a past fluid system can refine fluid flow simulation. As such, this contribution is to be seen as a complement to recent reviews dedicated to (1) how FTBs accommodate deformation through the development of meso-structures that damage reservoirs (Tavani *et al.* 2015); (2) the specific relationship between fault zones and permeability (Faulkner *et al.* 2010) and more generally fault zone hydrogeology (Bense *et al.* 2013); (3) the interplay between deformation and fluid flow at the fold scale (Evans & Fischer, 2012); (4) the prediction of past fluid flow in FTBs (Roure *et al.* 2005, 2010); (5) the petrophysical evolution of carbonates (Archie, 1952; Regnet *et al.* 2019); and (6) the interplay between chemistry and deformation in carbonates (Laubach *et al.* 2019).

## 2. Fault zones and fracture networks: witnesses of past fluid flow

### 2.a. Development of fault zones and fracture networks

Orogenic forelands, that can be either fold-and-thrust belt – foreland basin systems or broken forelands, are the external parts of orogens where the deformation of sedimentary rocks occurred under diagenetic to low-grade metamorphic conditions of pressure and temperature, and in that sense are opposed to the higher-grade metamorphic hinterland (Fig. 1). The depth and degree of the mechanical decoupling level within the continental crust activated during collision has been widely debated for many years. One view states that the sedimentary cover is detached from the underlying basement along a shallow, low-strength décollement and deformed by thrusts with ramp-flat geometries rooting into the décollement level (thin-skinned tectonic style). This thin-skinned tectonic style supposes large-scale displacements and duplication of the sedimentary sequence, the underlying basement remaining undeformed (Lacombe & Bellahsen, 2016; Pfiffner, 2017). The low-strength décollement where thrusts are rooting at depth can be either viscous (e.g. salt, as in the Potwar Basin, Pakistan) or frictional (e.g. shales, as in the Alberta Rocky Mountains, Canada), or it can be associated with salt-related tectonic structures (e.g. the Sivas Basin, Turkey; Hudec & Jackson, 2007; Callot *et al.* 2012). The alternative view states that shortening involves a significant part of the crust along crustal-scale ramps above a deep ductile detachment (thick-skinned tectonic style). These are two end-members, and superimposed thin-skinned and basement-involved deformation may occur in various parts of the belt (Lacombe & Bellahsen, 2016; Pfiffner, 2017). Broken forelands (Fig. 1b) are characterized by basement uplifts, forming arches in a possibly erratic sequence of basement fault reactivation. These uplifts segment the former basin (Jordan & Allmendinger, 1986; Horton *et al.* 2022). Examples of broken forelands are the Laramide province in the western USA and the Sierras Pampeanas in Argentina.

The porosity and permeability of carbonate rocks are modified very early by diagenesis and later by structural damage. The latter develops mesoscale structures: (1) surfaces/bands that create porosity/permeability by fracturing, with a displacement either perpendicular to their surfaces (Fig. 2a–g; joints, veins and dilation bands) or along/oblique to their surfaces (Fig. 2h, i; faults and shear bands); and (2) surfaces/bands that reduce porosity/permeability by pressure-solution/cataclasis, with a motion either perpendicular to their surfaces (stylolites and compaction bands) or along/oblique to their surfaces (slickolites/shear bands). The distribution of these mesoscale structures varies spatially and temporally according to the position of the considered strata in the FTB/BF (Fig. 1). Considering carbonates, the formation of the fracture network starts during burial with the development of along-strike and across-strike joints and veins and of bedding-parallel sedimentary stylolites, the latter potentially developing at very shallow depths (<400 m; Toussaint *et al.* 2018). During foreland flexure, along-strike and across-strike joints and veins oriented at high angle to bedding develop, along with normal faults, in the sedimentary series. These structures form in response to forebulge development and along-foredeep stretching (in blue in Fig. 1a). The folding event (Lacombe *et al.* 2021) starts with the layer-parallel shortening (LPS). LPS produces a network of structures comprising (1) joints and veins either at high angle to bedding and striking parallel to the shortening direction or parallel to bedding, (2) pressure solution cleavages, including tectonic stylolites, of which planes are oriented at high angle to bedding and perpendicular to the
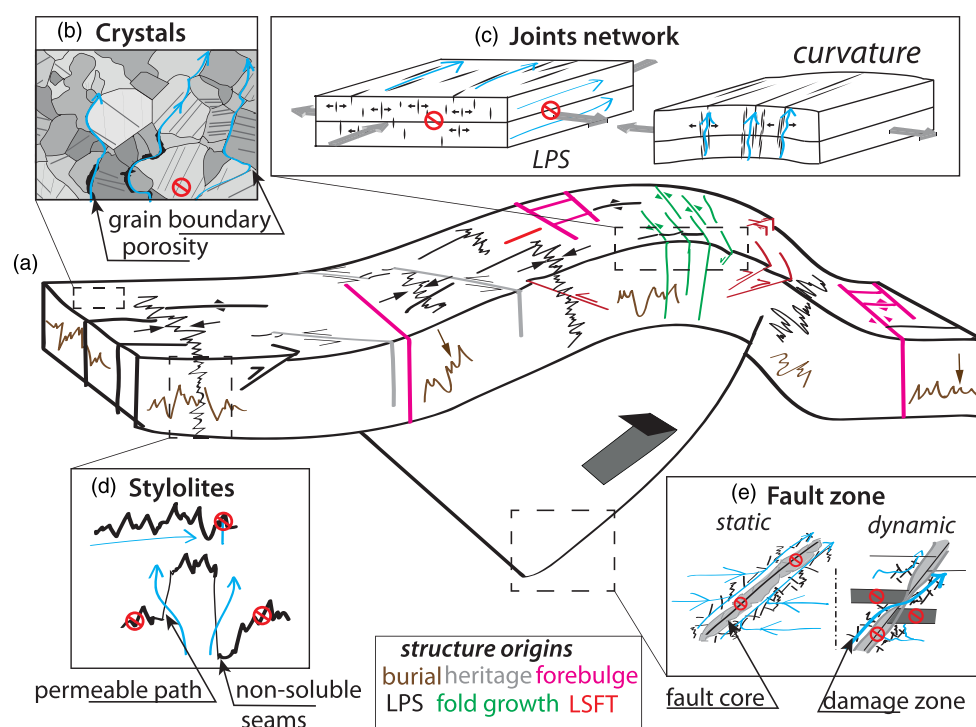
**Fig. 3.** (a) Expected distribution of the meso-scale fracture pattern at the fold scale, including faults, joints and stylolites. Colours show the relation between the feature and the stage of deformation: brown relates to burial, grey to pre-orogenic, pink to outer arc extension during flexure, black to the layer-parallel shortening, green to fold growth, red to late stage of fold tightening. (b–e) Zoom on the expected fluid flow in the structures depicted in (a): (b) matrix-scale reactive fluid migration pathways; (c) migration pathways in joint network; (d) migration pathways in stylolites; (e) migration pathways in fault zones and cores, with the static state and the dynamic state. See text for details and references.

shortening direction, and (3) conjugate strike-slip or reverse faults. The LPS may still affect strata at the onset of fold growth (Fig. 3) up to *c.* 30° of bed tilting (Tavani *et al.* 2015), and it can also develop bedding-parallel veins. In the orogenic foreland, fold growth is accommodated by flexural slip in the fold limbs and tangential longitudinal strain (e.g. outer-arc extension) at the fold hinge, the latter giving birth to along-strike joints at high angle to bedding as well as normal faults (Figs 1, 3). The fold 'locks' when limb rotation and/or kink-band migration cannot accommodate shortening anymore. At that stage, strata tilting is over but continuous horizontal shortening leads to late-stage fold tightening (LSFT), accommodated by mesoscale structures developing irrespective of bedding dip, such as (1) vertical conjugate strike-slip faults, (2) vertical joints striking parallel to the LPS-related ones, and (3) vertical tectonic stylolites oriented perpendicular to the shortening direction. At all stages of fold growth, earlier-formed fractures, either inherited from an ancient contractional event or from the foreland flexure preceding folding and thrusting, may also be reactivated (Guiton *et al.* 2003; Bergbauer & Pollard, 2004; Bellahsen *et al.* 2006b; Callot *et al.* 2010a; Sassi *et al.* 2012). The folding event, encompassing deformation from the LPS to the LSFT, spans from a few Myr to a few tenths of Myr, according to the structural style and to the distance between the front of the range and the location of the (future) fold (Lacombe *et al.* 2021). It is important to note that in some specific cases this sequence will see development of fractures geometrically identical at various times of the deformation history, such as outer-arc extension related to the forebulge and to fold growth, or fold-axis perpendicular, LSFT and LPS fractures in fold limbs. In such cases, the origin of the fracture can only be assessed by robust relative chronology observations and/or might be assessed by geochemical, temperature and absolute age constraints on the filling cements precipitated during deformation.

## 2.b. Fluid sources and fluid evolution during migration

FTB/BF develop with various structural styles, that affect (1) the availability of different fluid sources and (2) the triggers for the fluid migration (Fig. 1). Excluding magmatic fluids we can distinguish between various parent fluids at the time of precipitation: (1) surficial fluids such as meteoric fluids and formational water (seawater or fresh water); (2) crustal fluids, either described as basement fluids or as metamorphic fluids. The metamorphic fluids are either produced during retrograde metasomatic reactions (Yardley & Graham, 2002) or during prograde dehydration reactions (e.g. Hollocher, 1991) occurring deeper in the crust. The fluids flowing in the basement rocks, beyond magmatic fluids, are proven to be usually derived from surficial fluids (Yardley & Graham, 2002). Similarly, formational water can evolve during fluid migration by interacting with the host rock in the basin, making so-called brines (or basinal fluids) if interacting with host rocks.

The fluid migration is triggered by various mechanisms (Fig. 1). The most common is the water table migration, or topographically driven flow, based on topographic/burial difference of a given stratum, that triggers pressure gradients making fluids migrate from the deepest towards the shallowest/highest part of the strata (Bjørlykke, 1994, 2015), usually along the slope between the hinterland and the forebulge, or between synclines and anticlines. Migration can also be triggered by the stress gradient of units thrusting over others, expelling the fluid forelandwards. This mechanism, called squeegee, channelizes fluids along permeable horizons (Oliver, 1986) where fluid can migrate at a speed of 10 km Myr$^{-1}$ over several million years (Ge & Garven, 1994), with pulses up to 100 km Myr$^{-1}$ (Michael & Bachu, 2001). Local stress accumulation in fault zones may also trigger 'hot flashes', an along-plane fast upward migration of hot fluids (Fig. 1; Machel & Cavell, 1999). Fluids can also flow

downwards in fault zones following pressure gradients between the sealed and the broken domains during the seismic cycle (fault valve behaviour: Henderson & McCaig, 1996; Sibson, 2000), or by enhancing permeability in the fault zone by local overpressure (Ortiz *et al.* 2019). Local chemical gradients between fluids and rocks can also enhance fluid migration, typically by carbonate dissolution, developing wormholes due to the flow of meteoric water undersaturated with respect to carbonates (Szymczak & Ladd, 2009; Petrus & Szymczak, 2016). This mechanism is efficient at a very shallow crustal level (Fig. 1).

## 2.c. Fault zones and fluid migration

At the scale of fault zones, the link between tectonics and fluid dynamics has been extensively investigated. For instance, the hydrological behaviour of fault zones, first introduced by Caine *et al.* (1996), has received a lot of attention since, with a compelling review proposed by Faulkner *et al.* (2010). When displacement exceeds 1 m (Micarelli *et al.* 2006), a fault can be divided into two main zones characterized by very different hydraulic behaviours (Fig. 3): the fault core, usually clay-rich, is a non-permeable zone, acting as a transverse barrier to the fluid which is forced to flow along the fault plane. In the surrounding damage zone, fractures develop (Fig. 2i), progressively increasing the connected porosity (Bense *et al.* 2013). However, fast cement precipitation after hydrofracturing can potentially reduce the permeability, leading to an overpressure–failure cycle bound to the seismic cycle (Sibson, 1990; Vass *et al.* 2014). Regardless of the stress regime under which the fault developed, the damage zone is observed as being the main drain for the fluid, being especially efficient for a flow parallel to the fault plane (Agosta, 2008; Baietto *et al.* 2008; Sutherland *et al.* 2012).

## 2.d. Fracture network and fluid migration

At the scale of the mesostructures, and leaving aside deformation bands that are rare in carbonates (Tondi *et al.* 2006), two kinds of mesostructures exert a strong control on the fluid migration (Fig. 3c, d): the fractures, either opened in mode I (referred to as joints: Oliver & Bons, 2001; Sachau *et al.* 2015; Wennberg *et al.* 2016) or shear/hybrid in type (mode II or I + II), and the stylolites (Braithwaite, 1989). Regardless of the nature of the rock volume, the hydraulic efficiency of fractures is directly controlled by (1) the fracture aperture, (2) the orientation of the fracture plane with respect to the ambient stress field, (3) its vertical/lateral extent and (4) the density and connectivity of the fracture network. In carbonates, fracture density and permeability are linked to the diagenetic state of the reservoir and to the mechanical properties of the rock, namely stiffness and tensile strength. There are reciprocal controls between the diagenetic state of the rock and the fracture development, leading to the concept of mechanical stratigraphy (Ortega *et al.* 2010; Barbier *et al.* 2012a; Wennberg *et al.* 2016). An efficient vertical fluid flow is observed in various folds (Evans & Fischer, 2012), probably related to an enhanced vertical extension of the joint network during folding. In contrast, joints developed during the LPS allowed efficient stratified, lateral migration of fluids with no vertical mixing in various case studies (Beaudoin *et al.* 2014a, 2020c). These observations of different hydraulic behaviour for the same kind of joints led to the proposition that this difference is not due just to the different geometry, but probably also to the stress regime active, influencing fracture aperture (and its evolution during time) (Fig. 3). Indeed, joint networks developed during LPS under a strike-slip stress regime

favour lateral fluid flow and fluid system stratification while joint networks developed in response to strata curvature under a local extensional stress regime favour vertical fluid flow and fluid homogenization between reservoirs. Although less efficient for fluid flow than fault zones, the mesoscale structures are also an important part of the palaeohydrology at the scale of the FTB (Beaudoin *et al.* 2013), and the veins can reliably be used to reconstruct the fluid system related to both large-scale and local tectonics.

The role of stylolites on the fluid system remains vastly overlooked in that context, except to constrain the diagenesis related to the burial phase or the early LPS (Swennen *et al.* 2000; Roure *et al.* 2010; Vandeginste *et al.* 2012). Stylolites are mainly considered as efficient barriers for fluid flow, since they accumulate nonsoluble, non-permeable material along their dissolution plane, and redistribute cement around, clogging the porosity (Nelson, 1981). This consideration makes stylolites interpreted as structures able to compartmentalize a reservoir (Roure *et al.* 2010). Yet, a growing number of natural observations and experimental case studies reveal that stylolites can be efficient drains for fluid flow (Koehn *et al.* 2016; Heap *et al.* 2018; Martín-Martín *et al.* 2018; Toussaint *et al.* 2018; Bruna *et al.* 2019). The impact of stylolites on the fluid flow depends on the orientation of the stylolite with respect to the flow, i.e. guiding a fluid flow parallel to the dissolution plane, and blocking the flow perpendicular to the dissolution plane (Fig. 3). This behaviour, similar to that of a fault zone, was observed in nature with a channelization of the reactive fluid flow along a stylolite plane (Martín-Martín *et al.* 2018; Humphrey *et al.* 2019) and in experiments (Heap *et al.* 2018). Yet it is not the only controlling factor of permeability to fluid flow. Indeed, Koehn *et al.* (2016) have observed ore-bearing stylolites in the Zechstein carbonate units (Germany), which demonstrates a strong control of the stylolite morphology over the fluid flow. They proposed a new classification in which the morphology of the stylolite, i.e. rectangular, suture and sharp peak, seismogram and simple wave-like, itself controlled by the growth rate of the stylolite, controls its impact over the fluid flow. In the classification, the stylolites that have high-amplitude peaks undergo a growth that locally shifts the non-permeable residue layer, allowing a fluid flow across the stylolite plane. It is important to note that because of local stress perturbations (Aharonov & Karcz, 2019), cracks can open during pressure solution and be filled with cement that will record information in relation to the stylolite development. Considering the complexity of stylolite development and its potential impact on fluid flow, it appears necessary to further investigate stylolites and reappraise their role in past fluid systems.

Though beyond the scope of this review, it is worth mentioning that the fluid chemistry may itself impact fluid flow, for instance through dissolution or fluid-mediated replacement, that will affect the fluid dynamics down to the crystal scale. Classic examples of the latter in carbonates are dolomitization or apatitization processes, and recent experimental works (Jonas *et al.* 2014; Pedrosa *et al.* 2017; Weber *et al.* 2021) and natural observations (Centrella *et al.* 2021) highlighted the prominent role of grain boundaries and mineralogical defects like cleavage planes on the fluid flow at that scale (Fig. 3).

## 2.e. Past fluid flow markers

Reconstructing fluid flow in orogenic forelands requires identification of markers of past fluid flow. These witnesses can be indirect, like the contrasted colour halo in the host rock around a fracture

related to the migration of a fluid with a different redox state than the host (e.g. Eichhubl *et al.* 2004; Stel, 2009; Missenard *et al.* 2014). In such cases, quantitative information remains very limited. More interestingly, there is a wealth of direct markers of past fluid flow, like cements precipitating in breccia during hydrofracturing (Fig. 2i), even though the link between breccia texture and hydrofracturing is nowadays questioned (Centrella *et al.* 2022). Mineralogical phase transformation such as dolomitization is another example of a well-studied marker that allows reconstruction of the past fluid system (e.g. Martín-Martín *et al.* 2013; Koeshidayatullah *et al.* 2020*a*, *b*; Centrella *et al.* 2021; Motte *et al.* 2021). Yet, the most studied witness of the past fluid flow in contractional settings consists in the cements filling fractures (veins and faults), including the fluid inclusions they host (Bons *et al.* 2012; Laubach *et al.* 2019). In FTB and BF, the mineralogy of such filling, beyond calcite and quartz, can include fluorite, ores or gypsum.

## 3. Bounding cement precipitation from past fluid to deformation: the role of petrography

In order to reconstruct the past fluid properties during deformation, it is important to (1) unambiguously link cement precipitation to the timing of development of the studied structure (fault, vein, stylolite), and (2) check whether the cement has been altered or not by later diagenetic events. This is a prerequisite to any robust geochemical analysis of the past fluid system. In the case of cements associated to faults, the observation of either cement in cataclasites (Fig. 2i) or, better, of striated calcite steps (Fig. 2h) is a reliable way to ensure that the cement precipitated from a fluid involved during the deformation, provided the breccia cement is not a simple matter of recrystallization (Centrella *et al.* 2022). In the case of veins, a robust petrographic study is systematically required prior to any geochemical analysis being performed. First, the nature of the filling is an obvious yet ambiguous indicator of the nature of the fluid. For example, the occurrence of gypsum veins indicates the involvement of fluids that were in contact with evaporitic layers in the reservoir (Pichat *et al.* 2018), but it cannot argue in favour of the evaporites being the source of the fluids (dehydration during the tectonic remobilization of a salt layer) or part of the migration pathway of the fluid (a meteoric fluid percolating within a gypsum level; e.g. Travé *et al.* 2007). Another example is the content of the crystal fluid inclusions (halite crystals, hydrocarbons) that can also be informative about either the fluid origin or its pathways. In their review, Bons *et al.* (2012) illustrate what vein cement texture can tell us about the mode of deformation, and about the common timing between vein opening and cement precipitation (Fig. 2c–e). The coevality between precipitation of cement and deformation is obvious when the cement precipitates as fibrous crystals in opened veins (Bons *et al.* 2012), or when the vein growth is driven by crystallization forces during precipitation (Gratier *et al.* 2012; Cobbold *et al.* 2013). In the case of a syntaxial texture supporting the growth-induced opening of a vein (Fig. 2d), experimental data suggest that a very high fluid flow is required to keep the crystal growth rate sufficiently high (Lee & Morse, 1999; Hilgers & Urai, 2002*b*). In the case where the timing of precipitation is ambiguous with respect to the development of the fracture (e.g. in presence of blocky calcite; Fig. 2c), the process that triggered precipitation must be questioned. In the case of calcite, a mineral with a retrograde solubility (Segnit *et al.* 1962), oversaturation for a given fluid is reached when temperature increases or when $pCO_2$ decreases. Precipitation can be triggered by mixing between

hydrothermal migrating fluids and local fluids. In cases where fluid mixing is not supported by data, authors have considered that the opening of the fracture triggers the precipitation by locally reducing $pCO_2$ (Beaudoin *et al.* 2014*a*; Cruset *et al.* 2018). It is interesting to note that the recent study of Roberts and Holdsworth (2022) suggests that veins developed as crack seal are optimal to access the past fluid at the time of deformation, even though this needs to be considered with care as Bons *et al.* (2012) clearly showed that a crack seal can be related to multiple events of deformation.

When a cement is considered to be linked to the fracture development, a second mandatory petrographic step is to check that the cement was not altered by diagenesis. Indeed, calcite crystals can keep their initial chemical signature pristine at low-grade metamorphism (e.g. Dielforder *et al.* 2022), so it is important to discard the idea that dissolution/reprecipitation or recrystallization processes affected the cement. A classical tool used for that purpose is cathodoluminescence (Fig. 2f, g) ( Machel, 1985*a*; 1997). The natural luminescence of calcite (but also of quartz, fluorite, gypsum) in a vein is informative about (1) the number of cement phases in the fracture, and/or alteration events affecting the vein cements, (2) the redox state of the fluid, itself arguably relatable to the fluid origin (Machel, 1997), and (3) the rate of precipitation of calcite cement, variation of which can create luminescence zoning (Dromgoole & Walter, 1990; Boggs & Krinsley, 2006). For the latter, the relative part of the growth rate with regard to the surface growth preference has been debated (Reeder & Grams, 1987). Above all, ensuring that the cement filling the vein precipitated in a single phase (homogeneous luminescence; Fig. 2f), and that it has not been subsequently altered (Fig. 2g) is key to validate that the geochemical analysis of the cement actually yields information about the past fluid (e.g. van Geet *et al.* 2002; Hanks *et al.* 2006; Barbier *et al.,* 2012 *a*). That preliminary step is mandatory to allow further interpretation of a geochemical dataset with respect to the tectonic history of an area.

## 4. Geochemical proxies to reconstruct the past fluid system

In this section we review the basic concepts and pitfalls of the geochemical techniques that are used for, but not limited to, the reconstruction of part of the past fluid system when applied to calcite cement in tectonic structures. We first focus on the most classical techniques, then summarize the less developed/applied ones. Figure 4 presents an ideal workflow of how these techniques can be applied to a sample, with emphasis on what (combination of) analysis can be used to access specific parameters of the fluid system. For reviews of the use of geochemistry for past fluid beyond its relation to tectonics (e.g. diagenesis), we refer the reader to the existing literature (Emery & Robinson, 1993; Swart, 2015).

### 4.a. Fluid inclusions

Fluid inclusions are micrometre- to millimetre-scale inclusions – filled with fluids, or a combination of fluid, vapour and solid – that are ubiquitous in crystals (Goldstein & Reynolds, 1994). Three types of fluid inclusions are classically described (Roedder, 1984; Goldstein & Reynolds, 1994): (1) the primary fluid inclusions, that are defects related to the crystal growth itself. Primary fluid inclusions mainly occur along the crystal growth rims, and mostly have a shape corresponding to the crystal habitus. (2) Pseudo-secondary fluid inclusions are not directly distributed in a pattern linked to the crystal growth, yet they are lined onto deformation planes that
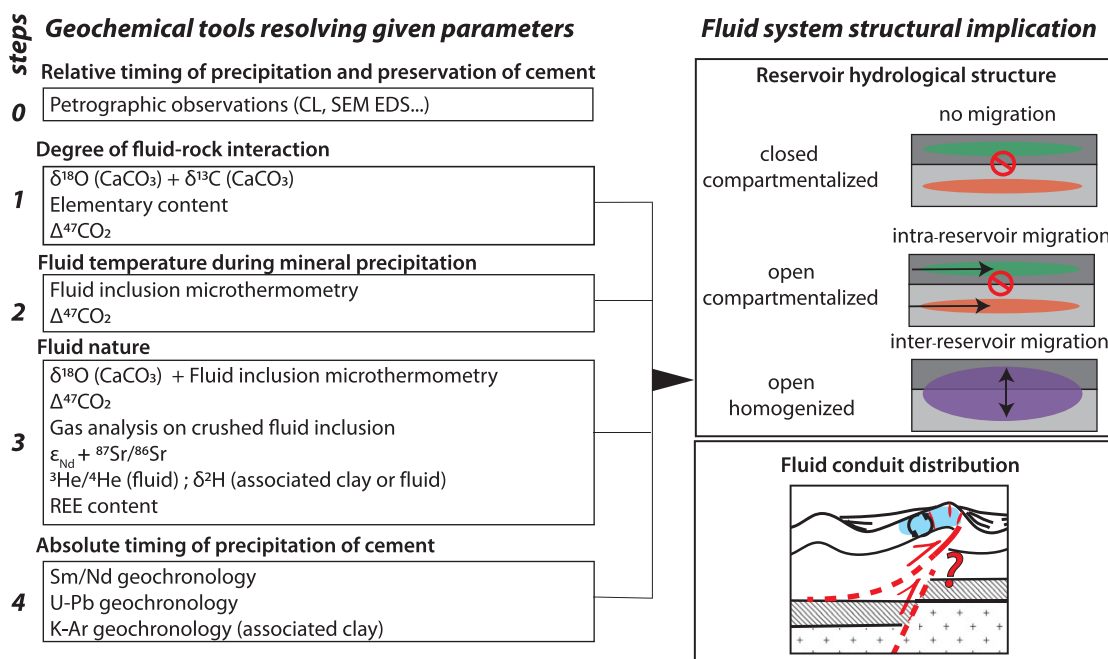
## Geochemical tools resolving given parameters

**steps**

**Relative timing of precipitation and preservation of cement**

**0** | Petrographic observations (CL, SEM EDS...)

**Degree of fluid-rock interaction**

**1** | $\delta^{18}O$ (CaCO₃) + $\delta^{13}C$ (CaCO₃)
Elementary content
$\Delta^{47}CO_2$

**Fluid temperature during mineral precipitation**

**2** | Fluid inclusion microthermometry
$\Delta^{47}CO_2$

**Fluid nature**

**3** | $\delta^{18}O$ (CaCO₃) + Fluid inclusion microthermometry
$\Delta^{47}CO_2$
Gas analysis on crushed fluid inclusion
$\epsilon_{Nd}$ + $^{87}Sr/^{86}Sr$
$^{3}He/^{4}He$ (fluid) ; $\delta^{2}H$ (associated clay or fluid)
REE content

**Absolute timing of precipitation of cement**

**4** | Sm/Nd geochronology
U-Pb geochronology
K-Ar geochronology (associated clay)

## Fluid system structural implication

**Reservoir hydrological structure**

no migration

closed compartmentalized

intra-reservoir migration

open compartmentalized

inter-reservoir migration

open homogenized

**Fluid conduit distribution**



**Fig. 4.** Concept of geochemistry-assisted structural geology. Left-hand side: representation of all parameters (bold) that can be reconstructed from geochemical analysis (framed) on calcite, organized in a suggested workflow. The suggestion is to pick at least one of the analyses of each box to reconstruct the past fluid system with the least ambiguity. Right-hand side: structural implication of the outcome of the past fluid system reconstruction, including a direct appraisal of the reservoir hydrological structure, and an inferred model of the fluid conduit distribution in time and space.

developed during the crystal growth, being limited to the crystal. (3) Secondary fluid inclusions appear as trails, the orientation of which is not related to the crystal growth; they can be considered as post-growth mode I joints at the crystal scale (e.g. André *et al.* 2001). Regardless of the type of inclusions, the mineralizing fluid is trapped at set pressure and temperature. Assuming that (1) the volume of the inclusion remains constant, (2) fluid–solid chemical exchanges are null and thus (3) the fluid chemistry is constant, the pressure and temperature decrease during the subsequent exhumation of the crystal triggers phase changes potentially leading to the development of a vapour bubble (e.g. Bourdet *et al.* 2008). Fluid inclusions might be one-phase, two-phase with vapour/liquid or liquid/solid, or three-phase with coexistence in the laboratory conditions of solid, vapour and liquid phases, the former being typical of highly saline fluids (Goldstein & Reynolds, 1994). In the following paragraphs, we do not mention techniques that rely on hydrocarbon-bearing fluid inclusions. For more information than is summarized hereinafter, please refer to the detailed technical review by Chi *et al.* (2020).

The original analysis conducted with fluid inclusions consists in reconstructing the temperature and pressure condition of fluid entrapment, i.e. at the time the crystal precipitated, by means of microthermometry. A thick section of mineral is heated up under the microscope using a temperature-controlled microthermometric stage in order to measure the temperature at which the vapour phase becomes homogeneous with the liquid one. This is called the temperature of homogenization ($T_h$), and corresponds to the minimal temperature of the fluids when it was trapped in the inclusion (Goldstein & Reynolds, 1994). Note that if the fluid temperature is lower than 50 °C at the time of entrapment, the vapour bubble will usually be absent or may not be visible in laboratory conditions, but it can be nucleated or enlarged by freezing the fluid. With the knowledge of, or by assuming, the fluid chemical system and the pressure of entrapment (i.e. depth), one can reconstruct the

absolute temperature of precipitation. By comparing it to the expected temperature at which the host rock was at the time of precipitation, by considering a geothermal gradient and a past depth, it is then possible to assess if the fluid is hydrothermal (hotter than the local temperature), geothermal (equal to the local temperature) or hydrofrigid (colder than the local temperature) *sensu* Machel and Lonnee (2002). Microthermometry is also used to estimate the type of salts and the salinity of the system. The protocol is to freeze the studied fluid inclusion, and to heat it back up slowly to measure (1) the temperature(s) at which the ice starts to melt (i.e. eutectic temperature(s) $T_e$), which relates to the fluid composition (Davis *et al.* 1990), and (2) the temperature at which the last cube of ice disappears, i.e. the ice melting temperature ($T_{m\ ice}$). In a simple H₂O–NaCl system, the temperature at which a frozen fluid inclusion becomes completely liquid is directly related to the fluid salinity.

Two major pitfalls affect fluid inclusion microthermometry in calcite cement. The first is that the approach is valid only under the assumption that the volume and chemistry of the inclusion remained constant. In weak crystals such as calcite (Goldstein, 1986; Bodnar, 2003), volume might easily vary (1) during the analysis and (2) throughout the crystal history, especially in deformed areas. The variation in volume of the inclusion will usually have a petrographic effect on the shape of the inclusion (e.g. stretching), or a visible effect on the vapour bubble membrane, making it impossible to consider the measured $T_h$ in the dataset of measurements. In order to avoid misleading temperature data, the norm is to conduct a rigorous petrographic study to distinguish between the different generations of fluid inclusions in a given cement, then first to measure the homogenization temperature of fluid inclusion populations before the eutectic and ice melting temperatures (as freezing likely will stretch the inclusions), and then to use the modal value of population distribution as representative of the $T_h$. When data is available, the

comparison of the distribution with current geothermal temperature might also indicate a thermal re-equilibration of the fluid inclusion population with the current temperature, involving volume variations within the studied fluid inclusions (Bodnar, 2003). The second pitfall is that, considering the usual size of inclusions in calcite (<10 μm), the eutectic and melting temperatures are usually very hard to constrain because of technical limitation related to their limited size.

Fluid inclusions can also grant direct access to the fluid composition. One method consists in evaporating the liquid phase following sample crushing (e.g. Blamey, 2012; Dassié *et al.* 2018) and analysing its elemental or isotopic composition by either mass spectrometry or gas chromatography. In spite of recent progress, allowing data to be obtained from down to 0.1 μL of fluid by crushing, the main limitation is related to the fact that it would be required to crush only primary/pseudo-secondary fluid inclusions, which appear to be complicated, even with a solid petrographic characterization. Böhlke and Irwin (1992) showed that it was possible to analyse the fluid inclusions directly, but at the time it worked only for $10^{-11}$ L of fluid, in inclusions of very large dimensions (hundreds of μm). Laser absorption spectroscopy allows the reduction of these dimensions to a few tens of μm (Affolter *et al.* 2014). Yet future development in mass spectrometry on the one hand and in spotted sampling such as laser ablation on the other hand might lead to exciting developments enabling study of the content of selected fluid inclusion related to specific tectonic stages without crushing. A second method to access the fluid trapped in inclusions is to perform Raman spectroscopy on the fluid inclusion (Rosasco *et al.* 1975). Raman spectroscopy is usually coupled to microthermometry to gradually heat up the inclusion during the measurement, and so to characterize and quantify the nature and amount of chemical components trapped in the fluid inclusion. This technique is mainly developed for oil-bearing fluid inclusions (e.g. Guillaume *et al.* 2003) and allows, when combined with other techniques, for proper computation of the chemical composition of the fluid inclusion, i.e. the isochore and isopleth curves (Bakker, 2003), or for direct determination of the salinity of aqueous fluid inclusions (Caumon *et al.* 2014). When aqueous fluid inclusion microthermometry is combined with coeval oil-bearing fluid inclusion microthermometry, it becomes possible to access the exact pressure and temperature of entrapment of the fluid (Pironon & Bourdet., 2008).

## 4.b. Established isotope-based techniques

### 4.b.1. Oxygen

Oxygen stable isotope measurements consist in measuring the ratio between the $^{18}$O and the $^{16}$O of the oxygen-bearing mineral (carbonates, but also quartz or clays), dividing it by the measured ratio between the $^{18}$O and $^{16}$O of a standard itself calibrated to a reference (Standard Mean Ocean Water (SMOW) for liquid phase, PeeDee Belemnite (PDB) for carbonates), as follows:

$$\delta^{18}O = \left( {\left( {}^{18}O/{}^{16}O \right)_{sample}} \middle/ {\left( {}^{18}O/{}^{16}O \right)_{standard}} - 1 \right) * 1000 \quad (1)$$

The $\delta^{18}$O is expressed in per mil with respect to the reference (‰ PDB or ‰ SMOW). This technique can be performed using a few μg of pure carbonate (40 μg) obtained from machine-assisted sampling, or using laser or ionic ablation (Becker, 2002). This ensures very easy data acquisition with minimal preparatory work,

at very low cost and with relatively high precision (0.1−0.5 ‰ depending on the set-up used) (Swart *et al.* 1991).

In the case of carbonates, studying oxygen isotopic ratio considers the exchange between the $H_2O$ content of the fluid and $CaCO_3$. The formula that links the $\delta^{18}$O value of the carbonate to the $\delta^{18}$O of the water is as follows:

$$\delta^{18}O_{CaCO_3} = \delta^{18}O_{H_2O} + 1000 \ln \alpha \quad (2)$$

The fractionation coefficient $\alpha$ is primarily controlled by the temperature at which the phase change occurs (precipitation or dissolution). Since the seminal work of Epstein *et al.* (1953) that used $CaCO_3$ mineralized by gastropods to show a relationship between the $\delta^{18}_{CaCO3}$ and the temperature of the fluid, numerous experimental studies have established palaeothermometers valid for different temperatures (e.g. Craig, 1957; Kim & O'Neil, 1997; Zheng, 1999; Hu & Clayton, 2003; Chacko & Deines, 2008; Horita, 2014). For instance, the most widely used equation might be that of Kim and O'Neil (1997):

$$1000 \ln \alpha_{(CaCO_3 - H_2O)} = 18.03(10^{-3} * T^{-1}) - 32.42 \quad (3)$$

where $T$ is the phase transition temperature in kelvin. In other words, the $\delta^{18}$O value of the carbonate phase decreases as the temperature of precipitation increases. Even though the carbonate veins are mostly exclusively filled with calcite in orogenic forelands, it is worth noting that the equivalent relationships were also calibrated for the other carbonates (most used equations are gathered online by Beaudoin and Therrien, 2004).

However, other physical and chemical processes affect the oxygen isotope fractionation in debated ways: the evaporation rate (Dreybrodt & Deininger, 2014) and the fluid composition and precipitation kinetics (Bottinga & Craig, 1968; Rye & Bradbury, 1988, Zeebe, 2007). Most of these secondary factors seem negligible in a tectonic system where calcite precipitates in veins or in faults, yet the direct use of the $\delta^{18}$O value alone as a palaeothermometer is arguable. Indeed, both $\delta^{18}O_{H2O}$ and $\delta^{18}O_{CaCO3}$ of the vein cement are required to access the temperature of precipitation of the cement at the time of deformation. The way around this is to assume the vein cement precipitated from a fluid that derives from the local fluids contained in the host rock. In that case, the value of $\delta^{18}O_{H_2O}$ can be calculated using the measured $\delta^{18}O_{CaCO3}$ in the host rock and a temperature of precipitation $T$ assumed from the reconstruction of the surface temperature at the time the host rock precipitated. The value of $T$ is then used in Eqn (3), the resulting value of 1000 ln α allowing for the calculation of the $\delta^{18}O_{H_2O}$ using Eqn (2).

Assuming that the cement filling the fractures derives from the local fluid (seawater or freshwater) leads to the conjecture that a single fluid is involved in the system. That allowed many authors to explain an isotopic trend commonly observed in the fracture cements (Fig. 5). Indeed, the joint decrease of the $\delta^{18}O_{CaCO3}/\delta^{13}C_{CaCO3}$ values in vein cements related to burial and LPS is a recurring pattern (e.g. de Graaf *et al.* 2019), usually interpreted as a remobilization of local fluid during progressive burial, at increasing temperatures (Fig. 5a (Beaudoin *et al.* 2011), Fig. 5d (de Graaf *et al.* 2019)). Such interpretation needs to be supported by independent temperature constraints. In case a, homogenization temperatures obtained from fluid inclusion microthermometry support the idea that some of the cements characterized by $\delta^{18}O_{CaCO3}$ >−15 ‰ PDB can be explained by cement precipitation from seawater during burial. Yet altogether

**Fig. 5.** Simplified representation of $\delta^{18}O$ vs $\delta^{13}C$ plots obtained in syn-kinematic calcite cements from the fracture network (a, b, d) and in thrust fault zone (c), along with interpretation of the related fluid system. The published interpretations are reported on each graph. (a) The Sheep Mountain Anticline past fluid system (modified after Beaudoin *et al.* 2011). (b) The Puig-Reig Anticline past fluid system (modified after Cruset *et al.* 2016). (c) The Mount Tancia thrust fault zone past fluid system (modified after Curzi *et al.,* 2020). (d) The past fluid system of the Albanide fold-and-thrust belt (modified after de Graaf *et al.* 2019). Note that the coloured frames in (a) locate the extension of plots (b–d). On all plots, the dashed grey frame represents the isotope values of the calcite fraction of the host rock when available. All values are given in ‰ PDB. *T* on plots refers to the measured temperatures of a given population, using an independent paleothermometer ($T_{47}$ for $\Delta^{47}CO_2$, $T_h$ for fluid inclusion homogenization temperatures). LPS stands for layer-parallel shortening.
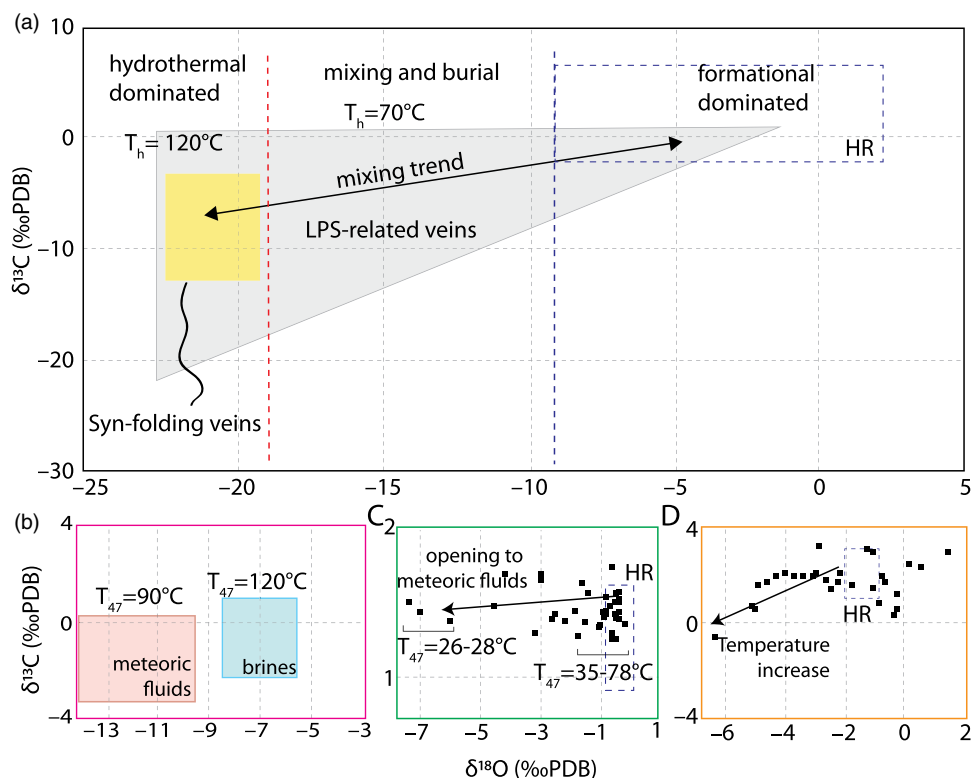
the combination of $T_h$ and $\delta^{18}O_{CaCO3}$ predicted that most of the cement had precipitated from a mixed fluid, highlighting extra-reservoir migrations. Cases b (Cruset *et al.* 2016) and c (Curzi *et al.* 2021) in Fig. 5 considerably challenge this classical 'burial' interpretation. Indeed, independent temperatures of deformation-related cements obtained using clumped isotopes $\Delta^{47}CO_2$ in both cases show that the cements exhibiting a more depleted $\delta^{18}O$ precipitated at a significantly lower temperature (*c.* 30 °C) than the cements exhibiting a less depleted $\delta^{18}O$ value. In that case, the isotopic pattern is interpreted as the precipitation from two different fluids (seawater and meteoric water) with no temperature effect relatable to burial or exhumation. These examples illustrate that an interpretation of a fluid system based solely on the classical $\delta^{18}O$–$\delta^{13}C$ must be treated with care as it is easy to misinterpret the isotopic data. Following this line of argument, it is important not to use just the $\delta^{18}O$–$\delta^{13}C$ of the vein and of the host rock to infer that the fluid is local or external to the reservoir. The isotopic equilibrium between the host rock and the vein cement is usually interpreted as due to rock buffering, i.e. a fluid/rock ratio strongly in favour of the rock, erasing the original fluid isotopic ratio. One needs to consider that with a fluid/rock ratio strongly in favour of the fluid, the isotopic ratio of the surrounding rock can be overprinted. Thus, it is important to couple with other techniques that will investigate the chemical equilibrium between the fluid and the host rock, such as elementary content.

### 4.b.2. Carbon
Carbon stable isotope measurements in carbonate phases deal with the ratio between $^{13}C$ and $^{12}C$, obtained with the same protocol as $\delta^{18}O$, and reported as ‰ PDB (see Eqn (1) for the formula, replacing O isotopes by C isotopes). In carbonates, the carbon is mainly provided by the dissolved carbonate species ($HCO_3^-$, $CO_3^{2-}$) and so the $\delta^{13}C$ values of host rock carbonate are mostly similar to $\delta^{13}C$

values of dissolved inorganic carbon, with other minor control parameters such as kinetics, pH and temperature of precipitation (Bottinga, 1969). Similarly, the $\delta^{13}C$ value of carbonate cement is bounded to the $\delta^{13}C$ value of the parent fluid. The latter can vary significantly, in particular under the influence of organic matter degradation due to bacterial activity (e.g. sulphate reduction or methanogenesis) or thermal degradation (Irwin *et al.* 1977; Curtis, 1987). $\delta^{13}C$ values of carbonates allow diagnosis of the bacterial activity related to oil and gas formation. $\delta^{13}C_{fluid}$ is positive in the case methanogenesis occurred, while $\delta^{13}C_{fluid}$ is negative in case there is an influence of a deeper methane source ($\delta^{13}C_{fluid}$ shows values down to −60 ‰ PDB). In the case there is oil production, the $\delta^{13}C_{fluid}$ values go down as far as −35 ‰ PDB (Peckmann & Thiel, 2004). $\delta^{13}C_{fluid}$ of the inorganic carbon in seawater is *c.* 0 ‰ PDB while it is *c.* −10 ‰ PDB in meteoric water. However, interpreting a $\delta^{13}C$ value in a calcite cement requires consideration of the mixing trends between end-members, $\delta^{13}C$ values of which are often assumed because seldom accessible to measurements. As such, it is impossible to distinguish between (1) a partial mixing between a calcite precipitated from 70 % of pristine marine seawater (0 ‰ PDB) and 30 % of a seawater where organic carbon has been altered (−30 ‰ PDB) (considering the abundances of carbon are identical in both seawaters, the mix would have a value of −9 ‰ PDB) and (2) a calcite precipitated from 100 % pristine meteoric water (−10 ‰ PDB). As for $\delta^{18}O$ values, the interpretation of $\delta^{13}C$ remains ambiguous when the fluid source is unknown (Fig. 5). On top of this, recent experimental work has proven that $\delta^{13}C$ values of carbonates precipitated from the same fluid source, at the same temperature, could present a shift of *c.* 3 ‰, due to the precipitation rate only (Yan *et al.* 2021). This parameter being elusive when studying tectonic structures, such study supports that $\delta^{13}C$ values must be used as a proxy with a great deal of care.

### 4.b.3. $\Delta^{47}CO_2$ palaeothermometry

The clumping of isotopes, i.e. the association of isotopes into specific mass ion groups, so-called isotopologues, has been studied for decades, yet it is only recently that the concept has been developed for unravelling carbonate precipitation temperature conditions. After methodological locks were lifted by Eiler and Schauble (2004), showing it is possible to measure $CO_2$ isotopologues with good accuracy, Ghosh *et al.* (2006) developed a thermometer based on the thermodynamical equilibrium of the doubly substituted isotopologue $^{13}C^{18}O^{16}O$. As defined by the authors, the enrichment of $^{13}C^{18}O^{16}O$ in $CO_2$ measured during acid digestion of $CaCO_3$ relative to stochastic distribution of isotopes among all isotopologues is temperature-dependent. This enrichment, called $\Delta^{47}CO_2$, relies on the fact the heavy isotopes $^{13}C$ and $^{18}O$ will be ordered in a different way (i.e. clumped or separated) according to the temperature. Since the clumping of heavy isotopes within a molecule is a purely stochastic process at high temperature but is systematically over-represented (relative to randomly distributing isotopes among molecules) at low temperature, the 'absolute' temperature of carbonate precipitation can be constrained using clumped-isotope abundances.

The coeval measure of $\Delta^{47}CO_2$ and $\delta^{18}O$ of a carbonate phase further allows reconstruction of both the absolute temperature of precipitation of the calcite and the $\delta^{18}O$ value of the fluid it precipitated from, overcoming the classic limitation of $\delta^{18}O$ measurements to reconstruct the past fluid temperature and origin. A growing community quickly applied this new tool that became a staple when it comes to characterization of diagenetic calcite and dolomite (Huntington *et al.* 2011; MacDonald *et al.* 2018; Mangenot *et al.* 2018), fault cements (Swanson *et al.* 2012; Bergman *et al*, 2013) and vein cements (Pagel *et al.* 2018; MacDonald *et al.* 2019; Beaudoin *et al.* 2020c; Hoareau *et al.*2021a; Labeur *et al.* 2021). Meanwhile, intensive calibration work has been conducted (Affek, 2012; Zaarur *et al.* 2013; Hough *et al.* 2014; Tang *et al.* 2014; Wacker *et al.* 2014; Bonifacie *et al.* 2017; Anderson *et al.* 2021), with notable recent effort to improve the analytical accuracy (Daëron, 2021) and to reduce the persistent discrepancy between measurements performed in the various analytical set-ups (Bernasconi *et al.*, 2018, 2021).

In spite of being widely used by the community, it is important to bear in mind the $\Delta^{47}CO_2$ palaeothermometry is still a recent methodology, that suffers from an incomplete understanding of how diagenesis might affect the chemical record (Chen *et al.* 2019; Hoareau *et al.* 2021a; Nooitgedacht *et al.* 2021). The method is limited indeed to samples that have not been brought to temperature exceeding *c.* 180 °C, at which the solid-state reordering by isotopic diffusion of $^{13}C$ and $^{18}O$ becomes stochastic (Stolper & Eiler, 2015). Solid-state reordering by isotopic diffusion is still active from lower temperature, and must systematically be corrected by thermodynamic modelling if the sample might have reached temperature >100 °C (e.g. Lloyd *et al.* 2018). One efficient way of checking would be to systematically conduct fluid inclusion microthermometry on the same cements, which would have the additional benefit of quantifying the fluid pressure at the time of cement precipitation (e.g. Mangenot *et al.* 2017).

### 4.b.4. Strontium

Strontium has four natural isotopes ($^{84}Sr$, $^{86}Sr$, $^{87}Sr$ and $^{88}Sr$), including one related to radioactive decay ($^{87}Rb$ to $^{87}Sr$). However, as calcite cements are very poor in Rb, the radiogenic isotope ratio for strontium, $^{87}Sr/^{86}Sr$, is very stable in calcite, making it a robust marker for fluid source and migration pathways (Graustein, 1989). Indeed, this ratio is only related to the source fluid radiogenic signature, and to the potential mixing between fluid sources. The evolution of the $^{87}Sr/^{86}Sr$ value of seawater through geological time (McArthur *et al.* 2001) makes the $^{87}Sr/^{86}Sr$ value of mineralization a good way to distinguish whether the fluids are seawater or not, even though there are numerous overlaps in the radiogenic signature of seawater during the geological history. For instance, the typical radiogenic values for the Oligocene seawater (0.7078–0.7082) are significantly different from the values for the Pliocene seawater (0.7091–0.7092) but similar to the values of the early Triassic seawater (0.7078–0.7082). Typical ranges of $^{87}Sr/^{86}Sr$ values vary according to the epoch and age considered, being lower from the Dogger to the early Cretaceous (0.7068–0.7074) than since the Maastrichtian (0.7077–0.7092), for instance. In a stratigraphic sequence that is otherwise well constrained, it is then possible to distinguish a local seawater origin of the fluid from which cement precipitated in the fractures. In orogenic forelands, the mineralizing fluid could have been in frequent contact with K- or Rb-rich rocks such as clays, sandstones or granites, i.e. lithologies with a high radiogenic signature ($^{87}Sr/^{86}Sr$ value > 0.710). Consequently, the $^{87}Sr/^{86}Sr$ value of a calcite cement has been used in numerous past fluid reconstructions, sometimes showing that fluids flowed in contact with radiogenic materials (Travé *et al.* 2000; Beaudoin *et al.* 2011, 2014a), and sometimes preserving a pristine seawater signature in spite of being buried to metamorphic conditions (Dielforder *et al.* 2015, 2022). Even if the $^{87}Sr/^{86}Sr$ ratio does not vary during dissolution and precipitation, the recrystallization of calcite during diagenesis can release Sr in the fluid, altering its $^{87}Sr/^{86}Sr$ ratio (Dielforder *et al.* 2022). Another example of misleading Sr radiogenic measurement has been documented in the vicinity of diapirs (Pichat *et al.* 2018), where the present-day seawater yields the radiogenic signature of the underlying evaporites. To reduce the risk of misinterpretation, a good understanding of the structural geology and a robust petrographic analysis to check that the calcite cement did not undergo recrystallization are mandatory. Also, the radiogenic value obtained can be due to mixing between different sources. Then, it is necessary to know the radiogenic value of each of the potential radiogenic rocks, i.e. the clays, evaporites, basement rocks, marine sediment, detrital-rich sandstone etc. This requires access to most of the sedimentary sequence, a condition that might not be fulfilled in a given study area.

### 4.b.5. Geochronology

The absolute dating of deformation by geochronology – a set of techniques that rely on the radioactive disintegration of parent isotopes in given parent–daughter isotope pairs – is long established, and there are a number of systems allowing the dating ofcarbonate cements related to tectonic activity. Some of these have restricted applicability, like Sm–Nd geochronology, which can be applied in contexts where mineralizing fluids are rich in REE. Such contexts include calcite veins associated to gold deposits (Xu *et al.* 2015), to basement-derived fluids (Barker *et al.* 2009; Gao *et al.* 2020) and to coal-bearing veins (Tonguç Uysal *et al.* 2007). U-series (also called U–Th) and U–Pb geochronology are increasingly popular in the field of tectonics thanks to their wider applicability to the calcite cements. Classically, the concentration in $^{230}Th$, $^{232}Th$, $^{234}U$ and $^{238}U$ for the U-series geochronology and in $^{235}U$, $^{238}U$, $^{207}Pb$,

$^{206}$Pb and $^{204}$Pb for U–Pb geochronology is obtained by isotope dilution followed by thermal ionization mass spectrometry (TIMS) or inductively coupled plasma – mass spectrometry (ICP-MS), a technique that has a high precision and accuracy but is time-consuming and expensive (Brannon *et al.* 1996; Rasbury & Cole, 2009), even though recent development makes it faster (Engel *et al.* 2020). The recent reduction of the concentration threshold for the detection of trace elements using laser ablation coupled to ICP-MS (LA-ICP-MS) has enabled a democratization of LA-ICP-MS geochronology, that paved the way to obtaining the U–Pb absolute age of syn-kinematic calcite cements in veins (see Roberts *et al.*, 2020, for a review) and faults (see Roberts & Holdsworth, 2022, for a review), with further developments of U–Pb dating of dolomite phases (Bar *et al.* 2021; Motte *et al.* 2021; Su *et al.* 2022). In contrast, the very low $^{230}$Th concentration in carbonates severely hampers the applicability of LA-ICP-MS to U-series geochronology (e.g. Lin *et al.* 2017), which is moreover restricted to ages younger than 500 to 600 kyr (Villemant & Feuillet, 2003; Andersen *et al.* 2008), thereby restricting the application to recent tectonic events. Alternatively, U–Pb does not suffer that limit and allows dating of cements as old as $10^8$ years. The growing size of the community using U–Pb geochronology leads to a variety of data treatment that permits either treating the cement as a bulk or providing a mapping of U–Pb ratio in microstructures (Drost *et al.* 2018; Hoareau *et al.* 2021b), and also an interest in expanding the limits of LA-ICP-MS detection (Kylander-Clark, 2020). Beyond being fast and relatively cheap, the LA-ICP-MS U–Pb geochronology has been successfully compared to other geochronometers (Mottram *et al.* 2020) like K–Ar, a system that has long been used in tectonics, especially through the dating of neoformed illite in fault gouges by K–Ar or Ar–Ar geochronology (Lyons & Snellenburg, 1971; van der Pluijm *et al.* 2001, 2006; Zwingmann *et al.* 2004; Haines & van der Pluijm, 2008; Clauer, 2013; Viola *et al.* 2013; Hnat & van der Pluijm, 2014; Scheiber *et al.* 2019).

However, it is important to underline that calcite does commonly incorporate more Pb than U, making it difficult to date in numerous cases (Mottram *et al.* 2020). Also, the role of diagenesis on the incorporation of U and Pb in carbonate minerals remains debated (Roberts *et al.* 2020). The potential Pb redistribution by solid-state diffusion related to crystal-scale deformation has been observed in other minerals (rutile) and causes variation of the obtained age at the mineral scale (Moore *et al.* 2020). Thus, the diagenetic state of the calcite vein cement has to be systematically studied, along with its elementary content, in order to properly perform the analysis. Another important point is that the ages obtained from vein cements might not be straightforwardly interpreted as representative of the entire duration of the deformation event that developed the veins, so a certain number of data might be required to cover the entire timespan during which a deformation phase affected the rock (Beaudoin *et al.* 2018). In faults, the age of a cement can be younger than the fault activity because of a subsequent fluid flow (Roberts *et al.* 2021; Roberts & Holdsworth, 2022). To check whether the U–Pb age legitimately represents the age of precipitation, a recent approach couples the $\Delta^{47}$CO$_2$ palaeothermometry to U–Pb geochronology to check whether the vein cement precipitated at thermal equilibrium with the host or not (Pagel *et al.* 2018; Hoareau *et al.* 2021a; Muñoz-López *et al.* 2022). In the Spanish Pyrenean foreland, Hoareau *et al.* (2021a) used this combination to validate that the cements precipitated during the last uplift phase and were not subject to any later burial, preserving their original $\Delta^{47}$CO$_2$ values.

## 4.c. Developing isotope-based techniques

Being the main constitutive element of carbonates, calcium has five stable isotopes, two ratios being used to reconstruct carbonate diagenesis: the $\delta^{44/40}$Ca and $\delta^{44/42}$Ca, the former being the most used and reported as $\delta^{44}$Ca (Swart, 2015). As the $\delta^{44}$Ca varies according to the fluid source, it is mainly used to characterize the source of calcium during events such as evaporation, weathering or dolomitization (e.g. Fantle & Higgins, 2014; Tostevin *et al.* 2019). The fractionation of $\delta^{44}$Ca between the fluid and a given mineral is related to temperature (Gussone *et al.* 2020) and precipitation rate (Tang *et al.* 2008). The few studies that rely upon application of $\delta^{44}$Ca to calcite cement in tectonic structures discussed the interaction between the fluid and the basement, or the origin of dolomitization (Husson *et al.* 2015).

Numerous secondary minerals can be found associated to carbonates, enabling the study of isotopes that can help unravel the past fluid system. Hydrogen isotopic ratio ($\delta^2$H or $\delta$D) is classically used along with $\delta^{18}$O values, both measured in the clay fractions in deformation features to access the fluid source. In fact, a restricted range of $\delta^2$H values and associated $\delta^{18}$O values of H$_2$O corresponds to meteoric waters (Craig, 1961; Sheppard, 1986). This approach has been used in several case studies where $\delta^2$H–$\delta^{18}$O values of clay fractions in fault gouges determine the ingress within major faults to either meteoric or deep-sourced fluids (e.g. Haines *et al.* 2016; Lynch & van der Pluijm, 2017; Lynch *et al.* 2019, 2021). $^7$Li/$^6$Li isotopic ratio ($\delta^7$Li) may prove valuable in the reconstruction of the past fluid system. While relatively recent, the fractionation of Li is related to the degree of weathering of the Li-rich igneous rocks. $\delta^7$Li is proven to be a good proxy for weathering intensity (Dellinger *et al.* 2015), and while it has been applied in modern rivers to date, future research could include a possible use on clay fractions to decipher the potential fluid migration pathway through the basement in orogenic forelands.

Ballentine and Burnard (2002) proposed that noble gases transported in fluids can be used to assess fluid origin and transportation process. Among these, the radiogenic isotope ratio for helium, $^3$He/$^4$He, is considered as the most efficient tracer of a deep source of fluid, either crustal or mantellic (e.g. Pik & Marty, 2009) and has been applied to syntectonic calcite veins (Smeraglia *et al.* 2018, 2021) to test whether the fault zone was a drain for deep-seated mantle-derived fluids. As gas will be accessed using crushing techniques (e.g. Blamey, 2012), a very rigorous petrographic study of fluid inclusions and their relation to diagenesis must be done beforehand. Recent efforts based on carbonate-bearing hydrocarbon seep-related deposits in the Cantabrian Basque Basin suggest that the use of neodynium isotopes in carbonates, $\epsilon_{Nd}$, is also a promising proxy to assess the volcanic origin of the fluids (Jakubowicz *et al.* 2022).

## 4.d. Elemental geochemistry

Elemental geochemistry relies upon studying the elemental composition of the mineral phases (here, calcite) by means of either bulk dissolution or electron probe microanalysis on sections (e.g. Centrella *et al.* 2018). The concentrations of several trace elements in calcite (Mn, Fe, Sr ...) can be interpreted in terms of fluid characteristics such as redox conditions at the time of precipitation (e.g. Curtis *et al.* 1986), or their origin (meteoric vs marine; e.g. Travé *et al.* 2007). In the published studies that use elemental geochemistry, the concentration of an element of the fluid is commonly calculated using a partition coefficient (Kd) (Parekh *et al.* 1977) and the measured concentration of this element in the cement. The Kd is

considered over a range of temperatures, and the concentration in the element of the fluid is compared to the expected concentration in each fluid source (meteoric, marine, deep-sourced, brine; e.g. Travé *et al.* 1997; Lacroix *et al.*, 2014). By doing so, researchers can derive the origin of the fluid, for example using one or all of Mg/Ca, Sr/Ca, Mn/Ca, Ca/Fe ratios. This approach remains arguable, because a number of assumptions have to be made. First, the precipitation of the crystal at chemical equilibrium with the fluid is of prime importance here, and such an assumption might be discussed (Paquette & Reeder, 1995). Second, the range of Kd used to calculate the past fluid elemental concentration comes from a specific experimental dataset where the fluid chemistry is by definition different from the precipitation fluid in the geological system, yet the Kd depends strongly on the fluid chemistry. In other words, an implicit assumption is made that for a given fluid origin (meteoric, basinal, marine) the chemistry is the same regardless of the context and remains constant in space and time. Nonetheless, elemental geochemistry has been applied in combination with other proxies to characterize the nature of the fluid. For instance the study of Travé *et al.* (2000) documents an alternation between flows of formation water and meteoric water along the major thrust zone of the El Guix anticline in the southern Pyrenees.

Rare earth elements (REE) are also used to reconstruct the fluid origin by means of a spider diagram, a diagram reporting normalized (to chondrite) REE concentrations from the lightest (La) to the heaviest (Lu). The pattern of the diagram might be diagnostic of the fluid source (Motte *et al.* 2021), as a negative anomaly in caesium is typical of seawater (Shields & Webb, 2004), and a positive anomaly in europium supports deep-sourced fluids (Bau & Möller, 1993). REE patterns have been successfully used to highlight (1) the migration of hydrothermal, potentially deep-sourced, fluids in the Abu Dhabi area (Morad *et al.* 2010); (2) large-scale fluid flow through crack-seal veins in the Eastern Belt of the Lachlan orogen (Australia) (Barker *et al.* 2006); (3) the link between travertine veins and hot fluid pulses in Turkey (Uysal *et al.* 2009); or (4) the seawater origin of the cement filling tectonic veins related to the Shizhu synclinorium (China) (Wang *et al.* 2017). However, it is important to consider that this approach relies on the debated assumption that the precipitation occurs at equilibrium with the fluid, and with no specific different distribution effect from one REE to another.

Other elemental analyses of interest can be obtained from the crushing of fluid inclusions, which grants access to the molecular ratios of the analysed gas, such as $N_2/Ar$, $Ar/He$ or $CO_2$–$SH_4$–$H_2$, and can help constrain if the fluid is derived from a meteoric source, a basinal source or its redox condition, respectively. Where conditions of concentration and preservation are met, a geothermometer can be derived from gas content, the most used one being the $CO_2/CH_4$ – H concentrations (D'Amore & Panichi, 1980; Henley *et al.* 1984; Giggenbach, 1996).

## 5. Reconstruction of the past fluid system at the local (fold/thrust) scale: case studies

### 5.a. Brief review of past fluid system studies over the past decade

At the scale of individual contractional structures like folds, numerous studies focused on the reconstruction of the past fluid system and its evolution during the deformation stages (LPS, fold growth, LSFT; see Section 2) of the so-called folding event (Lacombe *et al.* 2021). In these studies, effort was made to characterize the origin of the fluids and to picture the plumbing system.

Mozafari *et al.* (2015, 2017) used $\delta^{18}O$, $\delta^{13}C$, $^{87}Sr/^{86}Sr$ data along with fluid inclusion microthermometry and chemistry by Raman spectroscopy to show that in the Jabal Qusaybah anticline (Oman Mountains), fluids were rather local during LPS and evolved towards brines that interacted with siliciclastic strata during fold growth. Still in the Oman Mountains, Arndt *et al.* (2014) reconstructed a 50 m vertical fluid migration along the Jebel Shams fault zone using stable isotope geochemistry. In the southern Pyrenean foreland, fracture cements of the Puig Reig anticline, formed above a cover duplex, were studied by means of $\delta^{18}O$, $\delta^{13}C$, $\Delta^{47}CO_2$, $^{87}Sr/^{86}Sr$ data, fluid inclusion microthermometry along with elemental geochemistry of carbonate and fluid inclusions. Results revealed a lateral, reservoir-bounded forelandward fluid migration of hydrothermal brines along the thrust during LPS (Cruset *et al.* 2016). However, the cements within the curvature-related fractures precipitated from a mixture between downward-flowing meteoric fluids and upward-flowing brines (Cruset *et al.* 2016), suggesting a vertical fluid flow, hence the opening of the fluid system during folding. Still in the southern Pyrenean foreland, the fluid system within the Bóixols – Sant Corneli anticline was studied by means of $\delta^{18}O$, $\delta^{13}C$, $\Delta^{47}CO_2$, $^{87}Sr/^{86}Sr$ and elementary composition of the carbonate. Interpretations draw a fluid system first closed, then gradually opened to meteoric fluids flowing downwards, the décollement level being interpreted as an efficient barrier to deep-sourced fluids (Nardini *et al.* 2019; Muñoz-López *et al.* 2022). In the Montagna dei Fiori, an anticline from the Umbria Marche Apennine Ridge, Mozafari *et al.* (2019) used $\delta^{18}O$, $\delta^{13}C$, $^{87}Sr/^{86}Sr$ data along with fluid inclusion microthermometry to reconstruct two pulses of hydrothermal fluids sourced by evaporitic brines, one related to the pre-contractional history, i.e. the Jurassic rifting, and a second one related to the onset of the growth of the anticline. In the Cingoli anticline (Apennines, Italy), a fault-bend fold linked to a thrust the rooting depth of which is debated (Triassic evaporites vs basement), Labeur *et al.* (2021) showed, using $\delta^{18}O$, $\delta^{13}C$, $\Delta^{47}CO_2$ data, that the reservoir remained a compartmentalized system where syn-kinematic vein cements precipitated from thermally equilibrated evolved formational fluids during the whole fold development. In the Jura Mountains, the geochemistry ($\delta^{18}O$, $\delta^{13}C$, $\Delta^{47}CO_2$, $^{87}Sr/^{86}Sr$) of cements in fault zones and veins within folded strata above the internal Jura frontal thrust depicted a progressive opening of the reservoir to surficial meteoric fluids cooler than the environment (Smeraglia *et al.* 2020a). In the Bornes Massif (Subalpine belts), the reconstruction of the past fluid system associated to the development of the Parmelan anticline was based on $\delta^{18}O$, $\delta^{13}C$, $\Delta^{47}CO_2$, $^{87}Sr/^{86}Sr$ data, fluid inclusion microthermometry along with elemental geochemistry of carbonate. The fluid system was stratigraphically compartmentalized with hot meteoric fluids flowing laterally in the sedimentary cover during LPS and folding, then opened to meteoric fluids during the late stages of folding and during post-folding deformation development (Berio *et al.*, 2022). In the Vercors chain in southeastern France, Bilau *et al.* (2022) used U–Pb geochronology along with $\delta^{18}O$, $\delta^{13}C$ and $\Delta^{47}CO_2$ on syntectonic calcite veins and thrusts cements to picture a past fluid system dominated by heated brines.

### 5.b. General evolutionary trend of the past fluid system at the scale of the fold during the folding event

These recent studies support the conclusions presented in the review work conducted a decade ago by Evans and Fischer (2012). In many cases, the hydraulic structure of a folded reservoir
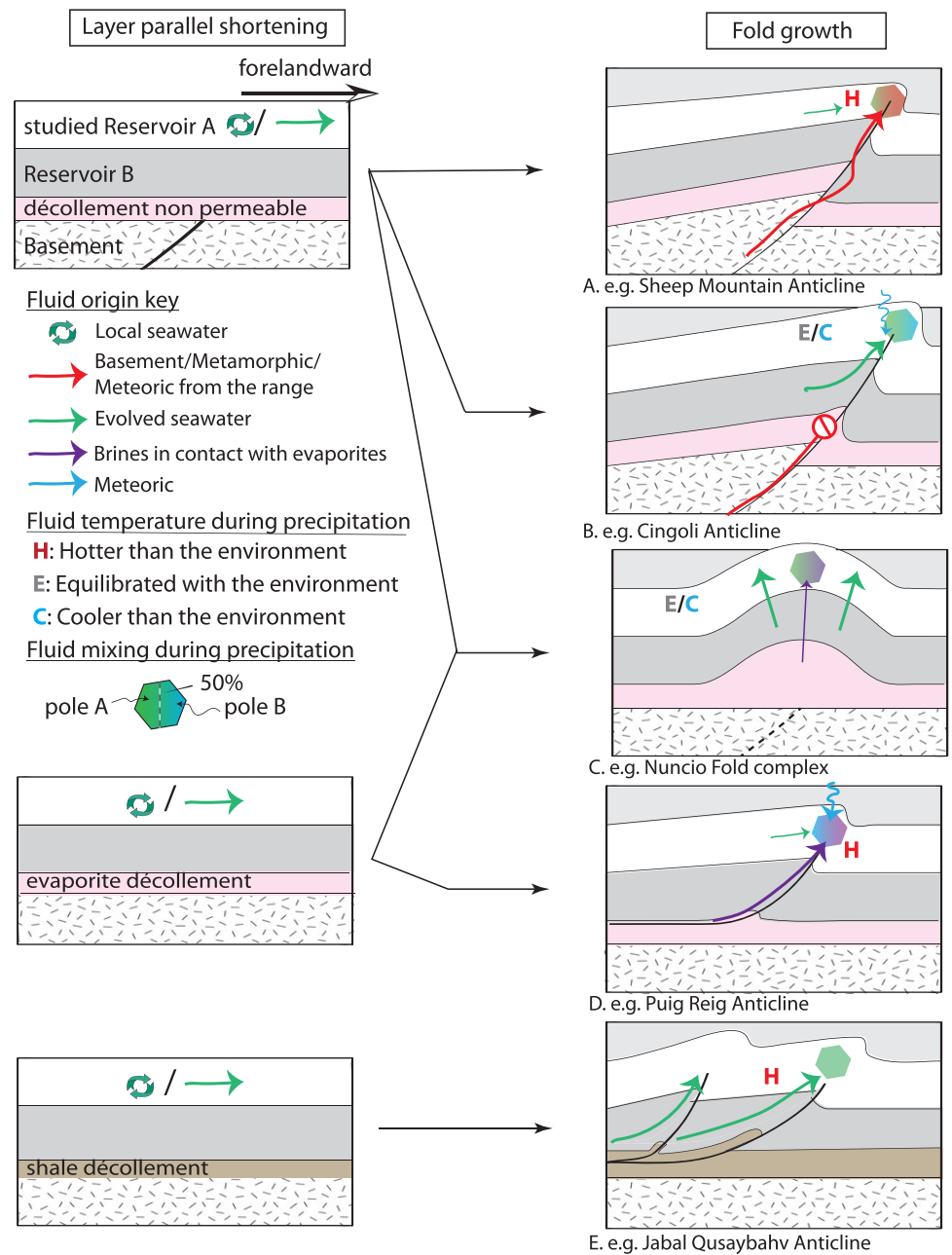
**Fig. 6.** Representation of the first-order evolution of the past fluid system at the scale of the individual fold or/and thrust. From an initial state related to layer-parallel shortening (left-hand side), the fluid system evolved according to the fault distribution/the décollement nature, and to the structural style of the structure. The resulting fluid from which cement precipitates is symbolized by a hexagon whose colour is related to the nature of the fluid, several colours representing a mixing with no implication on the ratio. Fluid temperature with respect to the local temperature is symbolized by C when cooler, H when hotter and E when at equilibrium.

evolves in a similar way from LPS to folding regardless of the tectonic settings, yet the nature of the fluids involved varies according to the structure (Fig. 6). During LPS, cements generally precipitated from formational fluid, suggesting a limited inter-reservoir connectivity. The fluid system can be considered either as closed if the fluid is formational with limited migration or as open if the formational fluid flowed laterally in the reservoir which remains stratigraphically compartmentalized (Fig. 4). In contrast, during fold growth, a switch occurs in the chemical signature of the cements and of the related fluids, with a notable input of either meteoric-derived fluids, saline brines or basement-derived fluids flowing upwards or downwards, according to the occurrence of an efficient conduit underneath the folded reservoir, in most cases a fault, but also the outer arc-related joints (e.g. Lefticariu *et al.* 2005; Beaudoin *et al.* 2014a). Such

fluid input proceeded to homogenize the fluid system at the reservoir scale, with various degrees of homogenization going from a mixing to a total overprint. Considering that the time required for thermal equilibration between the fluid and the rock is instantaneous at the geological timescale (e.g. Heinze *et al.* 2017), the fact a cement can precipitate at a temperature higher (or lower) than that of the surrounding host rock requires that the fluid did not thermally equilibrate before cement precipitated. That suggests (1) high flow and high precipitation rates together with limited exchanges with the host rock or (2) a very fast crystal growth, in line with the rate of few micrometres per second obtained in experimental set-ups (Lee & Morse, 1999; Hilgers & Urai, 2002a, b; Hilgers *et al.* 2004). Sometimes, however, the fluid system remains closed through the entire folding event (e.g. Labeur *et al.* 2021).

## 6. How geochemistry helps reconstruct the origin and large-scale migrations of fluids in forelands: insights from selected case studies

Most studies of past fluid systems were actually carried out at the scale of the foreland. Indeed, a past fluid flow obviously is not limited to individual structures like a fold or a thrust, and larger-scale processes are usually involved when it comes to fluid migration. For instance, the large-scale pressure and topographic gradients required for the migration of extra-reservoir fluids that distribute hydrocarbons and ore deposits like Pb–Zn Mississippian Valley-type (MVT) cannot be explained at the scale of the individual fold or thrust (Cathles, 1981; Roure *et al.* 2005). Hereinafter, we review how geochemical proxies helped to reconstruct the past fluid system which prevailed at the regional scale during the development of an orogenic foreland. To do that, we selected well-documented case studies: (1) the thin-skinned Canadian Rocky Mountains (Fig. 7) which extend southwards in the USA as the Rockies–Sevier belt (Fig. 8); (2) the thick-skinned Laramide province (USA; Fig. 8). Because the previous orogenic domains represent end-members in terms of tectonic style of deformation, hybrid cases where thin-skinned and thick-skinned deformations are superimposed are also considered; (3) the south Pyrenean FTB (Spain; Fig. 9), where the basement is also involved in shortening at depth under the internal Sierras; and (4) the Umbria–Marche Apennine Ridge in the central Apennines (Italy; Fig. 10), where the degree of basement involvement in shortening and its impact on the cover-scale deformation is debated.

### 6.a. The Canadian Rocky Mountains

One of the most iconic reconstructions of the past fluid system in a FTB might well be the one conducted in the Canadian Rockies and the Western Canada Sedimentary Basin (WCSB). The Canadian Rockies developed from the Upper Jurassic (155 Ma; DeCelles, 2004) as an effect of the subduction of the Farallon plate under the North America plate, leading to a thin-skinned belt referred to as the Sevier belt, going from Canada to Mexico (Fitz-Diaz *et al.* 2011*b*). In the Canadian Rockies and the WCSB, the contractional deformation has been accommodated in the sedimentary cover mainly through detachment folding to the north and thrust-related folding to the south, forming a belt up to 200 km wide. It is a paragon of an orogenic wedge where thrusts developed in a cratonward sequence (Paña & van der Pluijm, 2015) above a viscous décollement (Fig. 7). The large amounts of hydrothermal dolomite in Devonian carbonates, associated to important MVT ore deposits, are striking remnants of the fluid flows that have been characterized thanks to numerous studies (Mountjoy *et al.* 1992; Ge & Garven, 1994; Hairuo Qing & Mountjoy, 1994; Nesbitt & Muehlenbachs, 1995; Machel & Cavell, 1999; Al-Aasm *et al.* 2002; Vandeginste *et al.* 2012). The sum of the work done – mainly based on O, C and Sr isotopic analyses, so quite ambiguous; see Section 4 – depicted a debated past fluid flow during the contraction. In a first view, large-scale flow of basinal brines, pushed forelandwards through a squeegee-type flow due to the belt development and propagation, would explain the extensive dolomitization together with ore deposition (Bradbury & Woodwell,
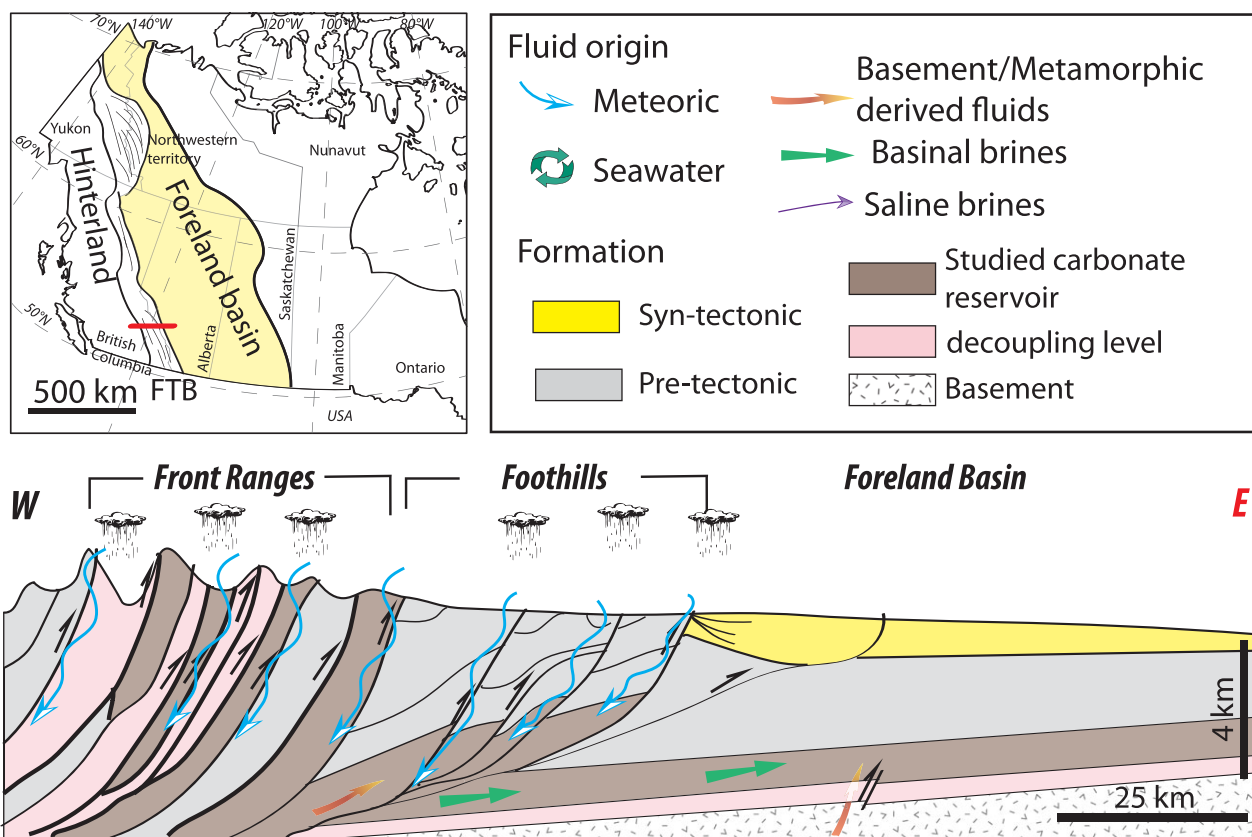


**Fig. 7.** Simplified cross-section and corresponding location of the Canadian Rocky Mountains fold-and-thrust belt where the past fluid system was reconstructed. The vertical exaggeration is *c.* 7:1. FTB stands for fold-and-thrust belt. The legend is transferable to the other cross-sections of Figures 8–10. In the present case, the decoupling level comprises argillites (Proterozoic). See text for details and references.

1987; Qing & Mountjoy, 1992; Ge & Garven, 1994; Al-Aasm *et al.* 2000). In an alternative view, the fluid migrations have been limited to inter-reservoir migrations, with local and transient hot-flash-type flow of basement-derived hydrothermal fluids during thrust activity (Nesbitt & Muehlenbachs, 1995; Machel & Cavell, 1999; Kirschner & Kennedy, 2001; Cooley *et al.* 2011; Vandeginste *et al.* 2012). Building on the geometry of the belt, numerical simulations of fluid flow predict that this lateral fluid migration in the reservoir occurred in response to thrusting at a speed of *c.* 2 km Myr$^{-1}$ ( Schneider, 2003). The difference between the two past fluid system models lies in the interpretation of high $^{87}$Sr/$^{86}$Sr values (>0.7120): while Qing and Mountjoy (1992) interpreted these in combination with elementary content as a marker of fluid migrations in contact with the basement rocks, Vandeginste *et al.* (2012) instead interpreted them in combination with δ$^{18}$O values as a witness of the contamination of the fluid by K-rich sedimentary strata. To support their revision of the former interpretation of the past fluid system, Vandeginste *et al.* (2012) invoke the impact of a complex diagenetic history, that may have altered fracture cements, enriching the original $^{87}$Sr/$^{86}$Sr content of the fluid. In their interpretation, Vandeginste *et al.* (2012) proposed that the notable input of meteoric fluid in the system was related to the post-orogenic evolution. By analysing clays in fault zones, Lynch *et al.* (2021) validated that the faults were efficient pathways to surficial, meteoric fluids, that were dominating (up to 90 %) the system compared to the existing but limited volume of metamorphic fluids.

### 6.b. The Laramide province (USA)

The Laramide province in the USA is an eastward continuation of the Sevier belt that extends from the southern part of Montana to the southern part of New Mexico (N–S) and from Arizona to South Dakota (W–E). From the end of Cretaceous times, a change in the mantle dynamic affected the subducting slab and led to a coupling between the slab and the lower crust (English *et al.* 2003; Yonkee & Weil, 2015), changing the direction of the shortening (Craddock & van der Pluijm, 1999) and reactivating inherited Precambrian structures (Marshak *et al.* 2000). The result of this history is a typical broken foreland, the Laramide province (Stone, 1967; Erslev, 1986; Marshak *et al.* 2000), where endorheic basins are separated by basement highs over a distance of 400 km (Fig. 8). Part of this broken foreland, the Bighorn Basin (Wyoming, USA), has been extensively studied for its fracture network and associated past fluid system. This Palaeocene–Eocene basin of *c.* 50 km width hosts basement-cored folds for which fracture patterns and related stress history have been extensively discussed (Craddock & van der Pluijm, 1989, 1999; Craddock & Relle, 2003; Bellahsen *et al.* 2006*a, b*; Neely & Erslev, 2009; Amrouch *et al.* 2010*a, b*, 2011; Beaudoin *et al.* 2011, 2012, 2014*b*, 2018, 2019*a*, 2020*a*; Thacker & Karlstrom, 2019). In the basin, the mesostructures developed during a deformation history that comprises three main stages: (1) pre-folding LPS fractures formed in response to the far-field stress transfer from the distant thin-skinned Sevier belt; (2) early folding LPS fractures formed as a result of Laramide contraction; (3) local extensional fractures striking parallel to fold axes and related to outer-arc extension due to strata curvature at fold hinges during Laramide fold growth. Studying the past fluid system associated to the fracture network enables one to reconstruct the evolution of the fluid sources, conditions of precipitation and migration pathways during the tectonic evolution, from being in the Sevier flexed foreland to becoming part of the Laramide broken foreland. Such reconstructions were based on O, C isotopic geochemistry, $^{87}$Sr/$^{86}$Sr ratios and fluid inclusion microthermometry on calcite cements of veins (Beaudoin *et al.* 2011, 2012, 2014*a*; Barbier *et al.* 2012*a*, 2012*b*, 2015) and more recently on U–Pb absolute dating (Beaudoin *et al.* 2018, 2019*a*).
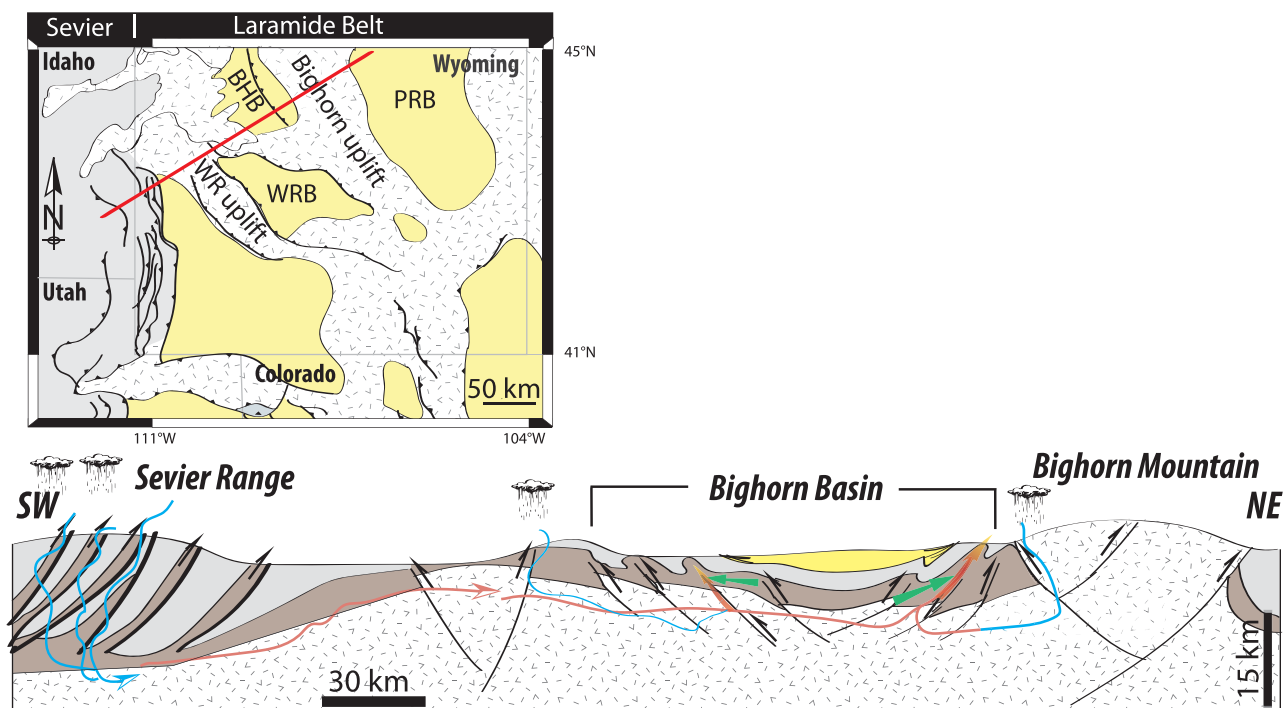


**Fig. 8.** Simplified cross-section and corresponding location of the Sevier range and Laramide province (USA) where the past fluid system was reconstructed. On the location map, the yellow colour indicates the intracratonic basins related to the exhumation of basement arches. The vertical exaggeration is about 2:1. WRB: Wind-River Basin; BHB: Bighorn Basin; PRB: Powder River Basin. See text for details and references. Key is given in Figure 7.

Combination of δ¹⁸O values with $T_h$ from fluid inclusions revealed that the fluids involved in the Ordovician–Permian reservoir during the Laramide deformation were a mixture of Palaeogene meteoric fluids and Palaeozoic seawater (Beaudoin *et al.* 2011; Barbier *et al.* 2012*b*). High ⁸⁷Sr/⁸⁶Sr signatures (>0.710) and high Th (>120 °C) suggested that the meteoric fluids first flowed into / in contact with the basement (Beaudoin *et al.* 2014*a*). This constrains the potential migration pathways, with a recharge zone of meteoric fluids in the highly elevated Sevier range to the west (Beaudoin *et al.* 2014*a*) and to the southwest (Barbier *et al.* 2012*b*). From there, a (north)eastward migration across the basin is suggested by the eastward decrease of the radiogenic values of the vein cements during the basin-scale LPS (Beaudoin *et al.* 2014*a*). At the time of folding, the radiogenic and heated fluids were expelled as pulses along the inherited basement faults reactivated as high-angle thrusts and flowed upwards into the sedimentary cover through the vertically persistent fractures related to outer-arc extension at fold hinges, overprinting the former, stratigraphically compartmentalized local fluid system. Pulses of hydrothermal, meteoric-derived fluids flowing upwards from the basement–cover interface also occurred earlier and later in the tectonic history of the basin, during the forebulge development related to the Sevier orogeny and during the post-orogenic (post-Laramide) extension (Beaudoin *et al.* 2014*a*). This evolution suggests a recharge mechanism for downward migration of meteoric fluids in the inner belt and an eastward squeegee-type flow (see Section 2.b) enhanced by an early basin-scale topographic gradient due to the early exhumation of the Bighorn Mountains easternmost basement arch (Fig. 8). This scenario of a large-scale eastward fluid migration was also supported by the reconstruction of the evolution of past fluid pressure at the basin scale using calcite twinning palaeopiezometry, fracture analysis and rock mechanics (Amrouch *et al.* 2011, Beaudoin *et al.* 2014*b*). The asymmetrical

evolution of the past fluid pressure during contraction, decreasing in the west as it increased in the east, suggested a lateral continuity of the Ordovician–Permian reservoir during the LPS, with a pressure gradient favouring an eastward fluid migration On the basis of the estimated age of the fracturing events (see Beaudoin *et al.* 2014*a*) the rate of the past fluid flow from the recharge area to the deformation site during LPS was estimated to be *c.* 8 km Myr⁻¹.

### 6.c. The south Pyrenean FTB (Spain)

The south Pyrenean FTB is a wide south-verging FTB formed at the expense of extensional basins developed during Aptian to Cenomanian times (Sibuet *et al.* 2004) and inverted during Late Cretaceous times during the Pyrenean orogeny, itself related to the convergence between the Iberian plate and the European plate (Choukroune, 1992). In the south Pyrenean FTB, the deformation is mainly distributed in the sedimentary cover along south-verging thrusts developed in a piggyback sequence and soling in the Triassic and Eocene evaporite décollement levels (Fig. 9). In the southernmost part of the Axial Zone, thrusts such as the Bielsa thrust or the Gavarnie thrust involve the basement (Fig. 9). The wealth of studies aiming at understanding the local or regional past fluid system makes this belt one of the most studied in the world (McCaig, 1988; Henderson & McCaig, 1996; Travé *et al.* 1997, 2000, 2007; McCaig *et al.* 2000; Caja *et al.* 2006; Lacroix *et al.* 2011, 2013, 2014, 2018; Beaudoin *et al.* 2015; Cruset *et al.* 2016, 2018, 2021; Crognier *et al.* 2018; Nardini *et al.* 2019; Hoareau *et al.* 2021*a*; Muñoz-López *et al.* 2022). Recent syntheses (Lacroix *et al.* 2011; Cruset *et al.* 2018; Crognier *et al.* 2018) on the past fluid system during the evolution of the FTB agreed on the general scenario (Fig. 9) involving a fluid system dominated by formational seawater where metamorphic fluids flowed from
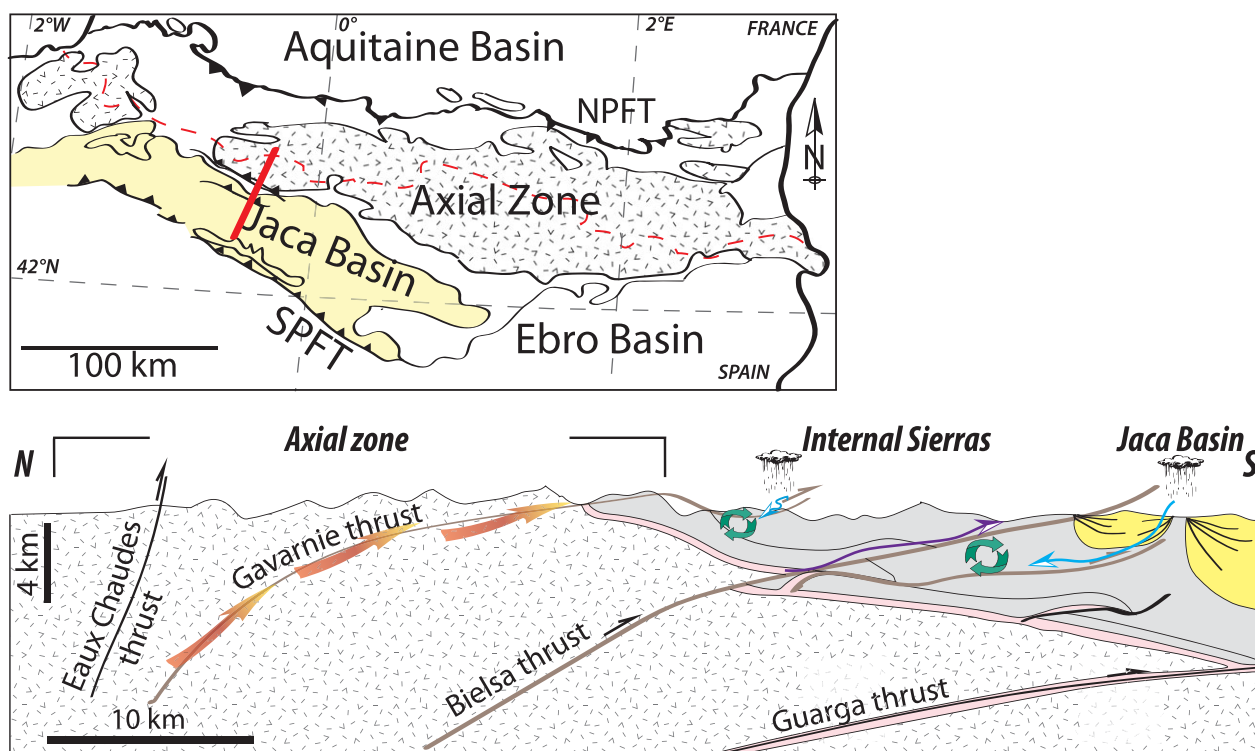


**Fig. 9.** Simplified cross-section and corresponding location of the southern Pyrenean FTB (Spain), where the past fluid system was reconstructed along the thrusts. The vertical exaggeration is *c.* 3:1. See text for details and references. Key is given in Figure 7. The nature of the décollement is evaporites (Triassic).

the Axial Zone along the basement-rooted thrusts and mixed to trigger cement precipitation in fault zones. A gradual opening of the system to meteoric fluids is also characterized during the late stage of thrust activity (e.g. Nardini *et al.* 2019; Cruset *et al.* 2021; Hoareau *et al.* 2021*a*; Muñoz-López *et al.* 2022) and, at fold scale, in fold-growth-related fractures (Beaudoin *et al.* 2015). The implication of extra-reservoir fluids has been proposed on the basis of the difference between $\delta^{18}O$ from cements in fault zones and $\delta^{18}O$ from local host rocks (Lacroix *et al.* 2014). Indeed, the vein – host-rock difference in $\delta^{18}O$ is much higher (10 ‰) in cements precipitated from metamorphic fluids than in cements precipitated from formational or meteoric fluids (1 ‰ and 4 ‰, respectively). Interestingly, the nature of the past fluids that migrated along the thrusts varies in space. For instance, the Gavarnie thrust enabled metamorphic fluids from the Axial Zone to flow into the foreland (Lacroix *et al.* 2011), while others such as the Bielsa thrust or the Boixols thrust do not host any geochemical imprint of deep-sourced fluids (e.g. Nardini *et al.* 2019). This difference in the nature of the fluid that flowed along the thrusts has been interpreted by Lacroix *et al.* (2014, 2018) as resulting from the location and timing of thrust activation: either the metamorphic fluids could not be efficiently transmitted by the thrusts that progressively formed at increasing distance from the feeding Axial Zone, and/or the sequence of basement thrusting did not coincide with the metasomatism releasing the metamorphic fluids.

### 6.d. The Umbria Marche Apennine Ridge (Italy)

The Apennines developed from the end of the Cretaceous to the Early Pleistocene in response to the convergence between the African and European plates. The resulting contractional deformation migrated eastwards following the retreat of the subducting Adriatic Plate under the European Plate since the Neogene (Elter *et al.* 2008). Post-orogenic extension affected the western part of the belt first, before propagating eastward, being active nowadays in the Umbria and Abruzzi areas. The recent/modern fluid system in relation to the active extensional tectonics in the westernmost part of the belt has been extensively studied by characterizing either fluid emanating from, or recent cementation within, active normal fault zones (Ghisetti & Vezzani, 2000; Minissale *et al.* 2000; Cello *et al.* 2001; Capozzi & Picotti, 2002; Agosta & Kirschner, 2003; Accaino *et al.* 2007; Smeraglia *et al.* 2018, 2021; Lucca *et al.* 2019; Curzi *et al.* 2020; Coppola *et al.* 2021; Vignaroli *et al.* 2022). The past fluid system associated with the development of the Apennine FTB and foreland basins has also

received attention (Ghisetti *et al.* 2001; Vannucchi *et al.* 2010; Gabellone *et al.* 2013; Beaudoin *et al.* 2020*c*; Curzi *et al.* 2020; Smeraglia *et al.* 2020*b*; Labeur *et al.* 2021). Namely, the Umbria Marche Apennine Ridge (central–northern Apennines; Fig. 10) was studied by Ghisetti *et al.* (2001) and Beaudoin *et al.* (2020*c*) along W–E transects. Ghisetti *et al.* (2001) reported stable isotopic values of calcite cements associated to thrusts along a WSW–ENE transect in the Central Apennines. The range of isotopic values of the cements ($\delta^{13}C = [-1$ to $3]$ ‰ PDB and $\delta^{18}O = [26$ to $33]$ ‰ SMOW) was equal to the range of isotopic values of the sedimentary host rocks. This was interpreted as a hint to consider that these thrusts were not allowing deep or superficial fluids to migrate into the studied formations, picturing a closed fluid system limited by the faults. To the north, in another portion of the Central Apennines, the Umbria Marche Apennine Ridge (UMAR; Fig. 10), Beaudoin *et al.* (2020*c*) carried out analyses of fracture networks in several anticlines along a transect running from the front of the Tuscan nappes to the Adriatic coast. The associated cements were analysed, and the values of the $\delta^{18}O$ in the veins were found to exceed the values of the $\delta^{18}O$ of the Jurassic–Palaeocene sedimentary host rocks. The $\Delta^{47}CO_2$ analysis revealed that the $\delta^{18}O$ of the fluid was positive (3 to 15 ‰ SMOW), suggesting either a deep-sourced fluid or a brine evolved from seawater. The former interpretation was discarded on account of the $^{87}Sr/^{86}Sr$ values, too low to relate to basement-derived fluids. Thus, Beaudoin *et al.* (2020*c*) proposed a lateral fluid flow of evolved brines in a stratigraphically compartmentalized reservoir (Fig. 10). This interpretation is further supported by the fact that in the innermost part of the belt, the hydrothermal regime of the fluids flowing in faults and veins (>140 °C) can be explained by a burial depth resulting from the cumulated thicknesses of Tuscan and Ligurian nappes, thrusted over the westernmost part of the UMAR at that time, if considering the past geothermal gradient of 24°C km$^{-1}$ as indicated by vitrinite reflectance (Caricchi *et al.* 2014). Note that a few veins related to LSFT host cements that precipitated from meteoric fluids characterized by a negative $\delta^{18}O$ value. To summarize, the UMAR is overall interpreted as a closed fluid system, with lateral migration of fluids related to the development of the FTB and nappes (Fig. 10).

## 7. Overview of other case studies

Section 6 reports detailed examples of how the fluid system related to the development of FTB/BF can be unravelled using geochemical proxies. It built on areas where an abundant literature was
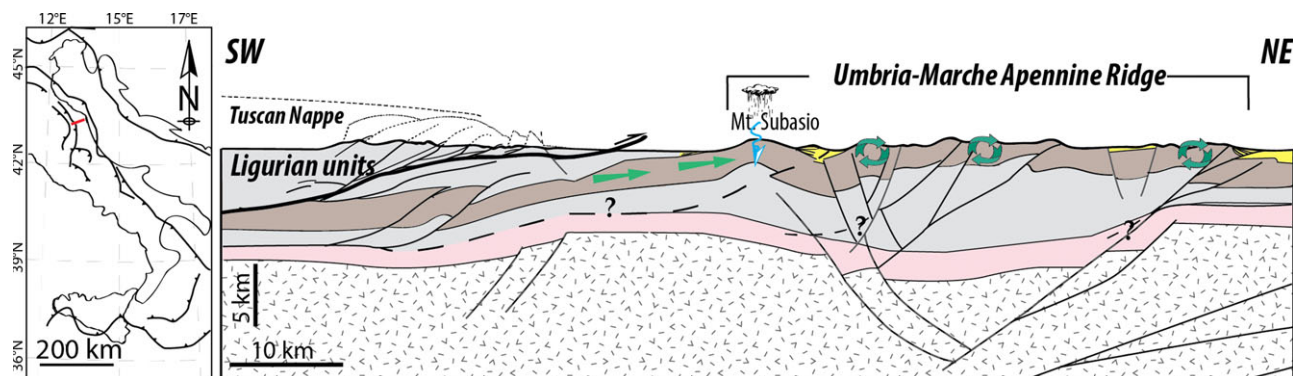


**Fig. 10.** Simplified cross-section and corresponding location of Umbria Marche Apennine Ridge (Italy), where the past fluid system was reconstructed. The vertical exaggeration is *c.* 2:1. See text for details and references. Key is given in Figure 7. The nature of the décollement is evaporites (Triassic).
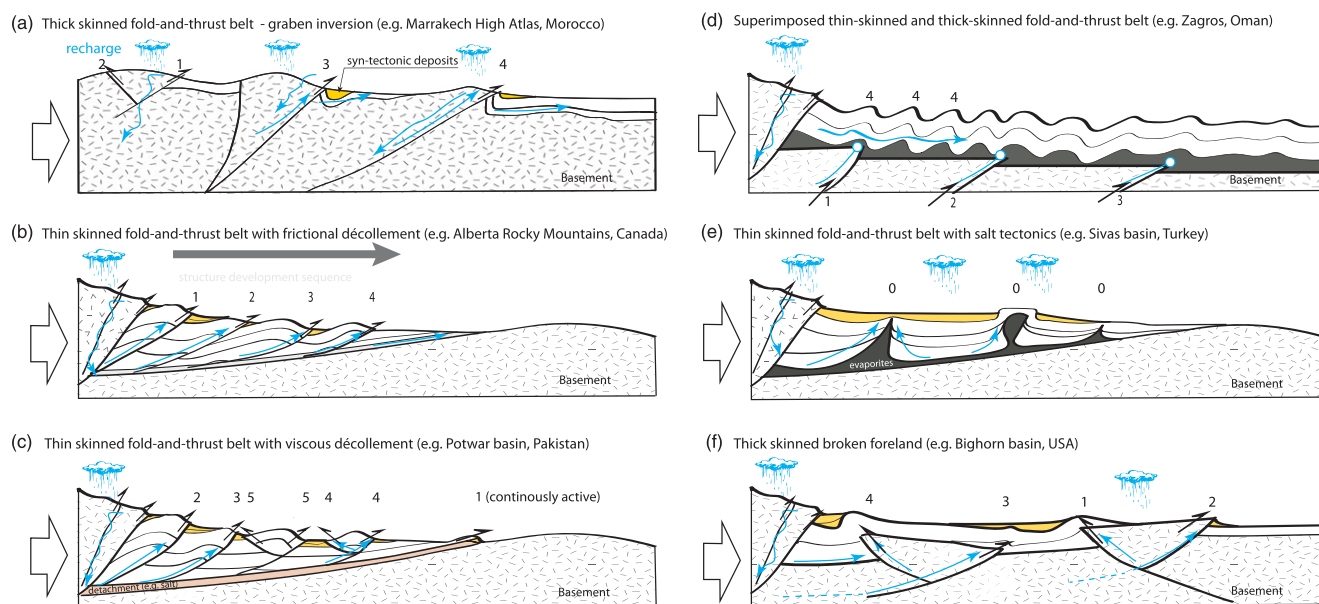
**Fig. 11.** Schematic cross-sections in the fold-and-thrust belts with respect to the structural style, inherited structures and rheology of the sediments. The expected order of structural development (thrust activation) is shown as numbers, along with the expected fluid migration at that scale (blue arrows).

available. We hereinafter complete these examples by reporting in a more succinct way the other FTB where a less significant number of geochemical studies have been conducted to depict the past fluid system with respect to the tectonic evolution at large scale or at mesoscale.

## 7.a. Thin-skinned fold-and-thrust belts: the Mexican Cordillera, the Appalachians and the Oman Mountains

The Mexican FTB is a thin-skinned FTB developed above a silici-clastic frictional décollement level (e.g. Fig. 11b) and where the past fluid system has been studied by Fitz-Diaz *et al.* (2011*a*). Although most vein cements from folds return $\delta^{18}O$ and $\delta^{13}C$ values buffered by the host rocks, $\delta^2H$ values of clays and fluid inclusions in veins are much higher in the undeformed foreland (up to 0 ‰ SMOW) than in the FTB (*c.* −60 ‰ SMOW). This spectacular increase supports a strong influence of meteoric fluids flowing during deformation near the hinterland, which fades away toward the foreland. Authors proposed that this isotopic pattern can be explained by a recharge zone in the west, where the higher part of the range is located, with a downward migration triggered by seismic pumping (Henderson & McCaig, 1996)

In the Sierra Madre (Fitz-Diaz *et al.* 2011*b*), the fluid system related to the detachment fold complex developed over thick Triassic evaporites (Nuncio fold complex) has been studied using isotope geochemistry and fluid inclusion microthermometry in calcite and quartz veins that developed in sequence from the burial until the syn-folding curvature (Fischer & Jackson, 1999; Lefticariu *et al.* 2005; Fischer *et al.* 2009). The fluid system was stratified and closed until folding, when it became homogenized and dominated by meteoric fluids. Eastwards, in the Cordoba platform and Veracruz Basin, i.e. the undeformed foreland, stable isotopes and fluid inclusion microthermometry were applied to cemented veins formed during LPS (Ferket *et al.* 2000, 2003, 2006, 2011; Gonzalez *et al.* 2012). The reconstructed fluid system involved a lateral migration of saline brines mixed with meteoric waters, with

a flow rate of 50–100 m Myr$^{-1}$ at the deformation front down to 0.1–2 m Myr$^{-1}$ further from it (Gonzalez *et al.* 2012).

The thin-skinned Appalachian FTB developed from the Ordovician to Permian times in the eastern part of the USA. Large-scale duplexes developed above Ordovician and Cambrian frictional clay levels (Fig 11b). Significant effort has been devoted to reconstructing the past fluid system at the scale of the entire FTB, especially in the Cambrian to Silurian Valley Ridge Province (Deloule & Turcotte, 1989; Evans & Battle, 1999; Ramsey & Onasch, 1999; Kirkwood *et al.* 2000; Evans & Hobbs, 2003; Evans, 2010; Evans *et al.* 2012). Fluid inclusion microthermometry and C, O isotopic studies helped define the P-T-X characteristics of the fluid system during deformation (Evans & Battles, 1999; Evans & Hobbs, 2003; Evans, 2010; Evans *et al.* 2012). During LPS, the past fluid system appears to be compartmentalized, with distinct reservoirs overlying each other. During folding, an efficient vertical migration and thus a breakage of horizontal seals occurred (Evans, 2010; Evans *et al.* 2012), with local thermal and isotopic disequilibrium with the host rock (Evans & Battle, 1999; Evans & Hobbs, 2003). These geochemical signatures hint at the input of extra-reservoir fluids into the reservoir rocks. However, no distinction can be made concerning the nature of the fluids, possibly being either meteoric or metamorphic. Yet, authors proposed that the topographic high to the west served as a recharge zone for these fluids that would have flowed as a squeegee over 60 km across the belt (Evans & Battle, 1999). Interestingly, not all the thrusts acted as drains to propel the fluids forelandwards: some of them acted as barriers restricting the fluid system according to their orientation and/or degree of reactivation (Ramsey & Onasch, 1999).

The Oman Mountains, in the United Arab Emirates, is a thin-skinned FTB in which the fluid system was characterized by studying hydrothermal dolomitization and fracture cements (Breesch *et al.* 2006, 2009, 2010, 2011; Holland *et al.* 2009*a*, *b*; Holland & Urai, 2010; Arndt *et al.* 2014). Authors discriminated a burial phase, a pre-LPS phase, a syn-folding phase and a post-deformation phase. During the burial phase, crack-seal cements precipitated from rock-buffered fluids, possibly formational, an

interpretation also proposed by Hilgers *et al.* (2006). The fracture cements in the LPS phase were interpreted as reflecting temperature increase during burial diagenesis. During contractional deformation including LPS, the fluid system was dominated by hydrothermal brines channelized from the basal décollement along a network of connected thrusts. Fluid flow simulations suggest hot flashes along the thrusts, the duration of which depends on the thrust activity (Callot *et al.* 2010b).

### 7.b. Thin-skinned fold-and-thrust belts with salt tectonics: the Albanides and the Sivas Basin

The past fluid system in the Albanides Foothills, mainly the Ionian Basin, located in the southwest of Albania, was reconstructed by van Geet *et al.* (2002), Vilasi *et al.* (2006, 2009), Roure *et al.* (2010) and de Graaf *et al.* (2019). This former Jurassic–Oligocene intracontinental rift basin was inverted during the Alpine orogeny, strongly mobilizing the Triassic evaporites as the main décollement with some inherited (and rejuvenated as well) diapirism, making this mountain range a thin-skinned FTB with salt tectonics influence (e.g. Fig. 11e). For van Geet *et al.* (2002), isotopic geochemistry on the fracture cements across the belt depicts a rather buffered fluid system during burial and LPS, with an enrichment in δ$^{18}$O during thrust activation that authors relate to interaction with Triassic evaporites. A similar enrichment is observed by Vilasi *et al.* (2006, 2009) coevally with the deposition of barite, strengthening the idea of interactions with the Triassic evaporites. Vilasi *et al.* (2006, 2009) also characterized a complex pre-deformational fluid system with input of meteoric fluids flowing through soil. The input of either meteoric or 'hydrothermal' fluids suggests an opening of the fluid system during contraction. De Graaf *et al.* (2019) proposed a slightly different scenario, with fluid interacting with evaporites since LPS in a reservoir that opened to meteoric fluid flow during the folding phase.

The Sivas Basin, located in the Anatolian plateau in Turkey, is an Oligocene to Pliocene foreland basin developed between the Taurides–Anatolides block and the Pontides block. Recent structural analyses have established the Sivas Basin as a striking example of a synorogenic salt tectonics-controlled basin (Fig. 11e), where the geometry at the time of deformation was directly controlled by the distribution and deformation of the Late Eocene evaporites of the Tuzhisar Fm (Kergaravat *et al.* 2016; Legeay *et al.* 2020). The influence of synorogenic salt tectonics can be illustrated from the geochemical characterization of the surrounding sandstones (Pichat *et al.* 2016) and of the evaporites collected around diapiric structures (Pichat *et al.* 2018). Salt tectonics enabled the complete clogging of sandstone porosity by precipitation of calcite and analcime in the vicinity of the diapiric structures early in its diagenetic evolution. Also, the Sr isotopic study of the evaporites shows that the saline waters currently at the surface yield the same radiogenic signature as the evaporites from the Tuzhisar Fm (Pichat *et al.* 2018), which suggests that current saline fluids are polluted by the Sr isotopic ratio of the salt through continuous diapiric recycling. This is a point to consider in basins where salt tectonics is present: as diapirs are dynamic structures, they may carry with them the radiogenic signature of their formation through mechanical advection or through secondary evaporite deposition. Consequently, any fluids flowing in contact with evaporites will presumably acquire their radiogenic signature, limiting the use of Sr-based tracers ($^{87}$Sr/$^{86}$Sr) or geochronometry (Rb–Sr) to infer the source and pathway of the fluids that interacted with the evaporites.

### 7.c. Fold-and-thrust belts with superimposed thin-skinned and thick-skinned styles of deformation: the Zagros FTB

Resulting from the ongoing collision of the Arabian plate with the Eurasian plate, the Zagros FTB in Kurdistan and Iran shows superimposed thin-skinned and thick-skinned tectonic styles of deformation (Fig. 11d; Ahmadhadi *et al.* 2007; Mouthereau *et al.* 2007, 2012; Lacombe & Bellahsen, 2016). The regional fluid system deduced from the study of the folds of the Zagros FTB was assessed using isotopic geochemistry and fluid inclusion microthermometry from mesoscale fracture networks from several major folds by Kareem *et al.* (2019). Authors depicted an early pervasive forelandward flow of hydrothermal brines, related to extensive dolomitization during LPS, followed by high flux of hydrothermal brines leading to another dolomitization event focused around the thrusts during their activation.

### 7.d. General evolutionary trend of the past fluid system at the scale of the orogenic foreland

The evolution of the fluid system as reported in the above case studies seemingly exhibits a common first-order pattern, independent of the structural style (Fig. 12). Indeed, as the pre-contraction strata now incorporated into the FTB likely were formerly parts of the undeformed foreland, they underwent (1) burial, (2) potentially extension related to the flexure/forebulge development, and (3) LPS. During burial, a closed fluid system is pictured, with the implication of local fluids (among others, van Geet *et al.* 2002; Hilgers *et al.* 2006; Vandeginste *et al.* 2012; Beaudoin *et al.* 2014a). However, the fluid flowing in fractures formed during forebulge development is usually not well documented. Indeed, unambiguously relating veins to outer-arc extension related to large-scale forebulge development requires careful observation of the chronological relationship between fractures and of their spatial distribution. Complementary microstructural study with techniques such as palaeostress reconstructions from calcite twins can support the timing of development of these fractures (e.g. Beaudoin *et al.* 2012). Consequently the paucity of published data limits our ability to propose a common trend for the fluid system related to the forebulge development, yet some authors suggest a transient vertical connection between reservoirs at that time, similar to that observed during folding (Beaudoin *et al.* 2014a). The systematic occurrence of such connection is still to be proven in other case studies, implying the need to properly decipher the fractures related to the forebulge development when studying the fracture network (Tavani *et al.* 2015). In contrast, the past fluid system bound to the LPS has been widely documented in all case studies, especially because LPS propagates deformation over hundreds of kilometres far into the stable craton (Craddock & Relle, 2003; van der Pluijm *et al.* 1997; Lacombe & Mouthereau, 1999; Lacombe, 2010; Beaudoin & Lacombe, 2018). During LPS, the mesostructures allow for a compartmentalized fluid system with lateral migration over kilometric distances, maintained by topographically driven or squeegee fluid flow. In contrast, almost all studies document a transient and strong enhancement of the vertical fracture permeability during thrusting and folding, leading to local opening to extra-reservoir fluids, either meteoric or basement-derived, that flow in fold hinges and along fault zones.

In spite of displaying a common evolution for the past fluid system, the timing and nature of fluids involved during thrusting and folding are strongly controlled by the structural style (Fig. 11). The impact of structural style at that time is twofold. On the one hand, the structural style imposes the nature of the fluids that can fill in

(a) Before fold-and-thrust belt
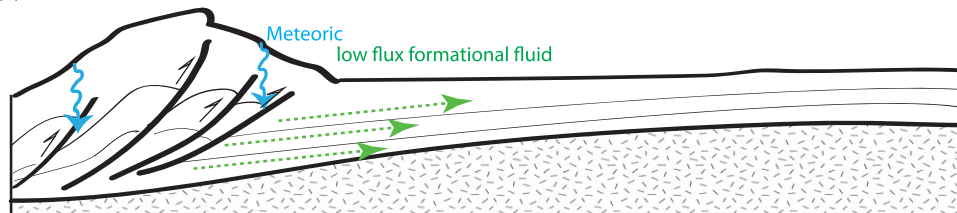


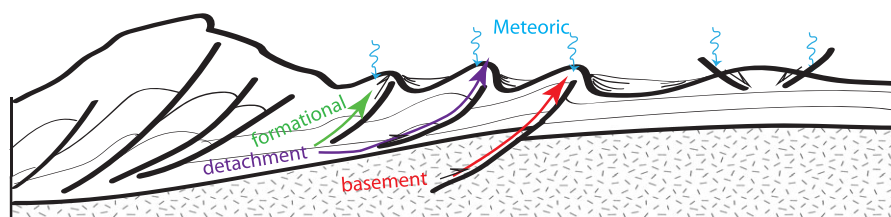(b) During the building of the fold-and-thrust belt



**Fig. 12.** Sketch illustrating the expected first-order evolution of the fluid system in FTB, without considering specificities related to structural style. (a) During layer-parallel shortening; (b) during folding/thrusting.

the reservoir in the sedimentary rocks: for instance, basement fluids are only encountered in forelands where the basement is involved in shortening. On the other hand, the structural style impacts the fluid flow by imposing a sequence of thrusting (Fig. 11). Thin-skinned tectonic wedges are usually associated with a sequence thrust activation and migration of the deformation front. In that case, the migration of fluids at the scale of the FTB occurs forelandwards (Fig. 11a), as documented in the Canadian Rocky Mountains (Vandeginste *et al.* 2012). In some cases, however, the development of thrusts can be out-of-sequence, with some inner thrusts developing later than the outer-most ones. This occurred in the southern Pyrenees (Henderson & McCaig, 1996; McCaig *et al.* 2000; Lacroix *et al.* 2014), where the fluids flowing along the thrusts are different in spite of the latter being of similar spatial extension (Fig. 9). Thick-skinned systems often display a more irregular and erratic sequence of deformation, especially in broken forelands. The sequence affects the timing of the fluid flowing from the basement into the sedimentary cover (Beaudoin *et al.* 2018). Finally, in FTB where the tectonics is linked to salt dynamics, the chemical signature of the fluids is strongly controlled by where and when diapiric structures develop and are dynamically involved in the shortening history (Pichat *et al.* 2018).

## 8. Discussion: towards geochemistry-assisted structural geology

### 8.a. Main feedbacks of past fluid system studies on structural geology

The very concept of geochemistry-assisted structural geology is to use the geochemical signatures of the past fluid to constrain sub-surface geology via the understanding of fluid sources and con-duits, with quantitative information about the temperature and age of the fluid from which the calcite cement precipitated. The overview of the case studies reveals a relationship between the fluid system evolution and tectonics that can be established by linking the opening of the fluid system in a reservoir to the structural style of deformation and/or the local or regional tectonic evolution. In the presented case studies, the interpretation of the past fluid system in terms of sources and pathways directly confronts the previous understanding of (1) the structure with an extended knowledge about the subsurface geometry thanks to wells or seis-mic imagery, and (2) deformation timing constrained by sedimen-tological, geochronological and structural observations and analyses. In turn, when the past fluid system is studied in order to unravel the spatial and temporal distribution of conduits and, by extension, the associated tectonic history, it appears possible to further constrain the structural geology whether at the scale of the individual structure or at the scale of the FTB. To do so and to be as unambiguous as possible in the interpretation of the geochemistry of calcite cements (e.g. Muñoz-López *et al.* 2022), we propose that the geochemical characteristics of the past fluid system should be built on (1) the interpretation of the difference in $\delta^{18}O$ and $\delta^{13}C$ between the vein cements and the local host rocks in terms of the degree of opening of the fluid system; and (2) a combination of $\delta^{18}O_{CaCO3}$ values of the cements with independent information on the temperature of the fluid at the time the cements precipitated as provided by another palaeothermometer (fluid inclusion microthermometry, $\Delta^{47}CO_2$). Such a combination ena-bles the characterization of the nature of the fluid (meteoric, sea-water or sedimentary). In some cases, other isotopic ($^4He$ or $\delta^2H$) analyses further help discriminate the fluid nature (metamorphic, mantellic, meteoric); (3) the use of tracers like $^{87}Sr/^{86}Sr$ or trace elementary composition, that help infer the specific lithologies through which the fluid has migrated (crystalline basement, evap-orites, clays), constraining the migration pathways and the exten-sion of the fracture network; and (4) age dating of the cements by means of geochronology, more specifically the uranium-based geochronology.

A direct instance comes from the Sheep Mountain Anticline (Laramide province), a fold developed above a blind basement-fault whose geometry at depth is unknown and still debated (see Bellahsen *et al.* 2006a). By reconstructing the past fluid system using isotopes and fluid inclusion microthermometry, Beaudoin *et al.* (2011) unravelled a two-step fluid system, compartmental-ized during LPS and homogenized during fold growth. The latter comprises a strong overprint of the seawater and evolved seawater by meteoric-derived fluids flowing from the basement, likely chan-nelized along the underlying high-angle thrust and precipitating in a hydrothermal regime. The distribution in map-view of the geo-chemical signature of the cements precipitated from these
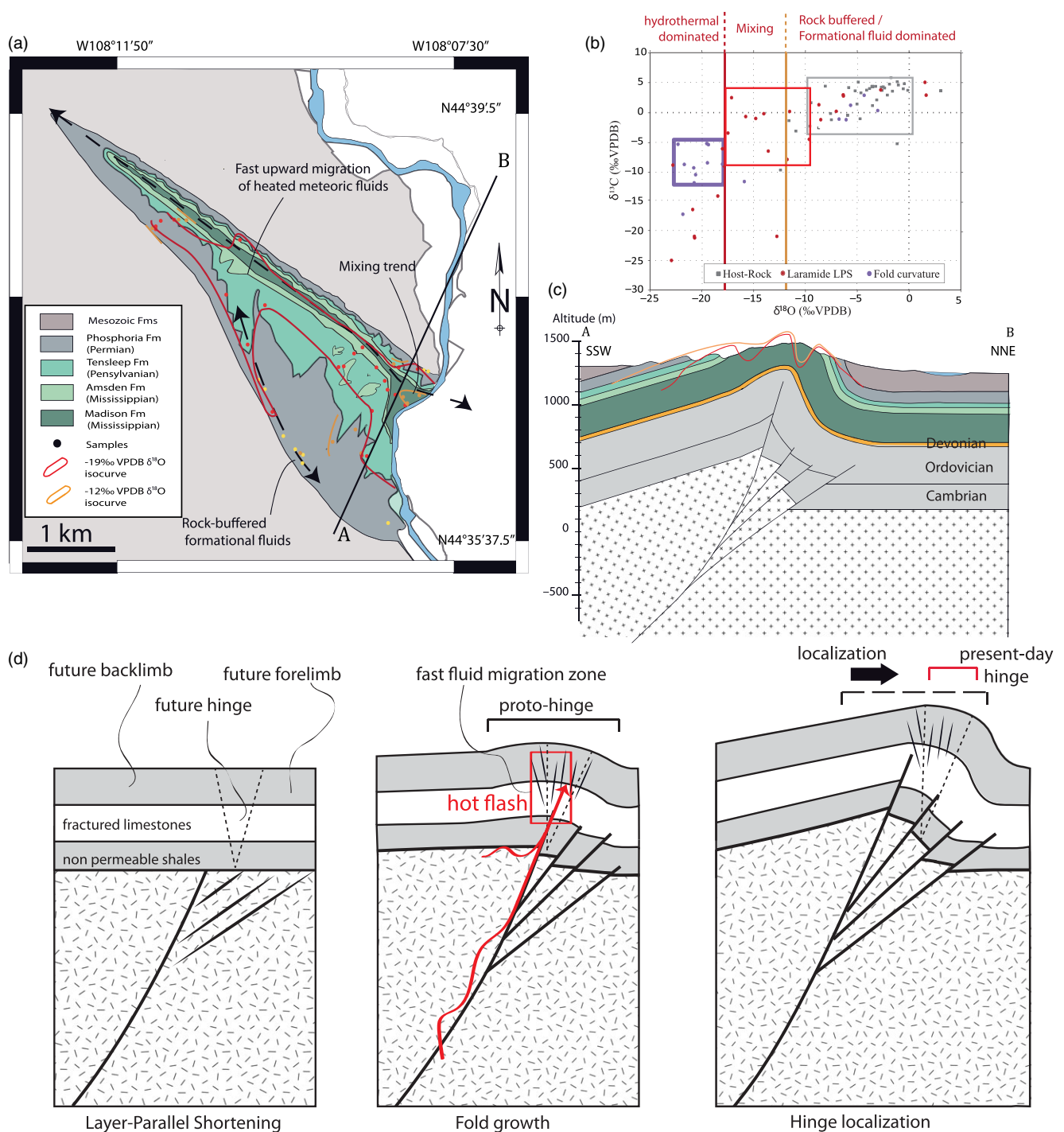
**Fig. 13.** Example of direct application of geochemistry-assisted structural geology, based on the case study of the Sheep Mountain Anticline (SMA; Beaudoin *et al.* 2011). (a) Geological map of the SMA, where the values of the δ18O of tectonic veins are reported as coloured points, and where iso-δ18O value curves are plotted. (b) Simplified δ18O vs δ13C plots of the cements in the fracture network. The colours of the dots and the corresponding frames relate to the deformation phase during which the vein developed. Red and orange vertical lines correspond to the past fluid system interpretation, in accordance with the curves plotted in (a). (c) Cross-section along the line located on (a), with the corresponding location of the iso-δ18O value curves, with a proposed subsurface geometry. (d) Interpretation of the deformation sequence accounting for a potential migration of the hinge during fold growth. (a) and (b) are modified after Beaudoin *et al.* (2011).

hydrothermal fluids, which display a typical and homogeneous range of δ18O values (from −19 ‰ PDB to −23 ‰ PDB; Beaudoin *et al.* 2011, 2014*a*; Fig. 13a), shows that the hydrothermal pulse was focused in a zone in the backlimb striking parallel to the current position of the hinge. The authors interpreted the distribution and orientation of this zone as a proxy to locate the fault tip at

the time of folding, and proposed a dynamic model of hinge migration during fold evolution (Fig. 13).

On the basis of the past fluid system reconstruction from numerous structures in the southern Pyrenees, Cruset *et al.* (2017) proposed to use the evolution of the chemical signatures of the successive calcite cements precipitated in a thrust zone to

infer whether the thrust (and the related fold) is detached through evaporites or clays. They observe two geochemical trends, in which the fluids are always a mixture of deep-sourced fluids and meteoric fluids. Where evaporites are involved in the décollement, the sequence of mineralization in the thrust zone shows successive calcite cements precipitated from a fluid with a gradually increasing $\delta^{18}O$ value with respect to the fluid from which the previous cement precipitated. Where the thrust is not soling into evaporites, the sequence of mineralization in the thrust zone shows successive calcite cements precipitated from a fluid with a decreasing $\delta^{18}O$ value and decreasing Fe and Sr contents with respect to the fluid from which the previous cement precipitated. If this rule looks very promising and could pave the way to a geochemical imagery of the nature of décollement based on fault/fracture calcite cements, it needs more applications to validate it further and to clarify the mechanisms that can explain this geochemical pattern.

Another striking example of geochemistry-assisted structural geology comes from past fluid system reconstruction in the southern Pyrenees (Lacroix *et al.* 2011). Coupling $\delta^{18}O$ $\delta^{13}C$ of cements in veins and fault zones to fluid inclusion microthermometry allowed those authors to show that the fluid system was closed to external fluids. Doing so, it is possible to estimate the depth at which a thrust was active, assuming a given geothermal gradient. That resulted in the picture of how the thrust evolved in the southern Pyrenees (Lacroix *et al.* 2011) or, when coupled to U–Pb absolute dating, in the reconstruction of the last stage of activity of the southernmost Pyrenean Thrust (Hoareau *et al.* 2021). By coupling the $\Delta^{47}CO_2$ temperature of cement precipitation in a closed system to a 1D burial-time model, a similar approach was also used in the Cingoli Anticline (Apennines, Italy) by Labeur *et al.* (2021) to estimate the absolute timing of the different stages of contractional deformation (LPS, folding, LSFT), in good agreement with the age of folding as constrained by growth strata.

Geochemistry-assisted structural geology is also a relevant approach to refine the large-scale structural geology in FTB where the structural style is debated, or has evolved over time. For example, in the Umbria Marches Apennine Ridge, Labeur *et al.* (2021) and Beaudoin *et al.* (2020*c*) reported that the main carbonate reservoir of the FTB hosted seawater fluids, i.e. with trace of neither evaporitic saline brines nor basement-derived fluids. In this FTB, where the degree of mechanical coupling between the basement and the sedimentary cover is strongly debated (Calamita *et al.* 2011; Scisciani *et al.* 2014, 2019), especially as thick evaporites lie in between, such an absence of extra-reservoir fluids is insightful. It can mean either that (1) thrusts in relation to which the folds were built are not rooting deep enough to reach either evaporites or basement, a hypothesis discarded by seismic imagery, or (2) the thrusts more likely root in the basement rather than in the evaporites. Authors favoured this interpretation, relating the absence of any basement-derived fluid signature to the fact that the impervious Triassic evaporites acted as a major barrier and prevented any upward fluid flow from the basement even along the (presumably limited) damage zone of the basement-rooted thrusts.

## 8.b. Timescales of deformation and fluid systems in orogenic forelands

An obvious side effect of understanding how fractures are related to the tectonic evolution of an area is that it grants a direct way of dating the tectonic event (see Roberts & Holdsworth, 2022, for a recent review). Of course, it is mandatory to have the best understanding of the diagenesis history of a fracture-filling cement to be

sure of what is actually dated, especially in fault zones where numerous dissolution–precipitation, recrystallization and/or successive fluid flow events can be recorded (e.g. Aubert *et al.* 2020). That being done, it becomes possible to date not only the timing of deformation, but also the duration of some events. For example, in the broken foreland of the Laramide province, U–Pb ages obtained in cements coeval with vein opening reveal that the Laramide LPS-related mesostructures developed over a duration of *c.* 30 Myr (Beaudoin *et al.* 2018, 2019*a*). This means that a tectonic deformation stage can last tens of millions of years, and in the case of the Laramide province, fractures from the LPS time are filled with fluids that flowed eastward at the scale of the basin (Barbier *et al.* 2012*b*; Beaudoin *et al.* 2014*a*). That means that during 30 Myr, the mesostructures developed in a way that maintained the required permeability of the sedimentary cover to enable the fluid migration at the basin scale in spite of cement precipitation in some of the fractures. Even the fractures related to strata curvature during fold growth have been estimated to develop over 1.5 to 15 Myr in various folds (Lacombe *et al.* 2021). Over these rather long timespans, the past fluid system remains isotopically homogeneous (see Section 5), with most of the curvature-related veins filled with cements precipitated either from basement-derived fluids (e.g. Beaudoin *et al.* 2011; Lacroix *et al.* 2014) or from meteoric fluids (e.g. Lynch *et al.* 2021). An overlooked but major implication of involving external fluids of the same source and chemistry over Myrs is that there is a need for long-lasting (> few Myrs) active recharge and migration mechanisms, e.g. convection cells at the scale of the FTB and/or the foreland basin (Gomez-Rivas *et al.* 2014. That brings into question the dynamics of the fluids and its timescale in FTB, which have been extensively investigated by means of numerical simulations of the past fluid system, especially when it comes to hydrocarbon exploration (see Roure *et al.* 2010, for a review). It must be kept in mind that measuring a migration speed for a given episode of deformation is out of reach when studying the past fluid system. Indeed, the absolute dating of a cement yields not the age of the fluid, but the age of the precipitation of the material dissolved within this fluid, and the fluid from which the cement precipitated in a fracture is therefore no longer available to mineralize another fracture. Nevertheless, in cases where the deformation event and related fracture development occurred over a short and well-constrained timespan, it becomes possible to estimate an average migration speed (e.g. Beaudoin *et al.* 2014*a*). Beyond that limitation, being able to perform the direct dating of a cement that is related to a specific fluid flow (e.g. basement-derived fluids) is a promising way to build a calendar of when fluid conduits developed, that can be related, for example, to the timing of basement thrust activation/propagation into the cover rocks.

## 8.c. Future developments

We have seen in this review that reconstructing the past fluid system from a simple mineralogical system (i.e. calcite) enables a better understanding of the evolution of the fluid migration, of the connectivity of the conduits and ultimately of the structural geology and tectonics of an area. Considering the case studies presented, the fracture network is depicted as an important drain in the palaeohydrology at the fold and the orogenic foreland scales. As the fracture network records much more information about the deformation history than thrusts and other seismic-scale faults, that means that the syn-kinematic cements precipitated in the fracture network are good targets to reconstruct the fluid system and its

evolution in relation to large-scale tectonics. In particular, the role of stylolites on the fluid system remains vastly overlooked in that context, except to constrain the diagenesis related to the burial phase or the early LPS (Swennen *et al.* 2000; Roure *et al.* 2010). As recent studies support that stylolites can be efficient conduits for fluid flow beyond the local scale (Koehn *et al.* 2016; Martín-Martín *et al.* 2018), and that they can develop during most of the folding stage (Beaudoin *et al.* 2016), it appears necessary to further investigate stylolites to reconstruct the past fluid system. This can be done simply by considering the tectonic and sedimentary stylolites, and by analysing cements precipitated in tension gashes or at the tip of stylolites (Aharonov & Karcz, 2019). On top of this, it is noteworthy that sedimentary stylolites yield quantitative estimates of the depth at which they developed, helping refine the expected temperature for a fluid flow event (Beaudoin *et al.* 2019b, 2020b). Another feature that deserves more attention to better appraise structural evolution and conduit distribution when reconstructing the past fluid system is the mineralogical transformation processes. As carbonates are extremely sensitive to fluid-mediated mineralogical transformation like dolomitization or apatitization of calcite, reconstructing the type of fluid that leads to the transformation can be insightful for the conduits. In the Maestrat Basin (Spain), such an approach revealed a deep-source fluid migrating over long timespans (Martin-Martin *et al.* 2018), which implies potential convection cells in the subsurface (Gomez-Rivas *et al.* 2014). Of course, such an approach is limited by our understanding of the fluid-mediated transformation process itself and the associated volume of fluids required. These are much debated to date (Davies & Smith, 2006; Merino & Canals, 2011; Jonas *et al.* 2014; Koeshidayatullah *et al.* 2020a; Centrella *et al.* 2021; Weber *et al.* 2021) and merit further investigation.

## 9. Conclusions

In this contribution, we provide a methodological and applicative review of published work focusing on the characterization of the past fluid system associated to orogenic forelands using geochemistry on fault and vein calcite cements. We also highlight/discuss whether and how past fluid system studies can shed light on tectonics. This review points out that some of the most commonly used geochemical tools like $\delta^{18}O$–$\delta^{13}C$ of carbonates can be very misleading if used alone, and that complementary methods are required in order to properly define a past fluid system, i.e. reconstructing the source fluid chemistry to infer the potential pathways. We can separate the geochemical proxies into three categories: (1) the palaeothermo(baro)meters, such as $\Delta^{47}CO_2$ and fluid inclusion microthermometry, which each have application domains limited by temperature (180 °C max for $\Delta^{47}CO_2$, 50 °C min for FIM in large inclusions); (2) the tracers, like $\delta^2H$, $^{87}Sr/^{86}Sr$, REE patterns, noble gas such as $^4He$, fluid inclusions and to a certain extent the trace element contents; and (3) the geochronometers, mainly U–Pb in carbonates. Of course, the fast-growing development of analytical capability, in both spatial and concentration resolution, has already made interpretation of the fluid chemistry less ambiguous and so provides a more reliable picture of the fluid system. One can be confident that ongoing analytical developments will democratize further the ability of the community to conduct convincing fluid system reconstructions in the future. For instance, extracting noble gases from fluid inclusions related to a given phase of deformation will enable more accessible ways to assess the source and chemistry of the fluids; lowering the detection threshold and improving the data treatment will allow dating of smaller volume

by means of U–Pb geochronology; coupling the clumped isotopy to LA-ICP-MS will allow characterization of the fluid nature and temperature at a higher spatial resolution. Nevertheless, the currently existing range of proxies, when used together, seem enough to comprehend most of the past fluid systems.

In published studies, there is a common trend of past fluid system evolution at the scale of the fold, the thrust and of the orogenic foreland (Fig. 12): (1) the system is closed or compartmentalized before the onset of folding/thrusting; (2) during folding/thrusting, the system opens to external fluids, either meteoric fluids, deep-sourced brines or metamorphic fluids according to what the structural geology allows for. However, there are variations according to the structural style of deformation in the belt and to the sedimentary succession of the area, with possibly no deep-sourced fluid in case the thrusts cross a layer of non-permeable material, like evaporites. The latter, however, always affect the fluid system of any thrust rooted in the evaporite layer. It is interesting to note that deciphering a past fluid system at the fold scale alone is always complicated by the fact that contractional structures in FTBs are mostly hydrologically connected with a strong influence of lateral migration during the tectonic history. Another important point to highlight is that even though large-scale fault zones remain an object of prime interest for reconstructing the past fluid system, numerous studies have established that the fracture network is of the utmost relevance to reconstruct the long-term past fluid system evolution. That supports that fractures below the seismic resolution are efficient drains and reliable recorders of the fluid system variation controlled by large-sale migration engines. The ambiguous impact of pressure solution on the fluid flow at the fracture-network scale remains to be better investigated in future studies.

The feedback that the characterization of the past fluid system grants to understand tectonics is twofold. (1) In cases where the subsurface is well known (i.e. seismic lines, wells), understanding the nature, temperature and preferential pathways of the fluid has been proven to be valuable for refining the structural-based basin models. This is mainly based on the fact the past fluid system helps better constrain the location of the drains and seals by reconstructing past pressure levels in reservoir, or to locate the extension of a thrust (refer to the numerous examples in the review of Roure *et al.* 2010). In that case, the recent democratization of geochronology in carbonates will improve the constraints on the time frame of deformation, refining further the 4D basin modelling. (2) In cases where little information is available about the subsurface, or if the tectonics is debated, it seems that past fluid flow holds some keys to comprehension. The isotopic and elemental signature of the cements precipitated in fractures is likely to reflect the source of the mineralizing fluid, especially in cases where the crystalline basement or evaporite levels are involved in shortening. That can help discussion of the tectonic style of deformation of an orogenic foreland, even though one needs to keep in mind that the absence of, for instance, basement fluids does not mean the basement is not involved at all in the deformation (e.g. Jura Mountains). At the fold scale, the geochemical signature of cements can be used to locate the main drains (e.g. underlying fault zone, hinge), which paves the way to alternative ways to discuss the structural geology. Finally, the past fluid system related to major faults and fractures allows the reconstruction of the absolute age of the deformation. To date, constraining the fluid dynamics in an orogenic foreland using that approach is out of reach, as only the age of the cement precipitation, and not of the source fluid, can be obtained. Yet, absolute ages grant another constraint to discuss how deformation affects strata

in forelands, and to put invaluable time constraints (timing, duration, rate) on dynamic events such as layer-parallel shortening, fold growth and thrust development.

We believe that geochemistry-based structural geology is a growing domain that will help refine predictive fluid flow models, beyond, obviously, the sole case of forelands, but the potential of which will also be developed, helping better understand the multiscale deformation history in the upper crust.

# References

**Accaino F, Bratus A, Conti S, Fontana D and Tinivella U** (2007) Fluid seepage in mud volcanoes of the northern Apennines: an integrated geophysical and geological study. *Journal of Applied Geophysics* **63**, 90–101.

**Affek HP** (2012) Clumped isotope paleothermometry: principles, applications, and challenges. *The Paleontological Society Papers* **18**, 101–14.

**Affolter S, Fleitmann D and Leuenberger M** (2014) New online method for water isotope analysis of speleothem fluid inclusions using laser absorption spectroscopy (WS-CRDS). *Climate of the Past* **10**, 1291–304.

**Agosta F** (2008) Fluid flow properties of basin-bounding normal faults in platform carbonates, Fucino Basin, central Italy. In *The Geodynamics of the Aegean and Anatolia* (eds T Taymaz, Y Yilmaz and Y Dilek), pp. 277–91. Geological Society of London, Special Publication no. 299.

**Agosta F and Kirschner DL** (2003) Fluid conduits in carbonate-hosted seismogenic normal faults of central Italy. *Journal of Geophysical Research: Solid Earth* **108**, 2221.

**Agosta F, Luetkemeyer PB, Lamarche J, Crider JG and Lacombe O** (2016) An introduction to the Special Issue on "The role of fluids in faulting and fracturing in carbonates and other upper crustal rocks". *Tectonophysics* **690**, 1–3.

**Aharonov E and Karcz Z** (2019) How stylolite tips crack rocks. *Journal of Structural Geology* **118**, 299–307.

**Ahmadhadi F, Lacombe O and Daniel JM** (2007) Early reactivation of basement faults in Central Zagros (SW Iran): evidence from pre-folding fracture populations in the Asmari Formation and Lower Tertiary paleogeography. In *Thrust Belts and Foreland Basins: From Fold Kinematics to Hydrocarbon Systems* (eds O Lacombe, J Lavé, J Vergés and F Roure), pp. 205–28. Berlin: Springer-Verlag.

**Al-Aasm I, Lonnee J and Clarke J** (2000) Multiple fluid flow events and the formation of saddle dolomite: examples from Middle Devonian carbonates of the Western Canada Sedimentary Basin. *Journal of Geochemical Exploration* **69–70**, 11–5.

**Al-Aasm IS, Lonnee J and Clarke J** (2002) Multiple fluid flow events and the formation of saddle dolomite: case studies from the Middle Devonian of the Western Canada Sedimentary Basin. *Marine and Petroleum Geology* **19**, 209–17.

**Amrouch K, Beaudoin N, Lacombe O, Bellahsen N and Daniel J-M** (2011) Paleostress magnitudes in folded sedimentary rocks. *Geophysical Research Letters* **38**, L17301.

**Amrouch K, Lacombe O, Bellahsen N, Daniel JM and Callot JP** (2010b) Stress and strain patterns, kinematics and deformation mechanisms in a basement-cored anticline: Sheep Mountain Anticline, Wyoming. *Tectonics* **29**, TC1005.

**Amrouch K, Robion P, Callot JP, Lacombe O, Daniel JM, Bellahsen N and Faure JL** (2010a) Constraints on deformation mechanisms during folding provided by rock physical properties: a case study at Sheep Mountain anticline (Wyoming, USA). *Geophysical Journal International* **182**, 1105–23.

**Andersen MB, Stirling CH, Potter E-K, Halliday AN, Blake SG, McCulloch MT, Ayling BF and O'Leary M** (2008) High-precision U-series measurements of more than 500,000 year old fossil corals. *Earth and Planetary Science Letters* **265**, 229–45.

**Anderson NT, Kelson JR, Kele S, Daëron M, Bonifacie M, Horita J, Mackey TJ, John CM, Kluge T, Petschnig P, Jost AB, Huntington KW, Bernasconi SM and Bergmann KD** (2021) A unified clumped isotope thermometer calibration (0.5–1,100°C) using carbonate-based standardization. *Geophysical Research Letters* **48**, e2020GL092069.

**André AS, Sausse J and Lespinasse M** (2001) New approach for the quantification of paleostress magnitudes: application to the Soultz vein system (Rhine graben, France). *Tectonophysics* **336**, 215–31.

**Andresen, KJ** (2012) Fluid flow features in hydrocarbon plumbing systems: what do they tell us about the basin evolution? *Marine Geology* **332**, 89–108.

**Archie GE** (1952) Classification of carbonate reservoir rocks and petrophysical considerations. *AAPG Bulletin* **36**, 278–98.

**Arndt M, Virgo S, Cox SF and Urai JL** (2014) Changes in fluid pathways in a calcite vein mesh (Natih Formation, Oman Mountains): insights from stable isotopes. *Geofluids* **14**, 391–418.

**Aubert I, Léonide P, Lamarche J and Salardon R** (2020) Diagenetic evolution of fault zones in Urgonian microporous carbonates, impact on reservoir properties (Provence – Southeast France). *Solid Earth* **11**, 1163–86.

**Baietto A, Cadoppi P, Martinotti G, Perello P, Perrochet P and Vuataz FD** (2008) Assessment of thermal circulations in strike-slip fault systems: the Terme di Valdieri case (Italian western Alps). In *The Geodynamics of the Aegean and Anatolia* (eds T Taymaz, Y Yilmaz and Y Dilek), pp. 317–39. Geological Society of London, Special Publication no. 299.

**Bakker RJ** (2003) Package FLUIDS 1. Computer programs for analysis of fluid inclusion data and for modelling bulk fluid properties. *Chemical Geology* **194**, 3–23.

**Ballentine CJ and Burnard, PG** (2002). Production, release and transport of noble gases in the continental crust. *Reviews in Mineralogy and Geochemistry* **47**, 481–538.

**Bar E, Nuriel P, Kylander-Clark A and Weinberger R** (2021) Towards in situ U-Pb dating of dolomite. *Geochronology* **3**, 337–49.

**Barbier M, Floquet M, Hamon Y and Callot JP** (2015) Nature and distribution of diagenetic phases and petrophysical properties of carbonates: the Mississippian Madison Formation (Bighorn Basin, Wyoming, USA). *Marine and Petroleum Geology* **67**, 230–48.

**Barbier M, Hamon Y, Callot JP, Floquet M and Daniel JM** (2012b) Sedimentary and diagenetic controls on the multiscale fracturing pattern of a carbonate reservoir: the Madison Formation (Sheep Mountain, Wyoming, USA). *Marine and Petroleum Geology* **29**, 50–67.

**Barbier M, Leprêtre R, Callot JP, Gasparrini M, Daniel JM, Hamon Y, Lacombe O and Floquet M** (2012a) Impact of fracture stratigraphy on the paleo-hydrogeology of the Madison Limestone in two basement-involved folds in the Bighorn basin, (Wyoming, USA). *Tectonophysics* **576–577**, 116–32.

**Barker SL, Cox SF, Eggins SM and Gagan, MK** (2006) Microchemical evidence for episodic growth of antitaxial veins during fracture-controlled fluid flow. *Earth and Planetary Science Letters* **250**, 331–44.

**Barker SLL, Bennett VC, Cox SF, Norman MD and Gagan MK** (2009) Sm–Nd, Sr, C and O isotope systematics in hydrothermal calcite–fluorite veins: implications for fluid–rock reaction and geochronology. *Chemical Geology* **268**, 58–66.

**Bau M and Möller P** (1993) Rare earth element systematics of the chemically precipitated component in early Precambrian iron formations and the evolution of the terrestrial atmosphere-hydrosphere-lithosphere system. *Geochimica et Cosmochimica Acta* **57**, 2239–49.

**Beaudoin N, Bellahsen N, Lacombe O and Emmanuel L** (2011) Fracture-controlled paleohydrogeology in a basement-cored, fault-related fold: Sheep Mountain Anticline, Wyoming, United States. *Geochemistry, Geophysics, Geosystems* **12**, Q06011.

**Beaudoin N, Bellahsen N, Lacombe O, Emmanuel L and Pironon J** (2014a) Crustal-scale fluid flow during the tectonic evolution of the Bighorn Basin (Wyoming, USA). *Basin Research* **26**, 403–35.

**Beaudoin N and Lacombe O** (2018) Recent and future trends in paleopiezometry in the diagenetic domain: insights into the tectonic paleostress and burial depth history of fold-and-thrust belts and sedimentary basins. *Journal of Structural Geology* **114**, 357–65.

**Beaudoin N, Lacombe O, Bellahsen N, Amrouch K and Daniel J-M** (2014b) Evolution of pore-fluid pressure during folding and basin contraction in overpressured reservoirs: insights from the Madison-Phosphoria carbonate formations in the Bighorn Basin (Wyoming, USA). *Marine and Petroleum Geology* **55**, 214–29.

**Beaudoin N, Lacombe O, Bellahsen N and Emmanuel L** (2013) Contribution of studies of sub-seismic fracture populations to paleo-hydrological reconstructions (Bighorn Basin, USA). *Procedia Earth and Planetary Science* **7**, 57–60.

**Beaudoin N, Leprêtre R, Bellahsen N, Lacombe O, Amrouch K, Callot J-P, Emmanuel L and Daniel J-M** (2012) Structural and microstructural evolution of the Rattlesnake Mountain Anticline (Wyoming, USA): new insights into the Sevier and Laramide orogenic stress build-up in the Bighorn Basin. *Tectonophysics* **576–577**, 20–45.

**Beaudoin G and Therrien P** (2004) The web stable isotope fractionation calculator. In *Handbook of Stable Isotope Analytical Techniques*, (ed P. de Groot), Elsevier pp. 1045–48.

**Beaudoin N, Gasparrini M, David ME, Lacombe O and Koehn D** (2019b) Bedding-parallel stylolites as a tool to unravel maximum burial depth in sedimentary basins: application to Middle Jurassic carbonate reservoirs in the Paris basin. *Geological Society of America Bulletin* **131**, 1239–54.

**Beaudoin N, Huyghe D, Bellahsen N, Lacombe O, Emmanuel L, Mouthereau F and Ouanhnon L** (2015) Fluid systems and fracture development during syn-depositional fold growth: an example from the Pico del Aguila anticline, Sierras Exteriores, southern Pyrenees, Spain. *Journal of Structural Geology* **70**, 23–38.

**Beaudoin N, Koehn D, Lacombe O, Lecouty A, Billi A, Aharonov E and Parlangeau C** (2016) Fingerprinting stress: stylolite and calcite twinning paleopiezometry revealing the complexity of progressive stress patterns during folding: the case of the Monte Nero anticline in the Apennines, Italy. *Tectonics* **35**, 1687–712.

**Beaudoin NE, Labeur A, Lacombe O, Koehn D, Billi A, Hoareau G, Boyce A, John CM, Marchegiano M, Roberts NM, Millar IL, Claverie F, Pecheyran C and Callot JP** (2020c) Regional-scale paleofluid system across the Tuscan Nappe-Umbria-Marche Apennine Ridge (northern Apennines) as revealed by mesostructural and isotopic analyses of stylolite-vein networks. *Solid Earth* **11**, 1617–41.

**Beaudoin N, Lacombe O, David ME and Koehn D** (2020a) Does stress transmission in forelands depend on structural style? Distinctive stress magnitudes during Sevier thin-skinned and Laramide thick-skinned layer-parallel shortening in the Bighorn Basin (USA) revealed by stylolite and calcite twinning paleopiezometry. *Terra Nova* **32**, 225–33.

**Beaudoin N, Lacombe O, Koehn D, David ME, Farrell N and Healy D** (2020b) Vertical stress history and paleoburial in foreland basins unravelled by stylolite roughness paleopiezometry: insights from bedding-parallel stylolites in the Bighorn Basin, Wyoming, USA. *Journal of Structural Geology* **136**, 104061.

**Beaudoin N, Lacombe O, Roberts NMW and Koehn D** (2018) U-Pb dating of calcite veins reveals complex stress evolution and thrust sequence in the Bighorn Basin, Wyoming, USA. *Geology* **46**, 1015–8.

**Beaudoin N, Lacombe O, Roberts NMW and Koehn D** (2019a) U-Pb dating of calcite veins reveals complex stress evolution and thrust sequence in the Bighorn Basin, Wyoming, USA: REPLY. *Geology* **47**, e481.

**Becker JS** (2002) State-of-the-art and progress in precise and accurate isotope ratio measurements by ICP-MS and LA-ICP-MS. *Journal of Analytical Atomic Spectrometry* **17**, 1172–85.

**Bellahsen N, Fiore PE and Pollard DD** (2006a) From spatial variation of fracture patterns to fold kinematics: a geomechanical approach. *Geophysical Research Letters* **33**, 1–4.

**Bellahsen N, Fiore P and Pollard DD** (2006b) The role of fractures in the structural interpretation of Sheep Mountain Anticline, Wyoming. *Journal of Structural Geology* **28**, 850–67.

**Bense VF, Gleeson T, Loveless SE, Bour O and Scibek J** (2013) Fault zone hydrogeology. *Earth-Science Reviews* **127**, 171–92.

**Bergbauer S and Pollard DD** (2004) A new conceptual fold-fracture model including prefolding joints, based on the Emigrant Gap anticline, Wyoming. *Bulletin of the Geological Society of America* **116**, 294–307.

**Bergman SC, Huntington KW and Crider JG** (2013) Tracing paleofluid sources using clumped isotope thermometry of diagenetic cements along the Moab Fault, Utah. *American Journal of Science* **313**, 490–515.

**Berio LR, Mittempergher S, Storti F, Bernasconi SM, Cipriani A, Lugli F and Balsamo F** (2022) Open-closed-open paleofluid system conditions recorded in the tectonic vein networks of the Parmelan anticline (Bornes Massif, France). *Journal of the Geological Society* **179** (5), 2021–117. https://doi.org/10.1144/jgs2021-117.

**Bernasconi SM, Daëron M, Bergmann KD, Bonifacie M, Meckler AN, Affek HP, Anderson N, Bajnai D, Barkan E, Beverly E, Blamart D, Burgener L, Calmels D, Chaduteau C, Clog M, Davidheiser-Kroll B, Davies A, Dux F, Eiler J, Elliott B, Fetrow AC, Fiebig J, Goldberg S, Hermoso M, Huntington KW, Hyland E, Ingalls M, Jaggi M, John CM, Jost AB, Katz S, Kelson J, Kluge T, Kocken IJ, Laskar A, Leutert TJ, Liang D, Lucarelli J, Mackey TJ, Mangenot X, Meinicke N, Modestou SE, Müller IA, Murray S, Neary A, Packard N, Passey BH, Pelletier E, Petersen S, Piasecki A, Schauer A, Snell KE, Swart PK, Tripati A, Upadhyay D, Vennemann T, Winkelstern I, Yarian D, Yoshida N, Zhang N and Ziegler M** (2021) InterCarb: a community effort to improve interlaboratory standardization of the carbonate clumped isotope thermometer using carbonate standards. *Geochemistry, Geophysics, Geosystems* **22**, e2020 GC009588.

**Bernasconi SM, Müller IA, Bergmann KD, Breitenbach SFM, Fernandez A, Hodell DA, Jaggi M, Meckler AN, Millan I and Ziegler M** (2018) Reducing uncertainties in carbonate clumped isotope analysis through consistent carbonate-based standardization. *Geochemistry, Geophysics, Geosystems* **19**, 2895–914.

**Bilau A, Bienveignant D, Rolland Y, Schwartz S, Godeau N, Guihou A, Deschamps P, Mangenot X, Brigaud B, Boschetti L and Dumont T** (2022) The Tertiary structuration of the Western Subalpine foreland deciphered by calcite-filled faults and veins. *Earth-Science Reviews* **236**, 104270.

**Bjørlykke K** (1994) Fluid-flow processes and diagenesis in sedimentary basins. In *Geofluids: Origin, Migration and Evolution of Fluids in Sedimentary Basins* (ed. J. Farrell), pp. 127–40. Geological Society of London, Special Publication no. 78.

**Bjørlykke K** (2015) Subsurface water and fluid flow in sedimentary basins. In *Petroleum Geoscience: From Sedimentary Environments to Rock Physics*, 2nd edn., pp. 279–300. Berlin: Springer.

**Blamey NJF** (2012) Composition and evolution of crustal, geothermal and hydrothermal fluids interpreted using quantitative fluid inclusion gas analysis. *Journal of Geochemical Exploration* **116–117**, 17–27.

**Bodnar RJ** (2003) Reequilibration of fluid inclusions. In Fluid Inclusions: Analysis and Interpretation (eds I Samson, A Anderson and D Marshall), pp. 213–30. Vancouver, Canada: Mineralogical Association of Canada Short Course 32.

**Boggs S and Krinsley D** (2006) *Application of Cathodoluminescence Imaging to the Study of Sedimentary Rocks*. Cambridge: Cambridge University Press.

**Böhlke JK and Irwin JJ** (1992) Laser microprobe analyses of noble gas isotopes and halogens in fluid inclusions: analyses of microstandards and synthetic inclusions in quartz. *Geochimica et Cosmochimica Acta* **56**, 187–201.

**Bonifacie M, Calmels D, Eiler JM, Horita J, Chaduteau C, Vasconcelos C, Agrinier P, Katz A, Passey BH, Ferry JM and Bourrand JJ** (2017) Calibration of the dolomite clumped isotope thermometer from 25 to 350 °C, and implications for a universal calibration for all (Ca, Mg, Fe) $CO_3$ carbonates. *Geochimica et Cosmochimica Acta* **200**, 255–79.

**Bons PD, Elburg MA and Gomez-Rivas E** (2012) A review of the formation of tectonic veins and their microstructures. *Journal of Structural Geology* **43**, 33–62.

**Bottinga Y** (1969) Calculated fractionation factors for carbon and hydrogen isotope exchange in the system calcite-carbon dioxide-graphite-methane-hydrogen-water vapor. *Geochimica et Cosmochimica Acta* **33**, 49–64.

**Bottinga Y and Craig H** (1968) Oxygen isotope fractionation between $CO_2$ and water, and the isotopic composition of marine atmospheric $CO_2$. *Earth and Planetary Science Letters* **5**, 285–95.

**Bourdet J, Pironon J, Levresse G and Tritlla J** (2008) Petroleum type determination through homogenization temperature and vapour volume fraction measurements in fluid inclusions. *Geofluids* **8**, 46–59.

**Bradbury HJ and Woodwell GR** (1987) Ancient fluid flow within foreland terrains. In *Petroleum Geology of the Continental Shelf of Northwest Europe: Oil and Source Rocks of the North Sea* (eds LV Illing and GD Hobson), pp. 87–102. Geological Society of London, Special Publication no. 34.

**Braithwaite CJR** (1989) Stylolites as open fluid conduits. *Marine and Petroleum Geology* **6**, 93–96.

**Brannon JC, Cole SC, Podosek FA, Ragan VM, Coveney RM, Wallace MW and Bradley AJ** (1996) Th-Pb and U-Pb dating of ore-stage calcite and Paleozoic fluid flow. *Science* **271**, 491–3.

**Breesch L, Swennen R, Dewever B, Roure F and Vincent B** (2011) Diagenesis and fluid system evolution in the northern Oman Mountains, United Arab Emirates: implications for petroleum exploration. *GeoArabia* **16**, 111–48.

**Breesch L, Swennen R and Vincent B** (2006) Dolomite formation in breccias at the Musandam Platform border, Northern Oman Mountains, United Arab Emirates. *Journal of Geochemical Exploration* **89**, 19–22.

**Breesch L, Swennen R and Vincent B** (2009) Fluid flow reconstruction in hanging and footwall carbonates: compartmentalization by Cenozoic reverse faulting in the Northern Oman Mountains (UAE). *Marine and Petroleum Geology* **26**, 113–28.

**Breesch L, Swennen R, Vincent B, Ellison R and Dewever B** (2010) Dolomite cementation and recrystallisation of sedimentary breccias along the Musandam Platform margin (United Arab Emirates). *Journal of Geochemical Exploration* **106**, 34–43.

**Bruna PO, Lavenu APC, Matonti C and Bertotti G** (2019) Are stylolites fluid-flow efficient features? *Journal of Structural Geology* **125**, 270–7.

**Caine JS, Evans JP and Forster CB** (1996) Fault zone architecture and permeability structure. *Geology* **24**, 1025–8.

**Caja MA, Permanyer A, Marfil R, Al-Aasm IS and Martín-Crespo T** (2006) Fluid flow record from fracture-fill calcite in the Eocene limestones from the South-Pyrenean Basin (NE Spain) and its relationship to oil shows. *Journal of Geochemical Exploration* **89**, 27–32.

**Calamita F, Satolli S, Scisciani V, Esestime P and Pace P** (2011) Contrasting styles of fault reactivation in curved orogenic belts: examples from the central Apennines (Italy). *Bulletin of the Geological Society of America* **123**, 1097–111.

**Callot JP, Breesch L, Guilhaumou N, Roure F, Swennen R and Vilasi N** (2010b) Paleo-fluids characterisation and fluid flow modelling along a regional transect in Northern United Arab Emirates (UAE). *Arabian Journal of Geosciences* **3**, 413–37.

**Callot JP, Robion P, Sassi W, Guiton MLE, Faure JL, Daniel JM, Mengus JM and Schmitz J** (2010a) Magnetic characterisation of folded aeolian sandstones: interpretation of magnetic fabrics in diamagnetic rocks. *Tectonophysics* **495**, 230–45.

**Callot JP, Sassi W, Roure F, Hill K, Wilson N and Divies R** (2017) Pressure and Basin modeling in Foothill belts: a study of the Kutubu area, Papua New Guinea Fold and Thrust Belt. AAPG Memoir 114, 165–89.

**Callot JP, Trocmé V, Letouzey J, Albouy E, Jahani S and Sherkati S** (2012) Pre-existing salt structures and the folding of the Zagros Mountains. In *Salt Tectonics, Sediments and Prospectivity* (ed. SG Archer), pp. 545–61. Geological Society of London, Special Publication no. 363.

**Capozzi R and Picotti V** (2002) Fluid migration and origin of a mud volcano in the Northern Apennines (Italy): the role of deeply rooted normal faults. *Terra Nova* **14**, 363–70.

**Caricchi C, Aldega L and Corrado S** (2014) Reconstruction of maximum burial along the Northern Apennines thrust wedge (Italy) by indicators of thermal exposure and modeling. *Bulletin of the Geological Society of America* **127**, 428–42.

**Cathles LM** (1981) Fluid flow and genesis of hydrothermal ore deposits. In *Economic Geology, Seventy-fifth Anniversary* Volume (1905–1980) (eds. Brian J Skinner), pp. 424–57. El Paso, USA: The Economic Geology Publishing Company.

**Caumon M-C, Dubessy J, Robert P and Tarantola A** (2014) Fused-silica capillary capsules (FSCCs) as reference synthetic aqueous fluid inclusions to determine chlorinity by Raman spectroscopy. *European Journal of Mineralogy* **25**, 755–63.

**Cello G, Invernizzi C, Mazzoli S and Tondi E** (2001) Fault properties and fluid flow patterns from Quaternary faults in the Apennines, Italy. *Tectonophysics* **336**, 63–78.

**Centrella S, Beaudoin NE, Derluyn H, Motte G, Hoareau G, Lanari P, Piccoli F, Pecheyran C and Callot JP** (2021) Micro-scale chemical and physical patterns in an interface of hydrothermal dolomitization reveals the governing transport mechanisms in nature: case of the Layens anticline, Pyrenees, France. *Sedimentology* **68**, 834–54.

**Centrella S, Beaudoin NE, Koehn D, Motte G, Hoareau G and Callot JP** (2022) How fluid-mediated rock transformations can mimic hydro-fracturing patterns in hydrothermal dolomite. *Marine and Petroleum Geology* **140**, 105657.

**Centrella S, Putnis A, Lanari P and Austrheim H** (2018) Textural and chemical evolution of pyroxene during hydration and deformation: a consequence of retrograde metamorphism. *Lithos* **296–299**, 245–64.

**Chacko T and Deines P** (2008) Theoretical calculation of oxygen isotope fractionation factors in carbonate systems. *Geochimica et Cosmochimica Acta* **72**, 3642–60.

**Chen S, Ryb U, Piasecki AM, Lloyd MK, Baker MB and Eiler JM** (2019) Mechanism of solid-state clumped isotope reordering in carbonate minerals from aragonite heating experiments. *Geochimica et Cosmochimica Acta* **258**, 156–73.

**Chi G, Diamond LW, Lu H, Lai J and Chu H** (2020) Common problems and pitfalls in fluid inclusion study: a review and discussion. *Minerals* **2021**, 7–11. https://doi.org/10.3390/MIN11010007.

**Choukroune P** (1992) Tectonic evolution of the Pyrenees. *Annual Review of Earth and Planetary Sciences* **20**, 143.

**Clauer N** (2013) The K-Ar and $^{40}$Ar/$^{39}$Ar methods revisited for dating fine-grained K-bearing clay minerals. *Chemical Geology* **354**, 163–85.

**Cobbold PR, Zanella A, Rodrigues N and Løseth H** (2013) Bedding-parallel fibrous veins (beef and cone-in-cone): worldwide occurrence and possible significance in terms of fluid overpressure, hydrocarbon generation and mineralization. *Marine and Petroleum Geology* **43**, 1–20.

**Cooley MA, Price RA, Kyser TK and Dixon JM** (2011) Stable-isotope geochemistry of syntectonic veins in Paleozoic carbonate rocks in the Livingstone Range anticlinorium and their significance to the thermal and fluid evolution of the southern Canadian foreland thrust and fold belt. *AAPG Bulletin* **95**, 1851–82.

**Coppola M, Correale A, Barberio MD, Billi A, Cavallo A, Fondriest M, Nazzari M, Paonita A, Romano C, Stagno V, Viti C and Vona JM** (2021) Meso- to nano-scale evidence of fluid-assisted co-seismic slip along the normal Mt. Morrone Fault, Italy: implications for earthquake hydrogeochemical precursors. *Earth and Planetary Science Letters* **568**, 117010.

**Craddock JP and Relle M** (2003) Fold axis-parallel rotation within the Laramide Derby Dome Fold, Wind River Basin, Wyoming, USA. *Journal of Structural Geology* **25**, 1959–72.

**Craddock JP and van der Pluijm BA** (1989) Late Paleozoic deformation of the cratonic carbonate cover of eastern North America. *Geology* **17**, 416–9.

**Craddock JP and van der Pluijm BA** (1999) Sevier-Laramide deformation of the continental interior from calcite twinning analysis, west-central North America. *Tectonophysics* **305**, 275–86.

**Craig H** (1957) Isotopic standards for carbon and oxygen and correction factors for mass-spectrometric analysis of carbon dioxide. *Geochimica et Cosmochimica Acta* **12**, 133–49.

**Craig H** (1961) Standard for reporting concentrations of deuterium and oxygen-18 in natural waters. *Science* **133**, 1833–4.

**Crognier N, Hoareau G, Aubourg C, Dubois M, Lacroix B, Branellec M, Callot JP and Vennemann T** (2018) Syn-orogenic fluid flow in the Jaca basin (south Pyrenean fold and thrust belt) from fracture and vein analyses. *Basin Research* **30**, 187–216.

**Cruset D, Cantarero I, Travé A, Vergés J and John CM** (2016) Crestal graben fluid evolution during growth of the Puig-Reig anticline (South Pyrenean fold and thrust belt). *Journal of Geodynamics* **101**, 30–50.

**Cruset D, Cantarero I, Vergés J, John CM, Muñoz-López D and Travé A** (2018) Changes in fluid regime in syn-orogenic sediments during the growth of the south Pyrenean fold and thrust belt. *Global and Planetary Change* **171**, 207–24.

**Cruset D, Vergés J, Benedicto A, Gomez-Rivas E, Cantarero I, John CM and Travé A** (2021) Multiple fluid flow events from salt-related rifting to basin inversion (Upper Pedraforca thrust sheet, SE Pyrenees). *Basin Research* **33**, 3102–36.

**Curtis CD** (1987) Inorganic geochemistry and petroleum exploration. In *Advances in Petroleum Geochemistry* (eds J Brooks and D Welte), pp. 91–141. London: Academic Press.

**Curzi M, Aldega L, Bernasconi SM, Berra F, Billi A, Boschi C, Franchini S, van der Lelij R, Viola G and Carminati E** (2020) Architecture and evolution of an extensionally-inverted thrust (Mt. Tancia Thrust, Central Apennines): geological, structural, geochemical, and K–Ar geochronological constraints. *Journal of Structural Geology* **136**, 104059.

**Curzi M, Bernasconi SM, Billi A, Boschi C, Aldega L, Franchini S, Albert R, Gerdes A, Barberio MD and Carminati E** (2021) U–Pb age of the 2016 Amatrice earthquake causative fault (Mt. Gorzano, Italy) and paleo-fluid circulation during seismic cycles inferred from inter-and co-seismic calcite. *Tectonophysics* **819**, 229076.

**Daëron M** (2021) Full propagation of analytical uncertainties in $\Delta^{47}$ measurements. *Geochemistry, Geophysics, Geosystems* **22**, e2020GC009592.

**D'Amore F and Panichi C** (1980) Evaluation of deep temperatures of hydrothermal systems by a new gas geothermometer. *Geochimica et Cosmochimica Acta* **44**, 549–56.

**Dassié EP, Genty D, Noret A, Mangenot X, Massault M, Lebas N, Duhamel M, Bonifacie M, Gasparrini M, Minster B and Michelot JL** (2018) A newly designed analytical line to examine fluid inclusion isotopic compositions in a variety of carbonate samples. *Geochemistry, Geophysics, Geosystems* **19**, 1107–22.

**Davies GR and Smith LB** (2006) Structurally controlled hydrothermal dolomite reservoir facies: an overview. *American Association of Petroleum Geologists Bulletin* **90**, 1641–90.

**Davis DW, Lowenstein TK and Spencer RJ** (1990) Melting behavior of fluid inclusions in laboratory-grown halite crystals in the systems NaCl-H₂O, NaCl-KCl-H₂O, NaCl-MgCl₂-H₂O, and NaCl-CaCl₂-H₂O. *Geochimica et Cosmochimica Acta* **54**, 591–601

**de Graaf S, Nooitgedacht CW, Goff JLE, van der Lubbe JHJL, Vonhof HB and Reijmer JJG** (2019) Fluid-flow evolution in the Albanide fold-thrust belt: insights from hydrogen and oxygen isotope ratios of fluid inclusions. AAPG Bulletin 103, 2421–45.

**del Sole L, Antonellini M, Soliva R, Ballas G, Balsamo F and Viola G** (2020) Structural control on fluid flow and shallow diagenesis: insights from calcite cementation along deformation bands in porous sandstones. *Solid Earth* **11**, 2169–195.

**DeCelles PG** (2004). Late Jurassic to Eocene evolution of the Cordilleran thrust belt and foreland basin system, western USA. *American Journal of Science* **304**, 105–68.

**Dellinger M, Gaillardet J, Bouchez J, Calmels D, Louvat P, Dosseto A, Gorge C, Alanoca L and Maurice L** (2015) Riverine Li isotope fractionation in the Amazon River basin controlled by the weathering regimes. *Geochimica et Cosmochimica Acta* **164**, 71–93.

**Deloule E and Turcotte DL** (1989) The flow of hot brines in cracks and the formation of ore deposits. *Economic Geology* **84**, 2217–25.

**Dielforder A, Villa IM, Berger A and Herwegh M** (2022) Tracing wedge-internal deformation by means of strontium isotope systematics of vein carbonates. *Geological Magazine.* https://doi.org/10.1017/ S0016756821001357

**Dielforder A, Vollstaedt H, Vennemann T, Berger A and Herwegh M** (2015) Linking megathrust earthquakes to brittle deformation in a fossil accretionary complex. *Nature Communications* **6**, 7504.

**Dreybrodt W and Deininger M** (2014) The impact of evaporation to the isotope composition of DIC in calcite precipitating water films in equilibrium and kinetic fractionation models. *Geochimica et Cosmochimica Acta* **125**, 433–9.

**Dromgoole EL.and Walter LM** (1990) Iron and manganese incorporation into calcite: effects of growth kinetics, temperature and solution chemistry. *Chemical Geology* **81**, 311–36.

**Drost K, Chew D, Petrus JA, Scholze F, Woodhead J D, Schneider JW and Harper DA** (2018) An image mapping approach to U-Pb LA-ICP-MS carbonate dating and applications to direct dating of carbonate sedimentation. *Geochemistry, Geophysics, Geosystems* **19**, 4631–48.

**Eichhubl P, Taylor WL, Pollard DD and Aydin A** (2004) Paleo-fluid flow and deformation in the Aztec Sandstone at the Valley of Fire, Nevada: evidence for the coupling of hydrogeologic, diagenetic, and tectonic processes. *GSA Bulletin* **116**, 1120–36.

**Eiler JM and Schauble E** (2004) $^{18}O^{13}C^{16}O$ in Earth's atmosphere. *Geochimica et Cosmochimica Acta* **68**, 4767–77.

**Elter P, Grasso M, Parotto M and Vezzani L** (2008) Structural setting of the Apennine-Maghrebian thrust belt. *Episodes* **26**, 205–11.

**Emery D and Robinson A** (1993) *Inorganic Geochemistry: Applications to Petroleum Geology*, 255 pp. Oxford, UK: Blackwell Scientific Publications.

**Engel J, Maas R, Woodhead J, Tympel J and Greig A** (2020) A single-column extraction chemistry for isotope dilution U-Pb dating of carbonate. *Chemical Geology* **531**, 119311.

**English JM, Johnston, ST and Wang K** (2003). Thermal modelling of the Laramide orogeny: testing the flat-slab subduction hypothesis. *Earth and Planetary Science Letters* **214**, 619–32.

**Epstein S, Buchsbaum R, Lowenstam HA and Urey HC** (1953) Revised carbonate-water isotopic temperature scale. *GSA Bulletin* **64**, 1315–26.

**Erslev EA** (1986) Basement balancing of Rocky Mountain foreland uplifts (USA). *Geology* **14**, 259–62.

**Evans MA** (2010) Temporal and spatial changes in deformation conditions during the formation of the Central Appalachian fold-and-thrust belt: evidence from joints, vein mineral paragenesis, and fluid inclusions. In *From Rodinia to Pangea: The Lithotectonic Record of the Appalachian Region* (ed. RP Tollo), pp. 417–518: Boulder, Colorado: Geological Society of America. GSA Memoir.

**Evans MA and Battle DA** (1999) Fluid inclusion and stable isotope analyses of veins from the central Appalachian Valley and Ridge province: implications for regional synorogenic hydrologic structure and fluid migration. *GSA Bulletin* **111**, 1841–60.

**Evans MA, Bebout GE and Brown CH** (2012) Changing fluid conditions during folding: an example from the central Appalachians. *Tectonophysics* **576–577**, 99–115.

**Evans MA and Fischer MP** (2012) On the distribution of fluids in folds: a review of controlling factors and processes. *Journal of Structural Geology* **44**, 2–24.

**Evans MA and Hobbs GC** (2003) Fate of 'warm' migrating fluids in the central Appalachians during the Late Paleozoic Alleghanian orogeny. *Journal of Geochemical Exploration* **78–79**, 327–31.

**Fantle MS and Higgins J** (2014) The effects of diagenesis and dolomitization on Ca and Mg isotopes in marine platform carbonates: implications for the geochemical cycles of Ca and Mg. *Geochimica et Cosmochimica Acta* **142**, 458–81.

**Faulkner DR, Jackson CAL, Lunn RJ, Schlische RW, Shipton ZK, Wibberley CAJ and Withjack MO** (2010) A review of recent developments concerning the structure, mechanics and fluid flow properties of fault zones. *Journal of Structural Geology* **32**, 1557–75.

**Ferket H, Guilhaumou N, Roure F and Swennen R** (2011) Insights from fluid inclusions, thermal and PVT modeling for paleo-burial and thermal reconstruction of the Córdoba petroleum system (NE Mexico). *Marine and Petroleum Geology* **28**, 936–58.

**Ferket H, Roure F, Swennen R and Ortuño S** (2000) Fluid migration placed into the deformation history of fold-and-thrust belts: an example from the Veracruz basin (Mexico). *Journal of Geochemical Exploration* **69–70**, 275–9.

**Ferket H, Swennen R, Ortuño S and Roure F** (2003) Reconstruction of the fluid flow history during Laramide forelandfold and thrust belt development in eastern Mexico: cathodoluminescence and δ¹⁸O-δ¹³C isotope trends of calcite-cemented fractures. *Journal of Geochemical Exploration* **78–79**, 163–7.

**Ferket H, Swennen R, Ortuño Arzate S and Roure F** (2006) Fluid flow evolution in petroleum reservoirs with a complex diagenetic history: an example from Veracruz, Mexico. *Journal of Geochemical Exploration* **89**, 108–11.

**Fischer MP, Higuera-Díaz IC, Evans MA, Perry EC and Lefticariu L** (2009) Fracture-controlled paleohydrology in a map-scale detachment fold: insights from the analysis of fluid inclusions in calcite and quartz veins. *Journal of Structural Geology* **31**, 1490–510.

**Fischer MP and Jackson PB** (1999) Stratigraphic controls on deformation patterns in fault-related folds: a detachment fold example from the Sierra Madre Oriental, northeast Mexico. *Journal of Structural Geology* **21**, 613–33.

**Fitz-Diaz E, Hudleston P, Siebenaller L, Kirschner D, Camprubí A, Tolson G and Puig TP** (2011a) Insights into fluid flow and water-rock interaction

during deformation of carbonate sequences in the Mexican fold-thrust belt. *Journal of Structural Geology* 33, 1237–53.

Fitz-Diaz E, Hudleston P and Tolson G (2011b) Comparison of tectonic styles in the Mexican and Canadian Rocky Mountain Fold-Thrust Belt. In *Kinematic Evolution and Structural Styles of Fold-and-Thrust Belts* (eds J Poblet and RJ Lisle), pp.149–67. Geological Society of London, Special Publication no. 349.

Fossen H, Schultz RA. Shipton ZK and Mair K (2007) Deformation bands in sandstone: a review. *Journal of the Geological Society* 164, 755–69.

Gabellone T, Gasparrini M, Iannace A, Invernizzi C, Mazzoli S and D'Antonio M (2013) Fluid channeling along thrust zones: the Lagonegro case history, southern Apennines, Italy. *Geofluids* 13, 140–58.

Gao J, He S, Zhao JX, He Z, Wu C, Feng Y, Nguyen AD, Zhou J and Yi Z (2020) Sm-Nd isochron dating and geochemical (rare earth elements, $^{87}Sr/^{86}Sr$, $\delta^{18}O$, $\delta^{13}C$) characterization of calcite veins in the Jiaoshiba shale gas field, China: implications for the mechanisms of vein formation in shale gas systems. *GSA Bulletin* 132, 1722–40.

Ge S and Garven G (1994) A theoretical model for thrust-induced deep groundwater expulsion with application to the Canadian Rocky Mountains. *Journal of Geophysical Research* 99, 13851–868.

Ghisetti F, Kirschner DL, Vezzani L and Agosta F (2001) Stable isotope evidence for contrasting paleofluid circulation in thrust faults and normal faults of the central Apennines, Italy. *Journal of Geophysical Research: Solid Earth* 106, 8811–25.

Ghisetti F and Vezzani L (2000) Detachments and normal faulting in the Marche fold-and-thrust belt (central Apennines, Italy): inferences on fluid migration paths. *Journal of Geodynamics* 29, 345–69.

Ghosh P, Adkins J, Affek H, Balta B, Guo W, Schauble EA, Schrag D and Eiler JM (2006) $^{13}C$-$^{18}O$ bonds in carbonate minerals: a new kind of paleothermometer. *Geochimica et Cosmochimica Acta* 70, 1439–56.

Giggenbach WF (1996) Chemical composition cf volcanic gases. In *Monitoring and Mitigation of Volcano Hazards*, (eds Scarpa/Tilling), pp. 221–56. Germany: Springer-Verlag Berlin.

Goldstein RH (1986) Reequilibration of fluid inclusions in low-temperature calcium-carbonate cement. *Geology* 14, 792–5.

Goldstein RH and Reynolds TJ (1994) *Systematics of Fluid Inclusions in Diagenetic Minerals. SEPM Short Course 31*, 213 pp.

Gomez-Rivas E, Corbella M, Martín-Martín JD, Stafford SL, Teixell A, Bons PD, Griera A and Cardellach E (2014) Reactivity of dolomitizing fluids and Mg source evaluation of fault-controlled dolomitization at the Benicàssim outcrop analogue (Maestrat basin, E Spain). *Marine and Petroleum Geology* 55, 26–42.

Gonzalez E, Ferket H, Callot J-P, Guillhaumou N, Ortuno S and Roure F (2012) Paleoburial, hydrocarbon generation, and migration in the Córdoba Platform and Veracruz Basin: insights from fluid inclusion studies and two-dimensional (2D) basin modeling. In *Analyzing the Thermal History of Sedimentary Basins: Methods and Case Studies* (ND Naeser and TH McCulloh), pp. 167–86. Tulsa, Oklahoma: SEPM Special Publication.

Gratier JP, Frery E, Deschamps P, Røyne A, Renard F, Dysthe D, Ellouz-Zimmerman N and Hamelin B (2012) How travertine veins grow from top to bottom and lift the rocks above them: the effect of crystallization force. *Geology* 40, 1015–18.

Graustein WC (1989) $^{87}Sr/^{86}Sr$ ratios measure the sources and flow of strontium in terrestrial ecosystems. In *Stable Isotopes in Ecological Research. Ecological Studies (Analysis and Synthesis)* (eds PW Rundel, JR Ehleringer and KA Nagy), pp. 491–512. New York: Springer.

Groshong RH, Kronenberg A, Couzens-Schultz BA and Newman J (2014) Fluids and structures in fold and thrust belts with recognition of the work of David Wiltschko. *Journal of Structural Geology* 69, 281–3.

Guillaume D, Teinturier S, Dubessy J and Pironon J (2003) Calibration of methane analysis by Raman spectroscopy in $H_2O$–NaCl–$CH_4$ fluid inclusions. *Chemical Geology* 194, 41–9.

Guiton MLE, Leroy YM and Sassi W (2003) Activation of diffuse discontinuities and folding of sedimentary layers. *Journal of Geophysical Research: Solid Earth* 108, 1–20.

Gussone N, Ahm ASC, Lau KV and Bradbury HJ (2020) Calcium isotopes in deep time: potential and limitations. *Chemical Geology* 544, 119601.

Haines S, Lynch E, Mulch A, Valley JW and van der Pluijm B (2016) Meteoric fluid infiltration in crustal-scale normal fault systems as indicated by $\delta^{18}O$ and $\delta^2H$ geochemistry and $^{40}Ar/^{39}Ar$ dating of neoformed clays in brittle fault rocks. *Lithosphere* 8, 587–600.

Haines SH and van der Pluijm BA (2008) Clay quantification and Ar–Ar dating of synthetic and natural gouge: application to the Miocene Sierra Mazatán detachment fault, Sonora, Mexico. *Journal of Structural Geology* 30, 525–38.

Hairuo Qing and Mountjoy EW (1994) Formation of coarsely crystalline, hydrothermal dolomite reservoirs in the Presqu'ile Barrier, Western Canada Sedimentary Basin. *AAPG Bulletin* 78, 55–77.

Hanks CL, Parris TM and Wallace WK (2006) Fracture paragenesis and microthermometry in Lisburne Group detachment folds: implications for the thermal and structural evolution of the northeastern Brooks Range, Alaska. *AAPG Bulletin* 90, 1–20.

Heap M, Reuschlé T, Baud P, Renard F and Iezzi G (2018) The permeability of stylolite-bearing limestone. *Journal of Structural Geology* 116, 81–93.

Heinze T, Hamidi S and Galvan, B. (2017). A dynamic heat transfer coefficient between fractured rock and flowing fluid. *Geothermics* 65, 10–16.

Henderson IHC and McCaig AM (1996) Fluid pressure and salinity variations in shear zone-related veins, central Pyrenees, France: implications for the fault-valve model. *Tectonophysics* 262, 321–48.

Henley R, Truesdell A, Barton P and Whitney J (1984) Fluid-mineral equilibria in hydrothermal systems. In *Reviews in Economic Geology 1* (eds Henley, Truesdell and Barton, Jr). Littleton, USA: Society of Economic Geologists.

Hilgers C, Dilg-Gruschinski K and Urai JL (2004) Microstructural evolution of syntaxial veins formed by advective flow. *Geology* 32, 261–4.

Hilgers C, Kirschner DL, Breton JP and Urai JL (2006) Fracture sealing and fluid overpressures in limestones of the Jabal Akhdar dome, Oman Mountains. *Geofluids* 6, 168–84.

Hilgers C and Urai JL (2002a) Experimental study of syntaxial vein growth during lateral fluid flow in transmitted light: first results. *Journal of Structural Geology* 24, 1029–43.

Hilgers C and Urai JL (2002b) Microstructural observations on natural syntectonic fibrous veins: implications for the growth process. *Tectonophysics* 352, 257–74.

Hnat JS and van der Pluijm BA (2014) Fault gouge dating in the Southern Appalachians, USA. *GSA Bulletin* 126, 639–51.

Hoareau G, Claverie F, Pecheyran C, Paroissin C, Grignard P-A, Motte G, Chailan O and Girard J-P (2021b) Direct U–Pb dating of carbonates from micron-scale femtosecond laser ablation inductively coupled plasma mass spectrometry images using robust regression. *Geochronology* 3, 67–87.

Hoareau G, Crognier N, Lacroix B, Aubourg C, Roberts NMW, Niemi N, Branellec M, Beaudoin N and Suarez Ruiz I (2021a) Combination of $\Delta^{47}$ and U-Pb dating in tectonic calcite veins unravel the last pulses related to the Pyrenean Shortening (Spain). *Earth and Planetary Science Letters* 553, 116636.

Holland M, Saxena N and Urai JL (2009a) Evolution of fractures in a highly dynamic thermal, hydraulic, and mechanical system-(II) remote sensing fracture analysis, Jabal Shams, Oman Mountains. *GeoArabia* 14, 163–94.

Holland M and Urai JL (2010) Evolution of anastomosing crack–seal vein networks in limestones: insight from an exhumed high-pressure cell, Jabal Shams, Oman Mountains. *Journal of Structural Geology* 32, 1279–90.

Holland M, Urai JL, Muchez P and Willemse EJM (2009b) Evolution of fractures in a highly dynamic thermal, hydraulic, and mechanical system – (I) Field observations in Mesozoic Carbonates, Jabal Shams, Oman Mountains. *GeoArabia* 14, 57–110.

Hollocher K (1991) Prograde amphibole dehydration reactions during high-grade regional metamorphism, central Massachusetts, USA. *American Mineralogist* 76, 956–70.

Horita J (2014) Oxygen and carbon isotope fractionation in the system dolomite–water–$CO_2$ to elevated temperatures. *Geochimica et Cosmochimica Acta* 129, 111–24.

Horton BK, Capaldi TN, Mackaman-Lofland C, Perez ND, Bush MA, Fuentes F and Constenius KN (2022) Broken foreland basins and the

influence of subduction dynamics, tectonic inheritance, and mechanical triggers. *Earth-Science Reviews*, **104193**.

Hough BG, Fan M and Passey BH (2014) Calibration of the clumped isotope geothermometer in soil carbonate in Wyoming and Nebraska, USA: implications for paleoelevation and paleoclimate reconstruction. *Earth and Planetary Science Letters* **391**, 110–20.

Hu G and Clayton RN (2003) Oxygen isotope salt effects at high pressure and high temperature and the calibration of oxygen isotope geothermometers. *Geochimica et Cosmochimica Acta* **67**, 3227–46.

Hudec MR and Jackson MPA (2007) Terra infirma: understanding salt tectonics. *Earth-Science Reviews* **82**, 1–28.

Humphrey E, Gomez-Rivas E, Koehn D, Bons PD, Neilson J, Martín-Martín JD and Schoenherr J (2019) Stylolite-controlled diagenesis of a mudstone carbonate reservoir: a case study from the Zechstein_2_Carbonate (Central European Basin, NW Germany). *Marine and Petroleum Geology* **109**, 88–107.

Huntington KW, Budd DA, Wernicke BP and Eiler JM (2011) Use of clumped-isotope thermometry to constrain the crystallization temperature of diagenetic calcite. *Journal of Sedimentary Research* **81**, 656–69.

Husson JM, Higgins JA, Maloof AC and Schoene B (2015) Ca and Mg isotope constraints on the origin of Earth's deepest $\delta^{13}C$ excursion. *Geochimica et Cosmochimica Acta* **160**, 243–66.

Irwin H, Curtis C and Coleman M (1977) Isotopic evidence for source of diagenetic carbonates formed during burial of organic-rich sediments. *Nature* **269**, 209–13.

Jakubowicz M, Agirrezabala LM, Belka Z, Siepak M and Dopieralska J (2022) Sr–Nd isotope decoupling at Cretaceous hydrocarbon seeps of the Basque-Cantabrian Basin (Spain): implications for tracing volcanic-influenced fluids in sedimented rifts. *Marine and Petroleum Geology* **135**, 105430.

Jin XY, Zhao JX, Feng YX, Hofstra AH, Deng XD, Zhao XF and Li JW (2021) Calcite U-Pb dating unravels the age and hydrothermal history of the giant Shuiyindong carlin-type gold deposit in the Golden Triangle, South China. *Economic Geology* **116**, 1253–65.

Jonas L, John T, King HE, Geisler T and Putnis A (2014) The role of grain boundaries and transient porosity in rocks as fluid pathways for reaction front propagation. *Earth and Planetary Science Letters* **386**, 64–74.

Jordan, TE and Allmendinger RW (1986). The Sierras Pampeanas of Argentina: a modern analogue of Rocky Mountain foreland deformation. *American Journal of Science* **286,** 737–64.

Kareem KH, Al-Aasm IS and Mansurbeg H (2019) Structurally-controlled hydrothermal fluid flow in an extensional tectonic regime: a case study of Cretaceous Qamchuqa Formation, Zagros Basin, Kurdistan Iraq. *Sedimentary Geology* **386**, 52–78.

Kergaravat C, Ribes C, Legeay E, Callot JP, Kavak KS and Ringenbach JC (2016) Minibasins and salt canopy in foreland fold-and-thrust belts: the central Sivas Basin, Turkey. *Tectonics* **35**, 1342–66.

Kim ST and O'Neil JR (1997) Equilibrium and nonequilibrium oxygen isotope effects in synthetic carbonates. *Geochimica et Cosmochimica Acta* **61**, 3461–75.

Kirkwood D, Ayt-Ougougdal M, Gayot T, Beaudoin G and Pironon J (2000) Paleofluid-flow in a foreland basin, Northern Appalachians: from syntectonic flexural extension to Taconian overthrusting. *Journal of Geochemical Exploration* **69–70**, 269–73.

Kirschner DL and Kennedy LA (2001) Limited syntectonic fluid flow in carbonate-hosted thrust faults of the Front Ranges, Canadian Rockies, inferred from stable isotope data and structures. *Journal of Geophysical Research: Solid Earth* **106**, 8827–40.

Koehn D, Rood MP, Beaudoin N, Chung P, Bons PD and Gomez-Rivas E (2016) A new stylolite classification scheme to estimate compaction and local permeability variations. *Sedimentary Geology* **346**, 60–71.

Koeshidayatullah A, Corlett H, Stacey J, Swart PK, Boyce and Hollis C (2020b) Origin and evolution of fault-controlled hydrothermal dolomitization fronts: new insight. *Earth and Planetary Science Letters* **541**, 116291.

Koeshidayatullah A, Corlett H, Stacey J, Swart PK, Boyce A, Robertson H, Whitaker F and Hollis C (2020a) Evaluating new fault-controlled hydrothermal dolomitization models: insights from the Cambrian Dolomite, Western Canadian Sedimentary Basin. *Sedimentology* **67**, 2945–73.

Kylander-Clark ARC (2020) Expanding the limits of laser-ablation U–Pb calcite geochronology. *Geochronology* **2**, 343–54.

Labeur A, Beaudoin NE, Lacombe O, Emmanuel L, Petracchini L, Daëron M, Klimowicz S and Callot JP (2021) Burial-deformation history of folded rocks unraveled by fracture analysis, stylolite paleopiezometry and vein cement geochemistry: a case study in the Cingoli Anticline (Umbria-Marche, Northern Apennines). *Geosciences* **11**, 135.

Lacombe O (2010) Calcite twins, a tool for tectonic studies in thrust belts and stable orogenic forelands. *Oil & Gas Science and Technology – Revue d'IFP Energies nouvelles* **65**, 809–38.

Lacombe O, Beaudoin NE, Hoareau G, Labeur A, Pecheyran C and Callot JP (2021) Dating folding beyond folding, from layer-parallel shortening to fold tightening, using mesostructures: lessons from the Apennines, Pyrenees, and Rocky Mountains. *Solid Earth* **12**, 2145–57.

Lacombe O and Bellahsen N (2016) Thick-skinned tectonics and basement-involved fold-thrust belts: insights from selected Cenozoic orogens. *Geological Magazine* **153**, 763–810.

Lacombe O and Mouthereau F (1999) What is the real front of orogens? The Pyrenean orogen as a case study. *Compte rendu de l'académie des sciences* **329**, 889–96.

Lacombe O and Rolland Y (2016) An introduction to the Special Issue on "Fluids in crustal deformation: fluid flow, fluid-rock interactions, rheology, melting and resources". *Journal of Geodynamics* **101**, 1–4.

Lacombe O, Swennen R and Caracausi A (2014) An introduction to the Special Issue on "Fluid-rock-tectonics interactions in basins and orogens". *Marine and Petroleum Geology* **55**, 1–5.

Lacroix B, Baumgartner LP, Bouvier AS, Kempton PD and Vennemann T (2018) Multi fluid-flow record during episodic mode I opening: a microstructural and SIMS study (Cotiella Thrust Fault, Pyrenees). *Earth and Planetary Science Letters* **503**, 37–46.

Lacroix B, Buatier M, Labaume P, Trave A, Dubois M, Charpentier D, Ventalon S and Convert-Gaubier D (2011) Microtectonic and geochemical characterization of thrusting in a foreland basin: example of the South-Pyrenean orogenic wedge (Spain). *Journal of Structural Geology* **33**, 1359–77.

Lacroix B, Leclère H, Buatier M and Fabbri O (2013) Weakening processes in thrust faults: insights from the Monte Perdido thrust fault (southern Pyrenees, Spain). *Geofluids* **13**, 56–65.

Lacroix B, Trave A, Buatier M, Labaume P, Vennemann T and Dubois M (2014) Syntectonic fluid-flow along thrust faults: example of the South-Pyrenean fold-and-thrust belt. *Marine and Petroleum Geology* **49**, 84–98.

Laubach SE, Eichhubl P, Hilgers C and Lander RH (2010) Structural diagenesis. *Journal of Structural Geology* **32**, 1866–72.

Laubach SE, Lander RH, Criscenti LJ, Anovitz LM, Urai JL, Pollyea RM, Hooker JN, Narr W, Evans MA, Kerisit SN, Olson JE, Dewers T, Fisher D, Bodnar R, Evans B, Dove P, Bonnell LM, Marder MP and Pyrak-Nolte L (2019) The role of chemistry in fracture pattern development and opportunities to advance interpretations of geological materials. Reviews of Geophysics 57, 1065–111.

Lee YJ and Morse JW (1999) Calcite precipitation in synthetic veins: implications for the time and fluid volume necessary for vein filling. *Chemical Geology* **156**, 151–70.

Lefticariu L, Perry EC, Fischer MP and Banner JL (2005) Evolution of fluid compartmentalization in a detachment fold complex. *Geology* **33**, 69–72.

Legeay E, Ringenbach JC, Kergaravat C, Pichat A, Mohn G, Vergés J, Sevki Kavak K and Callot JP (2020) Structure and kinematics of the Central Sivas Basin (Turkey): salt deposition and tectonics in an evolving fold-and-thrust belt. In *Fold and Thrust Belts: Structural Style, Evolution and Exploration* (ed. JA Hammerstein), pp. 361–96. Geological Society of London, Special Publication no. 490

Lin Y, Jochum KP, Scholz D, Hoffmann DL, Stoll B, Weis U and Meinrat OA (2017) In-situ high spatial resolution LA-MC-ICPMS $^{230}Th/U$ dating enables detection of small-scale age inversions in speleothems. *Solid Earth Sciences* **2**, 1–9.

Lloyd MK, Ryb U and Eiler JM (2018) Experimental calibration of clumped isotope reordering in dolomite. *Geochimica et Cosmochimica Acta* **242**, 1–20.

Lucca A, Storti F, Balsamo F, Clemenzi L, Fondriest M, Burgess R and Di Toro G (2019) From submarine to subaerial out-of-sequence thrusting

and gravity-driven extensional faulting: Gran Sasso Massif, central Apennines, Italy. *Tectonics* **38**, 4155–84.

Lynch EA, Mulch A, Yonkee A and van der Pluijm B (2019) Surface fluids in the evolving Sevier fold–thrust belt of ID–WY indicated by hydrogen isotopes in dated, authigenic clay minerals. *Earth and Planetary Science Letters* **513**, e2021GC009868.

Lynch EA, Panã D and van der Pluijm BA (2021) Focusing fluids in faults: evidence from stable isotopic studies of dated clay-rich fault gouge of the Alberta Rockies. *Geochemistry, Geophysics, Geosystems* **22**, e2021GC009868.

Lynch EA and van der Pluijm B (2017) Meteoric fluid infiltration in the Argentine Precordillera fold-and-thrust belt: evidence from H isotopic studies of neoformed clay minerals. *Lithosphere* **9**, 134–45.

Lyons JB and Snellenburg J (1971) Dating faults. *GSA Bulletin* **82**, 1749–52.

MacDonald JM, Faithfull JW, Roberts NMW, Davies AJ, Holdsworth CM. Newton M, Williamson S, Boyce A and John CM (2019) Clumped-isotope palaeothermometry and LA-ICP-MS U–Pb dating of lava-pile hydrothermal calcite veins. *Contributions to Mineralogy and Petrology* **174**, 1–15.

MacDonald JM, John CM and Girard JP (2018) Testing clumped isotopes as a reservoir characterization tool: a comparison with fluid inclusions in a dolomitized sedimentary carbonate reservoir buried to 2–4 km. In *From Source to Seep: Geochemical Applications of Hydrocarbon Systems* (ed. M Lawson), pp. 189–202. Geological Society of London, Special Publication no. 468.

Machel HG (1985a) Cathodoluminescence in calcite and dolomite and its chemical interpretation. *Geoscience Canada* **12**, 139–47.

Machel HG (1985b) Fibrous gypsum and fibrous anhydrite in veins. *Sedimentology* **32**, 443–54.

Machel HG (1997) Recrystallization versus neomorphism, and the concept of "significant recrystallization" in dolomite research. *Sedimentary Geology* **113**, 161–8.

Machel HG and Cavell PA (1999) Low-flux, tectonically-induced squeegee fluid flow ("hot flash") into the Rocky Mountain Foreland Basin. *Bulletin of Canadian Petroleum Geology* **47**, 510–33.

Machel HG and Lonnee J (2002) Hydrothermal dolomite – a product of poor definition and imagination. *Sedimentary Geology* **152**, 163–71.

Mangenot X, Bonifacie M, Gasparrini M, Götz A, Chaduteau C, Ader M and Rouchon V (2017) Coupling $\Delta^{47}$ and fluid inclusion thermometry on carbonate cements to precisely reconstruct the temperature, salinity and $\delta^{18}O$ of paleo-groundwater in sedimentary basins. Chemical Geology 472, 44–57.

Mangenot X, Gasparrini M, Rouchon V and Bonifacie M (2018) Basin-scale thermal and fluid flow histories revealed by carbonate clumped isotopes ($\Delta^{47}$) – Middle Jurassic carbonates of the Paris Basin depocentre. *Sedimentology* **65**, 123–50.

Marshak S, Karlstrom K and Timmons JM (2000) Inversion of Proterozoic extensional faults: an explanation for the pattern of Laramide and Ancestral Rockies intracratonic deformation, United States. *Geology* **28**, 735–8.

Martín-Martín JD, Gomez-Rivas E, Bover-Arnal T, Travé A, Salas R, Moreno-Bedmar JA, Tomás S, Corbella M, Teixell A, Vergés J and Stafford SL (2013) The Upper Aptian to Lower Albian syn-rift carbonate succession of the southern Maestrat Basin (Spain): facies architecture and fault-controlled stratabound dolostones. *Cretaceous Research* **41**, 217–36.

Martín-Martín JD, Gomez-Rivas E, Gómez-Gras D, Travé A, Ameneiro R, Koehn D and Bons PD (2018) Activation of stylolites as conduits for overpressured fluid flow in dolomitized platform carbonates. *Geological Society of London*, Special Publications **459**, 15776.

McArthur JM, Howarth RJ and Bailey TR (2001) Strontium isotope stratigraphy: LOWESS Version 3: best fit to the Marine Sr-Isotope Curve for 0–509 Ma and accompanying look-up table for deriving numerical age. *The Journal of Geology* **109**, 155–70.

McCaig AM (1988) Deep fluid circulation in fault zones. *Geology* **16**, 867–70.

McCaig AM, Tritlla J and Banks DA (2000) Fluid flow patterns during Pyrenean thrusting. *Journal of Geochemical Exploration* **69–70**, 539–43.

Merino E and Canals À (2011) Self-accelerating dolomite-for-calcite replacement: self-organized dynamics of burial dolomitization and associated mineralization. *American Journal of Science* **311**, 573–607.

Micarelli L, Benedicto A and Wibberley CAJ (2006) Structural evolution and permeability of normal fault zones in highly porous carbonate rocks. *Journal of Structural Geology* **28**, 1214–27.

Michael K and Bachu S (2001) Fluids and pressure distributions in the foreland-basin succession in the west-central part of the Alberta Basin, Canada: evidence for permeability barriers and hydrocarbon generation and migration. *AAPG Bulletin* **85**, 1231–52.

Minissale A, Magro G, Martinelli G, Vaselli O and Tassi GF (2000) Fluid geochemical transect in the Northern Apennines (central-northern Italy): fluid genesis and migration and tectonic implications. *Tectonophysics* **319**, 199–222.

Missenard Y, Bertrand A, Vergely P, Benedicto A, Cushing ME and Rocher M (2014) Fracture-fluid relationships: implications for the sealing capacity of clay layers – insights from field study of the Blue Clay formation, Maltese islands. *Bulletin de la Société Géologique de France* **185**, 51–63.

Moore J, Beinlich A, Porter JK, Talavera C, Berndt J, Piazolo S, Austrheim H and Putnis A (2020) Microstructurally controlled trace element (Zr, U–Pb) concentrations in metamorphic rutile: an example from the amphibolites of the Bergen Arcs. *Journal of Metamorphic Geology* **38**, 103–27.

Morad S, Al-Aasm IS, Sirat M and Sattar MM (2010) Vein calcite in Cretaceous carbonate reservoirs of Abu Dhabi: record of origin of fluids and diagenetic conditions. *Journal of Geochemical Exploration* **106**, 156–70.

Moragas M, Martínez C, Baqués V, Playà E, Travé A, Alías G and Cantarero I (2013) Diagenetic evolution of a fractured evaporite deposit (Vilobí Gypsum Unit, Miocene, NE Spain). *Geofluids* **13**, 180–93.

Motte G, Hoareau G, Callot JP, Revillon S, Piccoli F, Calassou S and Gaucher EC (2021) Rift and salt-related multi-phase dolomitization: example from the northwestern Pyrenees. *Marine and Petroleum Geology* **126**, 104932.

Mottram CM, Kellett DA, Barresi T, Zwingmann H, Friend M, Todd A and Percival JB (2020) Syncing fault rock clocks: direct comparison of U-Pb carbonate and K-Ar illite fault dating methods. *Geology* **48**, 1179–83.

Mountjoy EW, Qing H and McNutt RH (1992) Strontium isotopic composition of Devonian dolomites, Western Canada Sedimentary Basin: significance of sources of dolomitizing fluids. *Applied Geochemistry* **7**, 59–75.

Mourgues R and Cobbold PR (2003) Some tectonic consequences of fluid overpressures and seepage forces as demonstrated by sandbox modelling. *Tectonophysics* **376**, 75–97.

Mouthereau F, Lacombe O and Vergés J (2012) Building the Zagros collisional orogen: timing, strain distribution and the dynamics of Arabia/Eurasia plate convergence. *Tectonophysics* **532–535**, 27–60.

Mouthereau F, Tensi J, Bellahsen N, Lacombe O, de Boisgrollier T and Kargar S (2007) Tertiary sequence of deformation in a thin-skinned/thick-skinned collision belt: the Zagros Folded Belt (Fars, Iran). *Tectonics* **26**, TC5006.

Mozafari M, Swennen R, Balsamo F, Clemenzi L, Storti F, El Desouky H, Vanhaecke F, Tueckmantel C, Solum J and Taberner C (2015) Palofluid evolution in fault-damage zones: evidence from fault-fold interaction events in the Jabal Qusaybah Anticline (Adam Foothills, North Oman). *Journal of Sedimentary Research* **85**, 1525–51.

Mozafari M, Swennen R, Balsamo F, El Desouky H, Storti F and Taberner C (2019) Fault-controlled dolomitization in the Montagna dei Fiori Anticline (Central Apennines, Italy): record of a dominantly pre-orogenic fluid migration. *Solid Earth* **10**, 1355–83.

Mozafari M, Swennen R, Muchez P, Vassilieva E, Balsamo F, Storti F, Pironon J and Taberner C (2017) Origin of the saline paleofluids in fault-damage zones of the Jabal Qusaybah Anticline (Adam Foothills, Oman): constraints from fluid inclusions geochemistry. *Marine and Petroleum Geology* **86**, 537–46.

Muñoz-López D, Cruset D, Vergés J, Cantarero I, Benedicto A, Mangenot X, Albert R, Gerdes A, Beranoaguirre A and Travé A (2022) Spatio-temporal variation of fluid flow behavior along a fold: the Bóixols-Sant Corneli anticline (Southern Pyrenees) from U–Pb dating and structural, petrographic and geochemical constraints. *Marine and Petroleum Geology* **143**, 105788.

Nardini N, Muñoz-López D, Cruset D, Cantarero I, Martín-Martín JD, Benedicto A, Gomez-Rivas E, John CM and Travé A (2019) From early contraction to post-folding fluid evolution in the frontal part of the

Bóixols Thrust Sheet (Southern Pyrenees) as revealed by the texture and geochemistry of calcite cements. *Minerals* 9, 117.

**Neely TG and Erslev EA** (2009) The interplay of fold mechanisms and basement weaknesses at the transition between Laramide basement-involved arches, north-central Wyoming, USA. *Journal of Structural Geology* 31, 1012–27.

**Nelson RA** (1981) Significance of fracture sets associated with stylolite zones. *AAPG Bulletin* 65, 2417–25.

**Nesbitt BE and Muehlenbachs K** (1995) Geochemical studies of the origins and effects of synorogenic crustal fluids in the southern Ominecá Belt of British Columbia, Canada. *GSA Bulletin* 107, 1033–50.

**Nooitgedacht CW, van der Lubbe HJL, de Graaf S, Ziegler M, Staudigel PT and Reijmer JJG** (2021) Restricted internal oxygen isotope exchange in calcite veins: constraints from fluid inclusion and clumped isotope-derived temperatures. *Geochimica et Cosmochimica Acta* 297, 24–39.

**Oliver J** (1986) Fluids expelled tectonically from orogenic belts: their role in hydrocarbon migration and other geologic phenomena. *Geology* 14, 99–102.

**Oliver NHS and Bons PD** (2001) Mechanisms of fluid flow and fluid-rock interaction in fossil metamorphic hydrothermal systems inferred from vein-wall rock patterns, geometry and microstructure. *Geofluids* 1, 137–62.

**Ortega OJ, Gale JFW and Marrett R** (2010) Quantifying diagenetic and stratigraphic controls on fracture intensity in platform carbonates: an example from the Sierra Madre Oriental, northeast Mexico. *Journal of Structural Geology* 32, 1943–59.

**Ortiz JP, Person MA, Mozley PS, Evans JP and Bilek SL** (2019) The role of fault-zone architectural elements on pore pressure propagation and induced seismicity. *Groundwater* 57, 465–78.

**Pagel M, Bonifacie M, Schneider DA, Gautheron C, Brigaud B, Calmels D, Cros A, Saint-Bezar B, Landrein P, Sutcliffe C, Davis D and Chaduteau C** (2018) Improving paleohydrological and diagenetic reconstructions in calcite veins and breccia of a sedimentary basin by combining $\Delta^{47}$ temperature, $\delta^{18}O$ water and U-Pb age. *Chemical Geology* 481, 1–17.

**Paná DI and van der Pluijm BA** (2015) Orogenic pulses in the Alberta Rocky Mountains: radiometric dating of major faults and comparison with the regional tectono-stratigraphic record. *GSA Bulletin* 127, 480–502.

**Paquette J and Reeder RJ** (1995) Relationship between surface structure, growth mechanism, and trace element incorporation in calcite. *Geochimica et Cosmochimica Acta* 59, 735–49.

**Parekh PP, Möller P, Dulski P and Bausch WM** (1977) Distribution of trace elements between carbonate and non-carbonate phases of limestone. *Earth and Planetary Science Letters* 34, 39–50.

**Parry WT, Chan MA and Beitler B** (2004) Chemical bleaching indicates episodes of fluid flow in deformation bands in sandstone. *AAPG Bulletin* 88, 175–91.

**Peckmann J and Thiel V** (2004) Carbon cycling at ancient methane-seeps. *Chemical Geology* 205, 443–67.

**Pedrosa ET, Boeck L, Putnis CV and Putnis A** (2017) The replacement of a carbonate rock by fluorite: kinetics and microstructure. *American Mineralogist* 102, 126–34.

**Petrus K and Szymczak P** (2016) Influence of layering on the formation and growth of solution pipes. *Frontiers in Physics* 3, 1–13.

**Pfiffner OA.** (2017) Thick-skinned and thin-skinned tectonics: a global perspective. *Geosciences* 7, 71.

**Pichat A, Hoareau G, Callot J-P, Legeay E, Kavak KS, Révillon S, Parat C and Ringenbach J-C** (2018) Evidence of multiple evaporite recycling processes in a salt-tectonic context, Sivas Basin, Turkey. *Terra Nova* 30, 40–9.

**Pichat A, Hoareau G, Callot J-P and Ringenbach J-C** (2016) Diagenesis of Oligocene continental sandstones in salt-walled mini-basins – Sivas Basin, Turkey. *Sedimentary Geology* 339, 13–31.

**Pik R and Marty B** (2009) Helium isotopic signature of modern and fossil fluids associated with the Corinth rift fault zone (Greece): implication for fault connectivity in the lower crust. *Chemical Geology* 266, 67–75.

**Pironon J and Bourdet J** (2008) Petroleum and aqueous inclusions from deeply buried reservoirs: experimental simulations and consequences for overpressure estimates. *Geochimica et Cosmochimica Acta* 72, 4916–28.

**Qing H and Mountjoy E** (1992) Large-scale fluid flow in the Middle Devonian Presqu'ile barrier, western Canada sedimentary basin. *Geology* 20, 903–6.

**Ramsey DW and Onasch CM** (1999) Fluid migration in a cratonic setting: the fluid histories of two fault zones in the eastern midcontinent. *Tectonophysics* 305, 307–23.

**Rasbury ET and Cole JM** (2009) Directly dating geologic events: U-Pb dating of carbonates. *Reviews of Geophysics* 47, RG3001.

**Reeder RJ and Grams JC** (1987) Sector zoning in calcite cement crystals: implications for trace element distributions in carbonates. *Geochimica et Cosmochimica Acta* 51, 187–94.

**Regnet JB, David C, Robion P and Menéndez B** (2019) Microstructures and physical properties in carbonate rocks: a comprehensive review. *Marine and Petroleum Geology* 103, 366–76.

**Roberts NMW, Drost K, Horstwood MSA, Condon DJ, Chew D, Drake H, Milodowski AE, McLean NM, Smye AJ, Walker RJ, Haslam R, Hodson K, Imber J, Beaudoin N and Lee JK** (2020) Laser ablation inductively coupled plasma mass spectrometry (LA-ICP-MS) U–Pb carbonate geochronology: strategies, progress, and limitations. *Geochronology* 2, 33–61.

**Roberts NMW and Holdsworth RE** (2022) Timescales of faulting through calcite geochronology: a review. *Journal of Structural Geology* 158, 104578.

**Roberts NMW, Žák J, Vacek F and Sláma J** (2021) No more blind dates with calcite: fluid-flow vs. fault-slip along the Očkov thrust, Prague Basin. *Geoscience Frontiers* 12, 101143.

**Roedder E** (1984) *Fluid Inclusions: An Introduction to Studies of All Types of Fluid Inclusions, Gas, Liquid, or Melt, Trapped in Materials from Earth and Space, and Their Application to the Understanding of Geologic Processes*, Volume 12, 644 pp. Washington, DC: Mineralogical Society of America.

**Rosasco G, Roedder E and Simmons JH** (1975) Laser-excited Raman spectroscopy for nondestructive partial analysis of individual phases in fluid inclusions in minerals. *Science* 190, 557–60.

**Roure F, Andriessen P, Callot JP, Faure JL, Ferket H, Gonzales E, Guilhaumou N, Lacombe O, Malandain J, Sassi W, Schneider F, Swennen R and Vilasi N** (2010) The use of palaeo-thermo-barometers and coupled thermal, fluid flow and pore-fluid pressure modelling for hydrocarbon and reservoir prediction in fold and thrust belts. In *Hydrocarbons in Contractional Belts* (eds G Goffey, J Craig, T Needham and R Scott), pp. 87–114. Geological Society of London, Special Publication no. 348.

**Roure F, Swennen R, Schneider F, Faure JL, Ferket H, Guilhaumou N, Osadetz K, Robion P and Vandeginste V** (2005) Incidence and importance of tectonics and natural fluid migration on reservoir evolution in foreland fold-and-thrust belts. *Oil & Gas Science and Technology* 60, 67–106.

**Rye DM and Bradbury HJ** (1988) Fluid flow in the crust: an example from a Pyrenean thrust ramp. *American Journal of Science* 288, 197–235.

**Sachau T, Bons PD and Gomez-Rivas E** (2015) Transport efficiency and dynamics of hydraulic deformation networks. *Frontiers in Physics* 3, 1–13.

**Sassi W, Guiton MLE, Leroy YM, Daniel JM and Callot JP** (2012) Constraints on bed scale fracture chronology with a FEM mechanical model of folding: the case of Split Mountain (Utah, USA). *Tectonophysics* 576–577, 197–215.

**Scheiber T, Viola G, van der Lelij R, Margreth A and Schönenberger J** (2019) Microstructurally-constrained versus bulk fault gouge K-Ar dating. *Journal of Structural Geology* 127, 103868.

**Schneider F** (2003) Basin modeling in complex area: examples from eastern Venezuelan and Canadian Foothills. *Oil & Gas Science and Technology* 58, 313–24.

**Scisciani V, Agostini S, Calamita F, Pace P, Cilli A, Giori I and Paltrinieri W** (2014) Positive inversion tectonics in foreland fold-and-thrust belts: a reappraisal of the Umbria-Marche Northern Apennines (Central Italy) by integrating geological and geophysical data. *Tectonophysics* 637, 218–37.

**Scisciani V, Patruno S, Tavarnelli E, Calamita F, Pace P and Iacopini D** (2019) Multi-phase reactivations and inversions of Paleozoic–Mesozoic extensional basins during the Wilson cycle: case studies from the North Sea (UK) and the Northern Apennines (Italy). In *Fifty Years of the Wilson Cycle Concept in Plate Tectonics* (eds RW Wilson, GA Houseman, KJW McCaffrey, AG Dore and SJH Butler), pp. 205–43. Geological Society of London, Special Publication no. 470.

**Segnit ER, Holland HD and Biscardi, CJ** (1962). The solubility of calcite in aqueous solutions – I. The solubility of calcite in water between 75° and

200° at $CO_2$ pressures up to 60 atm. *Geochimica et Cosmochimica Acta* **26**, 1301–31.

**Sheppard SMF** (1986) Characterization and isotopic variations in natural waters. *Reviews in Mineralogy*, **16**, 165–83.

**Shields GA and Webb GE** (2004) Has the REE composition of seawater changed over geological time? *Chemical Geology* **204**, 103–7.

**Sibson RH** (1990) Conditions for fault-valve behaviour. In *Deformation Mechanisms, Rheology and Tectonics* (ed. RJ Knipe), pp. 15–28. Geological Society of London, Special Publication no. 54.

**Sibson RH** (2000) Fluid involvement in normal faulting. *Journal of Geodynamics* **29**, 469–99.

**Sibson RH** (2005) Hinge-parallel fluid flow in fold-thrust belts: how widespread? *Proceedings of the Geologists' Association* **116**, 301–9.

**Sibuet JC, Srivastava SP and Spakman W** (2004) Pyrenean orogeny and plate kinematics. *Journal of Geophysical Research: Solid Earth* **109**, 1–18.

**Smeraglia L, Aldega L, Bernasconi SM, Billi A, Boschi C, Caracausi A, Carminati E, Franchini S, Rizzo AL, Rossetti F and Vignaroli G** (2020b) The role of trapped fluids during the development and deformation of a carbonate/shale intra-wedge tectonic mélange (Mt. Massico, Southern Apennines, Italy). *Journal of Structural Geology* **138**, 104086.

**Smeraglia L, Bernasconi SM, Berra F, Billi A, Boschi C, Caracausi A, Carminati E, Castorina F, Doglioni C, Italiano F, Rizzo AL, Uysal IT and Zhao JX** (2018) Crustal-scale fluid circulation and co-seismic shallow comb-veining along the longest normal fault of the central Apennines, Italy. *Earth and Planetary Science Letters* **498**, 152–68.

**Smeraglia L, Fabbri O, Choulet F, Buatier M, Boulvais P, Bernasconi SM and Castorina F** (2019) Syntectonic fluid flow and deformation mechanisms within the frontal thrust of foreland fold-and-thrust belt: example from the Internal Jura, Eastern France. *Tectonophysics* **778**, 228178.

**Smeraglia L, Fabbri O, Choulet F, Buatier M, Boulvais P, Bernasconi SM and Castorina F** (2020a) Syntectonic fluid flow and deformation mechanisms within the frontal thrust of a foreland fold-and-thrust belt: example from the Internal Jura, Eastern France. *Tectonophysics* **778**, 228178.

**Smeraglia L, Giuffrida A, Grimaldi S, Pullen A, La Bruna V, Billi A and Agosta F** (2021) Fault-controlled upwelling of low-T hydrothermal fluids tracked by travertines in a fold-and-thrust belt, Monte Alpi, Southern Apennines, Italy. *Journal of Structural Geology* **144**, 104276.

**Stel H** (2009) Diagenetic crystallization and oxidation of siderite in red bed (Buntsandstein) sediments from the Central Iberian Chain, Spain. *Sedimentary Geology* **213**, 89–96.

**Stolper DA and Eiler JM** (2015) The kinetics of solid-state isotope-exchange reactions for clumped isotopes: a study of inorganic calcites and apatites from natural and experimental samples. *American Journal of Science* **315**, 363–411.

**Stone DS** (1967) Theory of Paleozoic oil and gas accumulation in Bighorn Basin, Wyoming. *AAPG Bulletin* **51**, 2056–114.

**Su A, Chen H, Feng Y-X, Zhao JX, Wang Z, Hu M, Jiang H and Duc Nguyen A** (2022) In situ U-Pb dating and geochemical characterization of multi-stage dolomite cementation in the Ediacaran Dengying Formation, Central Sichuan Basin, China: constraints on diagenetic, hydrothermal and paleo-oil filling events. *Precambrian Research* 368, 106481.

**Sutherland R, Toy VG, Townend J, Cox SC, Eccles JD, Faulkner DR, Prior DJ, Norris RJ, Mariani E, Boulton C, Carpenter BM, Menzies CD, Little TA, Hasting M, De Pascale GP, Langridge RM, Scott HR, Reid Lindroos Z, Fleming B and Kopf J** (2012) Drilling reveals fluid control on architecture and rupture of the Alpine Fault, New Zealand. *Geology* **40**, 1143–6.

**Swanson EM, Wernicke BP, Eiler JM and Losh S** (2012) Temperatures and fluids on faults based on carbonate clumped-isotope thermometry. *American Journal of Science* **312**, 1–21.

**Swart PK** (2015) The geochemistry of carbonate diagenesis: the past, present and future. *Sedimentology* **62**, 1233–304.

**Swart PK, Burns SJ and Leder JJ** (1991) Fractionation of the stable isotopes of oxygen and carbon in carbon dioxide during the reaction of calcite with phosphoric acid as a function of temperature and technique. *Chemical Geology: Isotope Geoscience section* **86**, 89–96.

**Swennen R, Muskha K and Roure F** (2000) Fluid circulation in the Ionian fold and thrust belt (Albania): implications for hydrocarbon prospectivity. **70**, 629–34.

**Szymczak P and Ladd AJC** (2009) Wormhole formation in dissolving fractures. *Journal of Geophysical Research: Solid Earth* **114**, 1–22.

**Szymczak P and Ladd AJC** (2014) Reactive-infiltration instabilities in rocks. Part 2. Dissolution of a porous matrix. *Journal of Fluid Mechanics* **738**, 591–630.

**Tang J, Dietzel M, Böhm F, Köhler SJ and Eisenhauer A** (2008) $Sr^{2+}/Ca^{2+}$ and $^{44}Ca/^{40}Ca$ fractionation during inorganic calcite formation: II. Ca isotopes. *Geochimica et Cosmochimica Acta* **72**, 3733–45.

**Tang J, Dietzel M, Fernandez A, Tripati AK and Rosenheim BE** (2014) Evaluation of kinetic effects on clumped isotope fractionation ($\Delta^{47}$) during inorganic calcite precipitation. *Geochimica et Cosmochimica Acta* **134**, 120–36.

**Tavani S, Storti F, Lacombe O, Corradetti A, Muñoz JA and Mazzoli S** (2015) A review of deformation pattern templates in foreland basin systems and fold-and-thrust belts: implications for the state of stress in the frontal regions of thrust wedges. *Earth-Science Reviews* **141**, 82–104.

**Thacker JO and Karlstrom KE** (2019) U-Pb dating of calcite veins reveals complex stress evolution and thrust sequence in the Bighorn Basin, Wyoming, USA. *Geology* **47**, e480.

**Tondi E, Antonellini M, Aydin A, Marchegiani L and Cello G** (2006) The role of deformation bands, stylolites and sheared stylolites in fault development in carbonate grainstones of Majella Mountain, Italy. *Journal of Structural Geology* **28**, 376–91.

**Tonguç Uysal I, Zhao J-X, Golding SD, Lawrence MG, Glikson M and Collerson KD** (2007) Sm-Nd dating and rare-earth element tracing of calcite: implications for fluid-flow events in the Bowen Basin, Australia. *Chemical Geology* **238**, 63–71.

**Tostevin R, Bradbury HJ, Shields GA, Wood RA, Bowyer F, Penny AM and Turchyn AV** (2019) Calcium isotopes as a record of the marine calcium cycle versus carbonate diagenesis during the late Ediacaran. *Chemical Geology* **529**, 119319.

**Toussaint R, Aharonov E, Koehn D, Gratier JP, Ebner M, Baud P, Rolland A and Renard F** (2018) Stylolites: a review. *Journal of Structural Geology* **114**, 163–95.

**Travé A, Calvet F, Sans M, Verges J and Thirlwall M** (2000) Fluid history related to the Alpine compression at the margin of the south-Pyrenean Foreland basin: the El Guix anticline. *Tectonophysics* **321**, 73–102.

**Travé A, Labaume P, Calvet F and Soler A** (1997) Sediment dewatering and pore fluid migration along thrust faults in a foreland basin inferred from isotopic and elemental geochemical analyses (Eocene southern Pyrenees, Spain). *Tectonophysics* **282**, 375–98.

**Travé A, Labaume P and Vergés J** (2007) Fluid systems in foreland fold-and-thrust belts: an overview from the Southern Pyrenees. In *Thrust Belts and Foreland Basins. Frontiers in Earth Sciences* (eds O Lacombe, F Roure, J Lavé and J Vergés) Heidelberg: Springer, Berlin. https://doi.org/10.1007/978-3-540-69426-7_5.

**Uysal, IT, Feng YX, Zhao JX, Isik V, Nuriel P and Golding, SD** (2009). Hydrothermal $CO_2$ degassing in seismically active zones during the late Quaternary. *Chemical Geology* **265**, 442–54.

**van der Pluijm BA, Craddock JP, Graham BR and Harris JH** (1997) Paleostress in cratonic North America: implications for deformation of continental interiors. *Science* **277**, 794–6.

**van der Pluijm BA, Hall CM, Vrolijk PJ, Pevear DR and Covey MC** (2001) The dating of shallow faults in the Earth's crust. *Nature* **412**, 172–5.

**van der Pluijm BA, Vrolijk PJ, Pevear DR, Hall CM and Solum J** (2006) Fault dating in the Canadian Rocky Mountains: evidence for late Cretaceous and early Eocene orogenic pulses. *Geology* **34**, 837–40.

**van Geet M, Swennen R, Durmishi C, Roure F and Muchez PH** (2002) Paragenesis of Cretaceous to Eocene carbonate reservoirs in the Ionian fold and thrust belt (Albania): relation between tectonism and fluid flow. *Sedimentology* **49**, 697–718.

**Vandeginste V, Swennen R, Allaeys M, Ellam RM, Osadetz K and Roure F** (2012) Challenges of structural diagenesis in foreland fold-and-thrust belts:

a case study on paleofluid flow in the Canadian Rocky Mountains West of Calgary. *Marine and Petroleum Geology* **35**, 235–51.

**Vannucchi P, Remitti F, Bettelli G, Boschi C and Dallai L** (2010) Fluid history related to the early Eocene-middle Miocene convergent system of the Northern Apennines (Italy): constraints from structural and isotopic studies. *Journal of Geophysical Research: Solid Earth* **115**, 5405.

**Vass A, Koehn D, Toussaint R, Ghani I and Piazolo S** (2014) The importance of fracture-healing on the deformation of fluid-filled layered systems. *Journal of Structural Geology* **67**, 94–106.

**Vignaroli G, Rossetti F, Petracchini L, Argante V, Bernasconi SM, Brilli M, Giustini F, Yu T-L, Shen C-C and Soligo M** (2022) Middle Pleistocene fluid infiltration with 10–15 ka recurrence within the seismic cycle of the active Monte Morrone Fault System (central Apennines, Italy) *Tectonophysics* **827**, 229269. doi: 10.1016/j.tecto.2022.229269.

**Vilasi N, Malandain J, Barrier L, Callot JP, Amrouch K, Guilhaumou N, Lacombe O, Muska K, Roure F and Swennen R** (2009) From outcrop and petrographic studies to basin-scale fluid flow modelling: the use of the Albanian natural laboratory for carbonate reservoir characterisation. *Tectonophysics* **474**, 367–92.

**Vilasi N, Swennen R and Roure F** (2006) Diagenesis and fracturing of Paleocene–Eocene carbonate turbidite systems in the Ionian Basin: the example of the Kelçyra area (Albania). *Journal of Geochemical Exploration* **89**, 409–13.

**Villemant B and Feuillet N** (2003) Dating open systems by the $^{238}$U–$^{234}$U–$^{230}$Th method: application to Quaternary reef terraces. *Earth and Planetary Science Letters* **210**, 105–18.

**Viola G, Zwingmann H, Mattila J and Käpyaho A** (2013) K-Ar illite age constraints on the Proterozoic formation and reactivation history of a brittle fault in Fennoscandia. *Terra Nova* **25**, 236–44.

**Wacker U, Fiebig J, Tödter J, Schöne BR, Bahr A, Friedrich O, Tütken T, Gischler E and Joachimski MM** (2014) Empirical calibration of the clumped isotope paleothermometer using calcites of various origins. *Geochimica et Cosmochimica Acta* **141**, 127–44.

**Wang X, Gao J, He S, He Z, Zhou Y, Tao Z, Zhang J and Wang Y** (2017) Fluid inclusion and geochemistry studies of calcite veins in Shizhu synclinorium, central China: record of origin of fluids and diagenetic conditions. *Journal of Earth Science* **28**, 315–32.

**Weber J, Cheshire MC, Bleuel M, Mildner D, Chang YJ, Ievlev A, Littrell KC, Ilavsky J, Stack AG and Anovitz LM** (2021) Influence of microstructure on replacement and porosity generation during experimental dolomitization of limestones. *Geochimica et Cosmochimica Acta* **303**, 137–58.

**Wennberg OP, Casini G, Jonoud S and Peacock DCP** (2016) The characteristics of open fractures in carbonate reservoirs and their impact on fluid flow: a discussion. *Petroleum Geoscience* **22**, 91–104.

**Xu WG, Fan HR, Hu FF, Santosh M, Yang KF, Lan TG and Wen BJ** (2015) Geochronology of the Guilaizhuang gold deposit, Luxi Block, eastern North China Craton: constraints from zircon U–Pb and fluorite-calcite Sm–Nd dating. *Ore Geology Reviews* **65**, 390–9.

**Yan H, Dreybrodt W, Bao H, Peng Y, Wei Y, Ma S, Mo B, Sun H and Liu Z** (2021) The influence of hydrodynamics on the carbon isotope composition of inorganically precipitated calcite. *Earth and Planetary Science Letters* **565**, 116932.

**Yardley BWD and Graham JT** (2002) The origins of salinity in metamorphic fluids. *Geofluids* **2**, 249–56.

**Yonkee WA and Weil AB** (2015) Tectonic evolution of the Sevier and Laramide belts within the North American Cordillera orogenic system. *Earth-Science Reviews* **150**, 531–93.

**Zaarur S, Affek HP and Brandon MT** (2013) A revised calibration of the clumped isotope thermometer. *Earth and Planetary Science Letters* **382**, 47–57.

**Zeebe RE** (2007) An expression for the overall oxygen isotope fractionation between the sum of dissolved inorganic carbon and water. *Geochemistry, Geophysics, Geosystems* **8**, Q09002.

**Zheng Y-F** (1999) Oxygen isotope fractionation in carbonate and sulfate minerals. *Geochemical Journal* **33**, 109–26.

**Zuluaga LF, Rotevatn A, Keilegavlen E and Fossen H** (2016) The effect of deformation bands on simulated fluid flow within fault-propagation fold trap types: lessons from the San Rafael monocline, Utah. *AAPG Bulletin* **100**, 1523–40.

**Zwingmann H, Offler R, Wilson T and Cox SF** (2004) K–Ar dating of fault gouge in the northern Sydney Basin, NSW, Australia: implications for the breakup of Gondwana. *Journal of Structural Geology* **26**, 2285–95.